Hydrology and sediments of a temperate estuary — Mallacoota Inlet, Victoria

G. E. Reinson

Bulletin 178

BUREAU OF MINERAL RESOURCES · GEOLOGY AND GEOPHYSICS · DEPARTMENT OF NATIONAL RESOURCES · AUSTRALIA

Cover photo:
Vertical aerial photograph taken 10 June 1971 from a height of 1800 m showing mouth of Genoa River at Mallacoota. North is to the left. The river's flood-tidal delta occupies most of the left half of the photo.

DEPARTMENT OF NATIONAL RESOURCES
BUREAU OF MINERAL RESOURCES, GEOLOGY AND GEOPHYSICS

BULLETIN 178

Hydrology and sediments of a temperate estuary — Mallacoota Inlet, Victoria

by

G. E. REINSON

Australian National University
Canberra

The author's present address is:
Geological Survey of Canada,
Bedford Institute of Oceanography,
Box 1006,
Dartmouth, Nova Scotia, Canada

AUSTRALIAN GOVERNMENT PUBLISHING SERVICE
CANBERRA 1977

DEPARTMENT OF NATIONAL RESOURCES

MINISTER: THE RT HON. J. D. ANTHONY, M.P.

SECRETARY: J. SCULLY

BUREAU OF MINERAL RESOURCES, GEOLOGY AND GEOPHYSICS

DIRECTOR: L. C. NOAKES, O.B.E.

ASSISTANT DIRECTOR, GEOLOGICAL BRANCH: J. N. CASEY

ABSTRACT

Mallacoota Inlet is a drowned river valley that is almost cut off from the sea by a barrier-beach complex. Additionally, a flood-tidal delta chokes the mouth of the estuary. Except for fluvial sand in the upper reaches of the estuary, sandy sediments are restricted to the seaward end where hydrodynamic activity is greatest. Muds are confined to basinal and deep-channel environments; silts occur where fresh-water discharge contributes to water circulation, and clays where circulation is restricted. In the coarse fraction of the sediments, feldspar and mica contents are highest, and quartz and carbonate are lowest, where fresh-water discharge contributes. The clay mineral assemblage in the estuarine sediments is generally similar to that of the soil and stream sediments in the source area. Geochemical results show that Fe, V, Cr, Ni, Zn, Cu, and P_2O_5 levels are highest in stagnant areas where organic-rich clay prevails, whereas Mn and Ti are highest in silts where fluvial discharge is dominant and water circulates relatively freely.

The results of the study suggest that the restricted basinal areas of the estuary are similar to fjords in terms of physical and chemical controls on sedimentation. The coastal barrier at Mallacoota was evidently formed by landward progradation during the Holocene, and overlies apparent remnants of a similar Pleistocene barrier. Many similar restricted estuaries exist along the south coast of New South Wales.

Published for the Bureau of Mineral Resources, Geology and Geophysics
by The Australian Government Publishing Service

ISBN 0 642 02903 2

MANUSCRIPT RECEIVED: MARCH 1974

REVISED MANUSCRIPT RECEIVED: AUGUST 1976

ISSUED: NOVEMBER 1977

Printed by Ambassador Press Pty Ltd, Granville, N.S.W. 2142.

CONTENTS

APPENDICES

TABLES

FIGURES

SUMMARY

Mallacoota Inlet, which is the estuary of the Genoa River, consists of an outer embayment partly enclosed by an extensive barrier-beach and dune-ridge complex, and a major drowned river valley and tributaries. Owing to the topography of the drowned river system, the estuary consists of three separate basins — Northern Basin, Southern Basin and Upper Lake. The three basins are interconnected by physically restricted passages. The basement topographic high on which the Goodwin Sands is situated isolates the Northern Basin almost completely from the Southern Basin. The Upper Lake is connected to the Southern Basin by the Narrows, a deep channel whose bathymetry and topography are similar to those of the main river channel in the upper part of the estuary. The main river channel is narrow, has very irregular, bedrock-controlled bottom topography, and is much deeper than the basinal areas. The water depth in the river channel is generally greater than 10 m, while the basinal areas are usually less than 6 m deep. The shallowest part of the estuary is at the seaward end where an extensive delta has formed immediately inside the entrance (see cover photo), and shallow-water banks rim the inside of the coastal barrier.

The temperature, composition, and circulation of the water in the estuary are controlled to a large extent by the physiography described above. Bottom topography and areal shape of the estuary, in addition to magnitude of river discharge, are the dominant factors controlling water circulation within the estuary.

The vertical circulation pattern consists of a two-layer flow system with entrainment of salt water into the upper, seaward-moving layer. The bottom topography helps to maintain this two-layer system in that the intruding sea water tends to sink down slopes into topographic lows, and as it moves slowly upstream is entrained in the opposite-moving upper layer of fresher water as it rises upslope on the other side. The upper layer decreases or increases in salinity depending on magnitude of river discharge. When discharge is high, entrainment of salt water increases, and when it is low the boundary between the two layers becomes diffuse and vertical mixing occurs throughout the water column. Seawater is never completely flushed out of the estuary, and a lens of salty water remains in the Narrows, Northern Basin, and Southern Basin even during periods of extreme runoff.

A complex lateral circulation pattern exists in the estuary. As seawater enters, it is channelled toward the right side of the estuary. It meets the seaward-flowing fresh water at right angles, and is deflected at the surface into the Northern Basin. This ponds up the fresh water in the southwest part of the Southern Basin. Some of the denser sea water sinks into the deeper areas of the Southern Basin and moves upstream through the Narrows, where again it is channelled to the right side of the Upper Lake and the fresher-water upper layer is again ponded up on the southwest side of Upper Lake.

The physiographic divisions delineate the estuary's three major subaqueous sedimentary environments: basinal, deep-channel and deltaic/shallow bank. The deltaic/shallow bank environments are characterized by sandy sediments, and the basinal and deep-channel environments by mud. Net landward movement of coarse marine detritus in the delta region is indicated by the sedimentary bed-forms, and accounts for the shallowing at the seaward end of the estuary, and the predominance of sand in the sediment of this region. Fluvial sand dominates the sediments of the river channel in the uppermost reaches of the estuary. Except for these fluvial sands and minor sand accumulations in the Upper Lake, sediments dominated by sand are restricted to the seaward end of the estuary, where hydrodynamic activity is at a maximum. Muds are restricted to basinal and deep-channel environments where hydrodynamic activity is minimal.

The water circulation pattern is reflected in the distribution pattern of clay and silt. Sediments rich in clay occur on the 'sea-water' side of the estuary where water circulation is restricted (Northern Basin), but sediments rich in silt occur on the fresh-water side, or the side where the water circulation is controlled also by fresh-water discharge (Upper Lake). The area where fresh water and sea water collide in the Upper Lake is marked by a linear accumulation of sandy mud.

The mineralogy of the coarse fraction of the sediments is directly related to the lateral water circulation pattern existing in the estuary. Feldspar and mica contents are lowest in that part of the estuary where sea water dominates, and are highest where fresh-water discharge makes a contribution. Conversely, contents of quartz and carbonate are highest where sea-water dominates and lowest where fresh-water discharge has the greater influence.

The distribution of organic matter in the sediments is also related to the water circulation pattern. The highest content of organic carbon occurs in sediments rich in clay in areas where water circulation is negligible. These organic-rich sediments are black and smell of H_2S, suggesting anoxic reducing conditions.

The clay-mineral assemblage of the estuarine sediments is similar to the clay-mineral assemblage in soil and stream sediment in the source area. Illite is slightly more abundant than kaolinite, vermiculite occurs in lesser amounts, and mixed-layer clays are minor. No extensive transformation of the clay minerals occurs upon entry into the marine environment and there is no significant variation in the clay-mineral assemblage throughout the estuary. The major difference observed between the continental and estuarine clays is the expanding nature of the vermiculite of the estuarine clays as compared to the soil clays, where it is stable. The estuarine clay-mineral assemblage is controlled largely by the clay minerals generated by weathering in, and supplied by erosional processes from, the source area. The minor changes in the land-derived clays when released to the estuarine environment can be explained by halmyrolytic and early diagenetic reactions with sea-water.

The distribution and concentration of the transition metals and P_2O_5 in the muddy sediments are controlled largely by fine-grained detrital mineralogy, and to a lesser extent, by the abundance of organic matter. Highest Fe, V, Cr, Ni, Zn, Cu and P_2O_5 concentrations occur in stagnant areas, where organic-rich, clay-size sediment prevails. Mn and Ti are most highly concentrated in silt-

rich sediments in areas where fluvial discharge prevails and the water circulates relatively freely.

The concentrations of transition metals and organic carbon in the Genoa estuarine muds are similar to those in muds from fjords and large reducing marine basins such as the Black Sea. This tends to suggest that the restricted basinal areas of the estuary are not radically different from fjords in terms of the physical and chemical controls on sedimentation.

The formation of the coastal barrier at Mallacoota appears to be a result of the landward progradation of bar and spit-sand deposits during the Holocene. These Holocene deposits seem to be superimposed on semi-indurated sand-rock deposits of discontinuous lateral extent. It is suggested that the sand-rock deposits may be remnants of a former Pleistocene inner barrier, which was drowned during the rapid marine transgression that followed the last glacial epoch.

Lagoonal or restricted estuaries like Mallacoota Inlet are common all along the south coast of New South Wales. Sand thresholds (flood-tidal deltas) and late-Holocene barrier complexes seal-off these estuaries from the open sea, giving rise to similar depositional and hydrological patterns within them. Lagoonal estuaries can thus be characterized as basinal-lagoonal areas receiving predominantly muddy sediments, which are terminated at the seaward end by marine barrier-sand and threshold-sand deposits, and at the landward end by fluvial channel-sand or deltaic-sand deposits. Consequently, the Genoa River estuary can serve as a model (with respect to hydrology, and texture, mineralogy and geochemistry of sediments) for other estuaries in southern New South Wales and eastern Victoria.

INTRODUCTION

This study resulted from the formation of an Estuary Study Group within the Bureau of Mineral Resources. The Estuary Study Group was organized in 1970 by P. J. Cook of the Phosphate Group, following the completion of detailed investigations of the Cambrian phosphorites of the Georgina Basin in northwest Queensland. De Keyser and Cook (1972) considered that some of the Cambrian sediments of the Georgina Basin may have been deposited under estuarine conditions, and, since little was known about the distribution of phosphorus in estuaries, it was decided to investigate some modern estuarine environments in detail. Before the investigation began, it was apparent that in order to understand the mechanism controlling the distribution of phosphorus it was necessary to study a wide range of variables that may have influenced phosphorus concentrations, such as hydrology, grain size, clay mineralogy, biogenic activity, Holocene history, and major and trace element geochemistry. Consequently it was decided to make the investigations as comprehensive as possible.

Two estuaries were chosen for study: Broad Sound, a tropical estuary on the central Queensland coast, and Mallacoota Inlet, a temperate estuary in the southeastern corner of Victoria. These two estuaries were chosen because they have contrasting climates and because there is no significant supply of phosphorus, from domestic, agricultural or industrial effluent, into either of them. The Broad Sound study was undertaken entirely by Bureau of Mineral Resources personnel (Cook & Mayo, in press). The Mallacoota study forms the basis for this Bulletin, and was undertaken by the writer with the assistance of BMR personnel from time to time, as part of a Ph.D. project at the Australian National University.

Mallacoota Inlet, which is the estuary of the Genoa River (Fig. 1), is situated just south of the New South Wales/Victoria border. The Genoa-Wallagaraugh river system drains an area of 1950 km^2. Estimated average run-off from the drainage basin is 4.4 x 10^8 m^3/yr (New South Wales Water Conservation and Irrigation Commission, 1968).

The two townships within the drainage basin — Mallacoota, on the southwest shore of the estuary, and Genoa, 24 km inland from Mallacoota (Fig. 1) — are both small. Consequently the estuary is relatively unaltered and unpolluted by man. Mallacoota has a permanent population of less than 300, and is within Mallacoota National Park, which surrounds the estuary but does not include much of the estuary shoreline within its boundaries. Mallacoota is a popular resort area, and a large camping site occupies the southwest shore of the inlet. Genoa, with a permanent population of less than 25, serves as regional headquarters of the Victoria Forestry Commission, and for the supply of food, dry goods, and postal services to residents of Mallacoota and vicinity.

There are no major industries in the Genoa River drainage basin. Minor logging operations have been in existence in the eastern part of the Wallagaraugh catchment for some time, and logging operations have been intensified recently in conjunction with the wood-chip industry based at Eden, NSW. Sheep and cattle properties occupy a minor part of the total drainage area; the location of three of the larger properties, Nungatta, Wangarabell, and Rockton, is shown in Figure 1. Commercial fishing, in particular abalone fishing, is an important industry at Mallacoota. This industry is organized by the local divers and the Victorian Government, and care is exercised to ensure that abalone beds are not excessively exploited.

Hydrological and sedimentological studies were undertaken in the Genoa River estuary with the following objectives in mind:

1) to determine the hydrological parameters of the estuary, and the subsequent sedimentary response,

2) to delineate the changes that have occurred in the source material during transport from the continental environment, and during deposition as sediment in the marginal-marine environment of the estuary,

3) to characterize the various sedimentary environments within the estuary, and to delineate the processes governing the chemical and mineralogical changes occurring in the sediments within these environments,

4) to investigate factors likely to influence the distribution of phosphorus in the estuary.

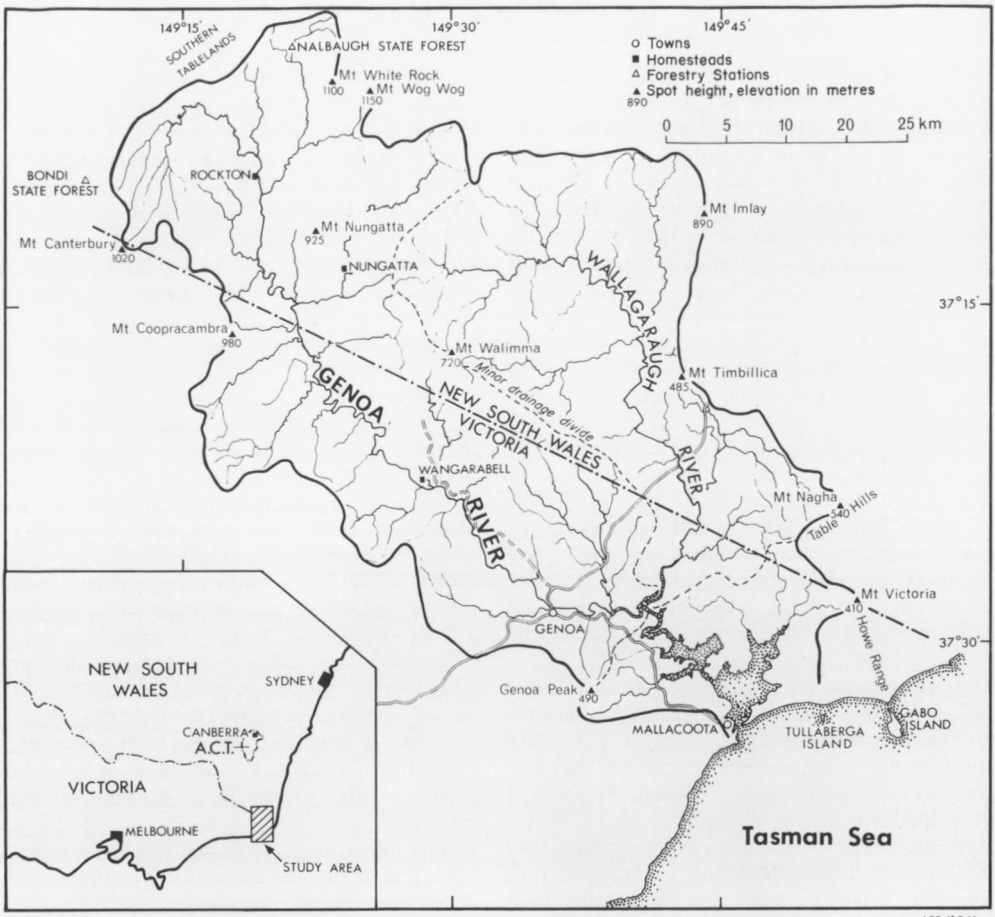

1. Mallacoota Inlet and Genoa River drainage basin

ACKNOWLEDGMENTS

This study was jointly supported by the Australian National University and the Bureau of Mineral Resources. The Australian National University supplied research facilities and supported the writer financially for three years through his tenure of an ANU Ph.D. Research Fellowship. The Bureau of Mineral Resources provided personnel and equipment during the field-work and some chemical analyses subsequently. I am grateful to Professor D. A. Brown and Mr J. N. Casey for supporting this project in their respective roles as Head of the Geology Department, ANU, and Assistant Director, Geological Branch, BMR. I am also deeply indebted to Dr P. J. Cook (BMR) and Dr K. A. W. Crook (ANU) who acted as joint Ph.D. supervisors, and gave valuable advice and assistance during the course of the study. Dr B. W. Chappell, Mr R. Freeman and Mrs M. Kaye, Department of Geology, ANU, aided the writer in the use of X-ray fluorescent analytical methods, Dr M. Sterns, Department of Chemistry, ANU, provided X-ray diffraction equipment for clay and silt analysis, and Mr W. Mayo (BMR), provided advice and expertise on sampling and statistical techniques. I wish to acknowledge a number of other individuals: in particular, Mr G. Taylor, with whom I had many fruitful discussions regarding modern sediment deposition, and Messrs R. Cliff, J. Morrow, J. Pennington and J. Wasik, all of ANU, whose logistic and technical assistance was greatly appreciated.

GENOA RIVER DRAINAGE BASIN

Climate

The climate in this region of southeast Australia is warm-temperate and subhumid according to the Koppen-Geiger classification (Strahler, 1969, plate 2). Mean annual precipitation is about 900 mm, and is fairly evenly distributed over the drainage basin. The eastern and northern margins of the catchment receive slightly more (1000 to 1100 mm), which is probably due to anomalous orographic features. Monthly rainfall is nearly evenly spread throughout the year. Monthly records indicate that at some gauging stations there is lower rainfall from July to November, but at others no such trend is evident. Snowfalls are fairly common during winter in upper regions of the drainage basin, above an elevation of 600 m.

Gabo Island has a mean annual temperature of 15°C, whereas at Nalbaugh and Bondi State Forests the mean annual temperature is about 10°C (Linforth, 1969; New South Wales Water Conservation and Irrigation Commission, 1968). The difference in mean minimum and mean maximum temperature is only about 6°C throughout the year at Gabo Island, whereas in the headwaters region the difference ranges from 10°C in June to about 15°C in January. Gabo Island has a mean monthly temperature ranging from 11°C in July to 18.6°C in February, whereas Nalbaugh State Forest has mean monthly temperatures ranging from 5°C in July to 17.5°C in January. From this data it is evident that significant seasonal change in temperature exists throughout most of the drainage basin except for the coastal areas. Generally, as elevation increases, so does the seasonal variation. Elevation and distance from maritime influence are the main factors that control minor temperature variations within the drainage basin.

Topography and vegetation

The Genoa River drainage system occupies predominantly mountainous terrain, the gently undulating areas being confined to the lower part of the catchment, around Genoa and Mallacoota Inlet.

The bulk of the vegetation in the drainage basin is sclerophyll forest characterized by species of *Eucalyptus* (Ashton, 1969). Understorey consists of abundant ferns and shrubs, and in coastal gullies and deeply incised creek areas undergrowth is dense. The entire drainage basin is covered by thick vegetation, except for those areas cleared by man, which comprise less than 5 percent of the total area of the basin.

Geology and soils

Previous geological investigations undertaken in this area have been mainly of a regional nature.

The Mallacoota 1 inch to 4 miles geological map published by the Geological Survey of New South Wales, and accompanying explanatory notes (Hall, 1959), and the Geological Survey of Victoria's Provisional Edition map (1:250 000) of the same Sheet area (1967), provided the basis for the more detailed map in this Bulletin (Fig. 2). Early geological investigations were conducted in this region by Carne (1897, 1898) and Dun (1897, 1898); these and subsequent works are dealt with at length by Hall (1959). More recent and detailed works, pertinent to this study, are those of Steiner (1966) and Gibson (1971). Steiner investigated the Devonian volcanic and sedimentary strata in the Eden-Pambula district, north of the drainage basin, and Gibson studied the surficial and solid geology of the upper part of the Genoa River drainage basin in conjunction with the present study (see also Reinson, 1973).

The geological age and areal distribution of the major rock types are shown in Figure 2. Ordovician metasediments are intruded by granitoid plutonic rocks of Middle Devonian(?) age. These are unconformably overlain by fluvial sediments of Late Devonian(?) age. Poorly consolidated Tertiary sediments unconformably overlie Ordovician sediments nearer the coast. Localized deposits of sand and mud of Quaternary age occur in low-lying areas of major stream channels, and on the coast. The stratigraphic succession is discussed in more detail by Hall (1959) and Gibson (1971).

Ordovician metasediments

Metasediments of Ordovician age are the most abundant rocks of sedimentary origin within the drainage basin. They are mainly fine-grained, low-grade metamorphics. Greenish-grey phyllites and slates predominate in the exposed sequences throughout the area, but interbeds of greywacke, siltstone, micaceous sandstone, and quartzite are common. Close to igneous contacts, micaceous schist and hornfels are present.

These Ordovician rocks are intensely folded and deformed, displaying numerous small-scale and large-scale structural features. These features are best seen in the coastal outcrops near Mallacoota, and around the shore of the estuary, which is surrounded almost entirely by steep cliffs of near-vertically dipping and tightly folded strata.

Steiner (1966), who informally termed these strata the 'Mallacoota Beds', noted that they crop out in a continuous belt adjacent to the coast from

Mallacoota northward to Eden with no significant variation in lithology and structure. Lithologically similar Ordovician strata crop out as isolated linear bodies in the drainage basin (Fig. 2), invariably situated between major igneous intrusions. Thin sections reveal that quartz and micaceous minerals (especially sericite), are the dominant minerals in these rocks. Feldspar occurs in lesser amounts. Biotite is absent, except in hornfels.

Devonian fluvial sediments

Fluvial sequences of Late Devonian(?) age are limited in areal extent within the drainage basin, and are confined mainly to the upper Genoa River area, although a few outcrops occur on the eastern boundary (Fig. 2). The strata on the Genoa River have been informally termed the 'Genoa River Beds' by Carne (1897) and Hall (1959), and on the basis of fossil plants Dun (1898) considered that these rocks may be correlated with Upper Devonian sediments in the Eden-Pambula district to the north.

The sequence as a whole consists of buff-coloured, arkosic conglomerate and sandstone interbedded with red mudstone, sandstone and siltstone. The Genoa River Beds, which exceed 270 m in thickness, consist of red mudstone overlain by interbedded, coarse arkosic sandstone and conglomerate (Gibson, 1971). The equivalent sequences on Mount Imlay and Mount Timbillica (Figs. 1 and 2), together are more than 760 m thick, and both the basal and uppermost beds are red mudstones (Hall, 1959). Coarse-grained clastic rocks, however, predominate over fine-grained varieties in all the outcrops observed in the study area.

2. Bedrock geology, Genoa River drainage basin

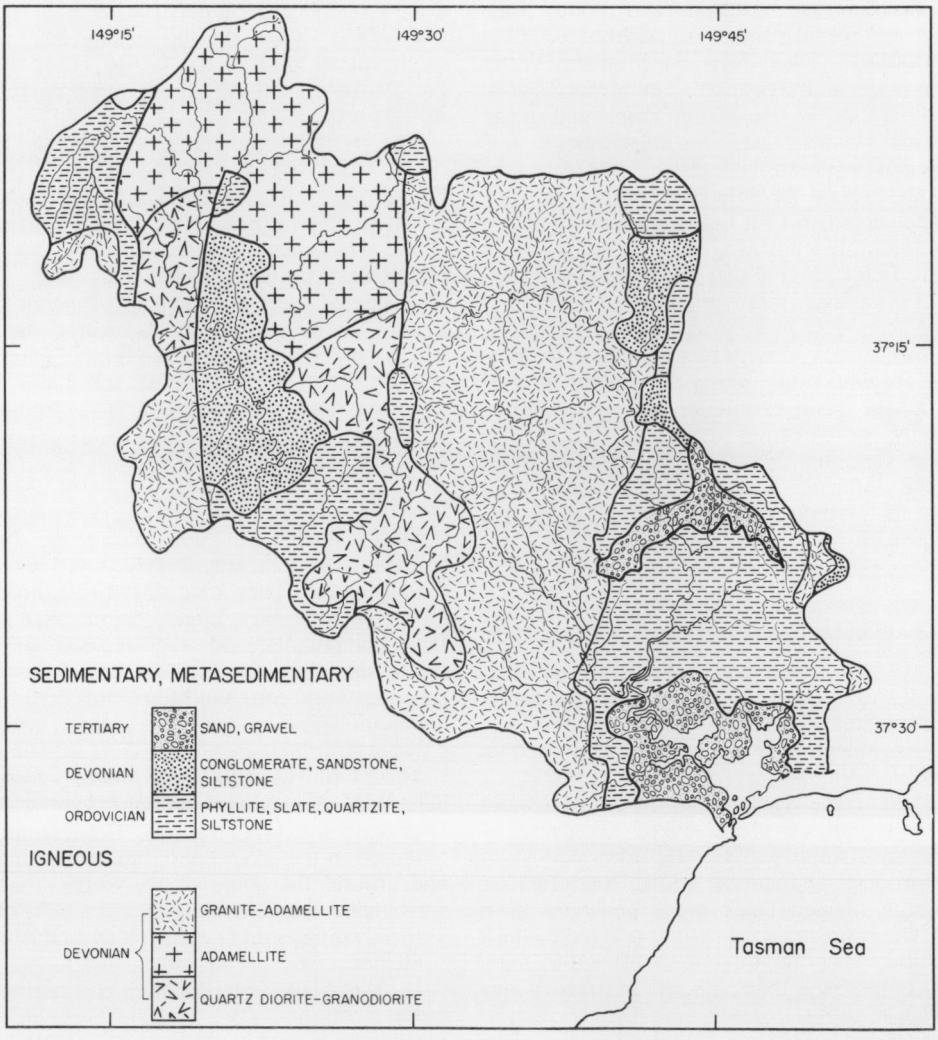

These Devonian strata are generally flat-lying or gently-dipping within the study-area, and form prominent, resistant cliffs in the Upper Genoa River area and along the eastern boundary of the drainage basin. The reader is referred to Steiner (1966) and Gibson (1971) for detailed stratigraphical and lithological descriptions of these and equivalent rocks in adjacent areas.

Tertiary sediments

Deposits of pre-Holocene, poorly-consolidated sediments resting on denuded surfaces of Devonian and older strata were tentatively given a Tertiary age by Hall (1959). These deposits are of very minor areal and vertical extent, and are confined to near-coastal areas of the drainage basin. Surficial deposits of sand and gravel, up to 30 m thick, occur in the lower Wallagaraugh River area near Mount Timbillica (Figs. 1 and 2). The hills around the Genoa River estuary are capped by up to 10 m of both unconsolidated and consolidated sediments. Loose sands and gravels are generally underlain by more resistant and highly ferruginous conglomerates and coarse sandstones. The Tertiary beds are considered by Hall (1959) and Steiner (1966) to represent fluvial and lacustrine deposits.

Devonian plutonic rocks

Most of the Genoa River drainage basin is underlain by granitoid plutonic rocks of the Bega Batholith. In the study-area this large composite batholith consists mainly of granite-adamellite, adamellite, and quartz diorite-granodiorite (Fig. 2). Gradations exist between these three granitoid intrusive rock types. Basic and acid dykes, and porphyry stocks are common within them. No attempt was made to map these minor intrusions, but the areal distribution of the three major intrusions was delineated as far as possible in the time available.

Granite-adamellite is the most abundant plutonic rock of the drainage basin. It is medium to coarse-grained, displaying typical granitic texture. Quartz content ranges from 25 to 48 percent. Potassium feldspar occurs mainly as microcline-perthite, but orthoclase is common also. The K-feldspar occurs as large anhedral, interstitial grains constituting 22 to 54 percent of the rock. Plagioclase is subhedral to euhedral, amounting to 15 to 28 percent in this rock-type. It ranges in composition from An_{10} to An_{45}, frequently falling in the intermediate oligoclase range (An_{16} to An_{26}). Biotite was found to be the only ferromagnesian mineral in the rock, and varies in abundance from 4 to 9 percent.

The adamellite rock unit is gradational in composition between granite-adamellite and quartz diorite-granodiorite, and occurs mainly in the Upper Genoa River area. It is medium to coarse-grained, and quartz content ranges from 27 to 45 percent. Potassium feldspar occurs mainly as perthitic microcline with lesser amounts of orthoclase, and forms 18 to 31 percent of the rock. Plagioclase occurs as subhedral to euhedral crystals with compositions from about An_{30} to An_{49}. The average composition is sodic andesine. Both hornblende and biotite occur in this rock-type, together amounting to 5 to 12 percent. Biotite is the dominant ferromagnesian; hornblende comprises less than 2 percent of the rock.

Quartz diorite/granodiorite in general has a major mineral composition lying close to the quartz diorite/granodiorite boundary. It is medium-grained, with quartz content ranging from 25 to 45 percent. Potassium feldspar, the least abundant of the three major constituents (2 to 18 percent) is usually untwinned, and of the orthoclase variety. Plagioclase commonly occurs as strongly zoned, subhedral to euhedral crystals, and ranges in composition about An_{25} to An_{60}, with an average composition in the An_{40} (intermediate andesine) range. The ferromagnesian minerals, biotite and hornblende, constitute up to 21 percent of the rock. Biotite is the more abundant, but hornblende can form up to 7 percent.

Soils

Red and yellow podzolic soils predominate throughout the drainage basin. The zone of weathered bedrock (or saprolitic zone) is thickly developed on all rocks except the highly resistant ridge-forming types. On granitoid bedrock, the solum (A and B horizons) is generally extensively developed, but on metasedimentary bedrock its thickness is highly variable. Solum cover is virtually absent on ridge-forming Ordovician quartzite and Devonian sandstone.

The processes of soil formation, soil-clay mineralogy, and the chemical weathering of various bedrocks in the Genoa drainage basin are discussed in detail elsewhere (Reinson, 1973, 1976).

ESTUARINE PHYSIOGRAPHY AND HYDROLOGY

MARITIME SETTING

The Genoa River estuary is located on a high-wave-energy coast, characterized by wave-cut cliffs and platforms in resistant bedrock, and by long curving beaches called 'surf beaches' by Bird (1964). The main ocean current, the East Australian current, moves southward along the coast but is some distance offshore and consequently has little effect on coastal morphology. Longshore drift in this area is to the northeast, as a result of the generation of longshore currents by northwest-directed wave action in the nearshore zone, and beach drifting in the surf zone.

The Mallacoota Inlet area is considered by Easton (1970) to be in the Eastern Australian tidal zone. The tides in this area are semi-diurnal with significant diurnal inequalities. The mean range of tide at Gabo Island is about 1.0 m at springs and 0.7 m at neaps (Easton, 1970, p. 165). Tidal range within the estuary is considerably less, because of the small entrance relative to the size of the body of water behind it (Fig. 3). Water level may vary about 0.7 m near the entrance, but over a tidal cycle is negligible in the central and upper parts of the estuary.

Winds have a significant effect on the water level

3. Aerial photograph of Genoa River estuary and hinterland, 1965; taken from elevation of 7600 m, by Royal Australian Air Force. (BMR Neg. No. GA 3934)

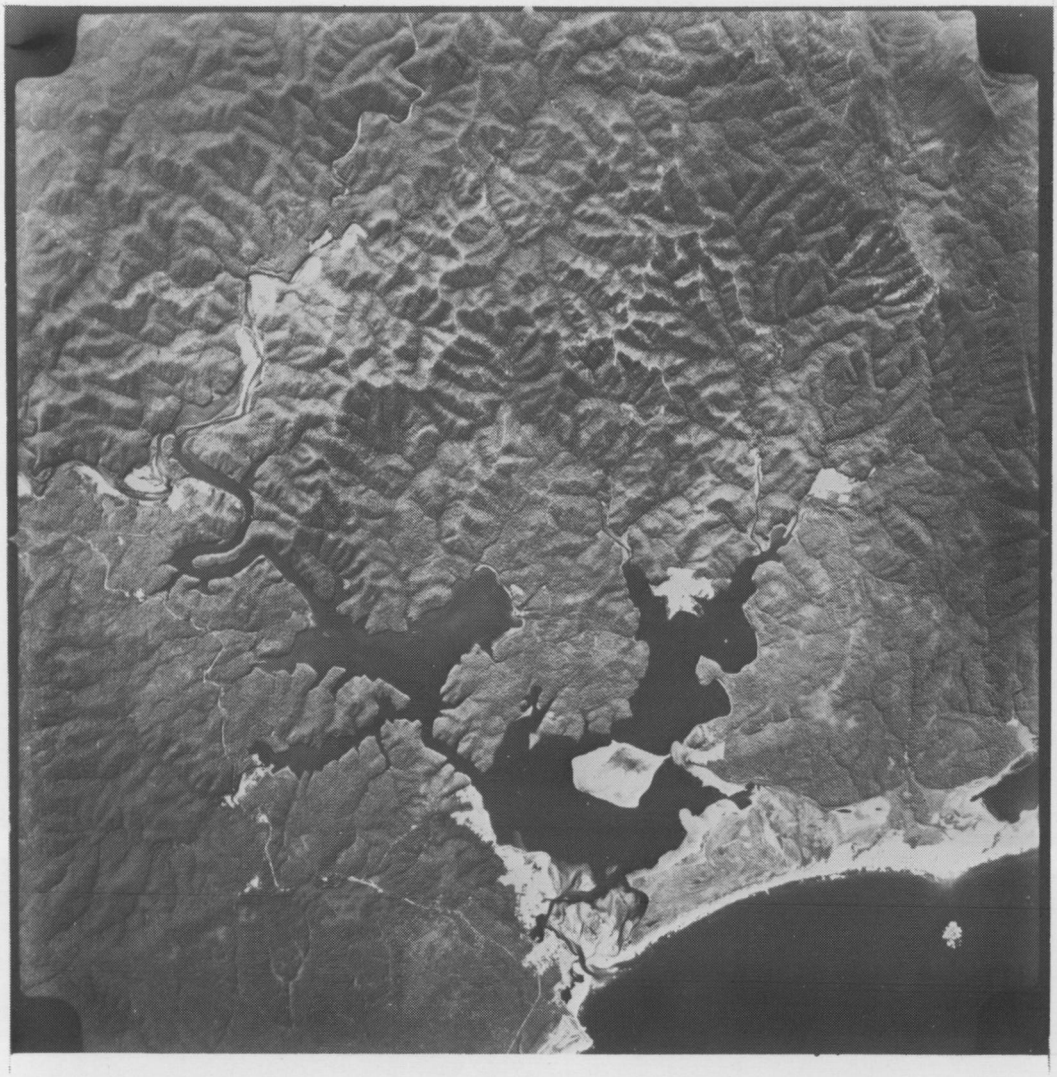

in the estuary, and on the water exchanged over a tidal cycle. Prolonged northerly winds may lower the relative water level as much as 1 m. Conversely, prolonged southerlies may raise it by a similar amount. Wind records from Gabo Island indicate that the dominant wind directions are from the northeast and southwest (Fig. 4). A seasonal pattern is evident, in that winds from the southwest are more dominant in the winter and spring. There is also a change to a predominant southwesterly wind in the afternoon, relative to morning wind directions, throughout the year (Fig. 4). Wind velocities are generally less than 30 knots,

4. Wind directions at Gabo Island, 1965-69. Twice-daily readings. Data supplied by Bureau of Meteorology

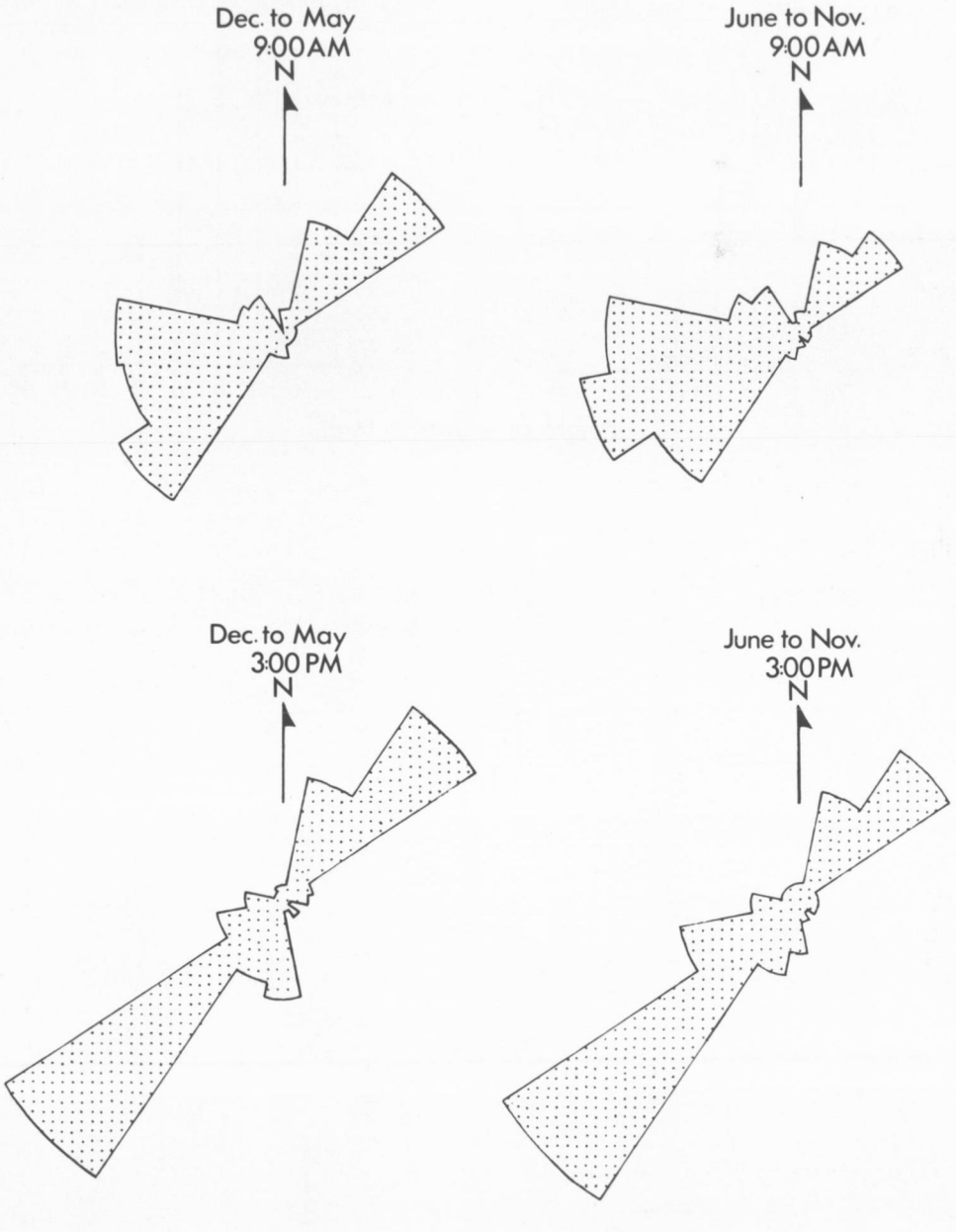

J55/A8/6

5. Sea and swell data, Gabo Island. Compiled from data supplied by Bureau of Meteorology

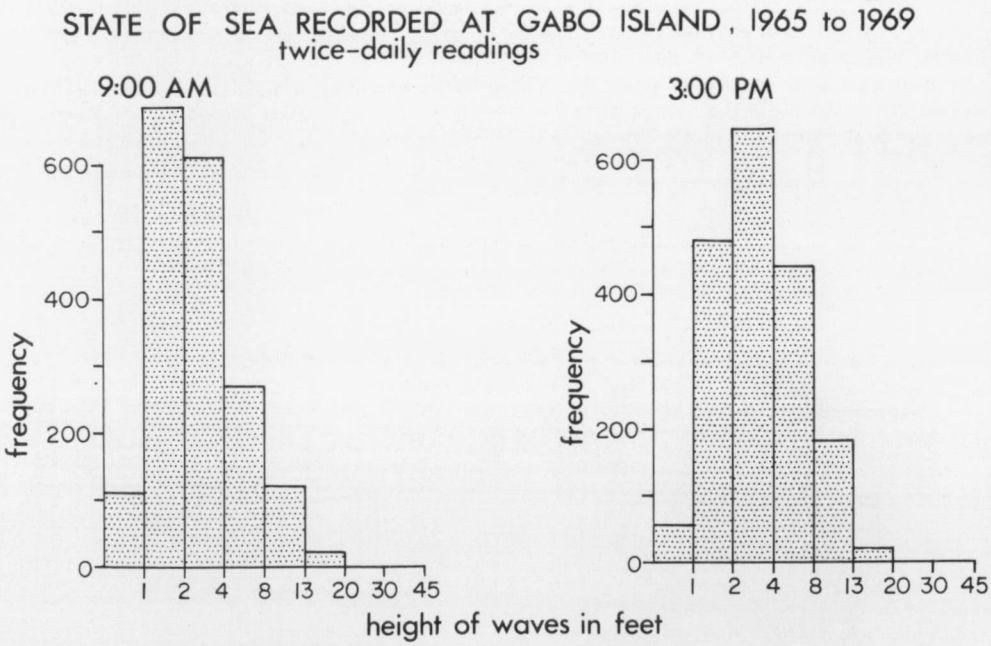

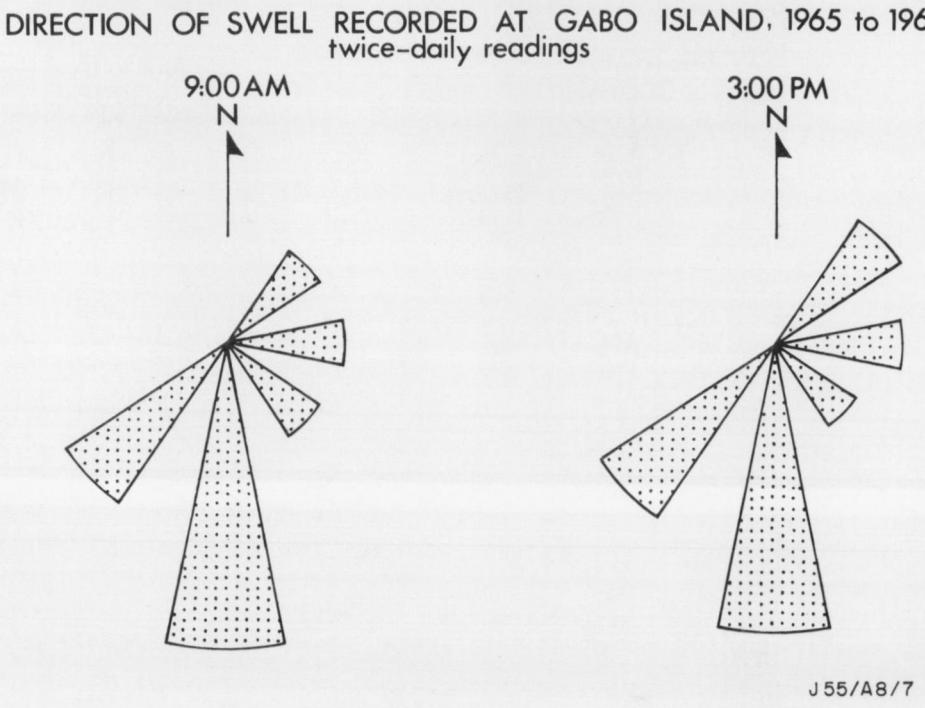

although higher velocities are more frequent in late winter and spring.

State of sea, and swell direction data collected at Gabo Island have been plotted in Figure 5. The state of the sea is dominantly smooth (wave height 1 to 2 ft) to slight (wave height 2 to 4 ft) in the morning, but changes to a slight to moderate sea (wave height 4 to 8 ft) by mid-afternoon. Rose diagrams of the direction from which swell is moving indicate dominant directions are south-southwest with very little diurnal variation. This substantiates the data plotted by Bird (1965, p. 27) for the years 1954-56, in which he reported a dominant southerly swell at Gabo Island. The swell in this area is generally a low swell of short or average length, or a swell of moderate height, with short to average length (Commonwealth Bureau of Meteorology, written communication).

River discharge data are scarce for this area. Only one gauging station, at Wangarabell (Fig. 1), has existed for any length of time. From the ten years of records accumulated, the average discharge of the Genoa is calculated to be 3.22 m^3/second (New South Wales Water Conservation and Irrigation Commission, 1968).

Physiography

Pritchard (1967) considers that there are four geomorphological types of estuaries: (1) drowned river valleys; (2) fjord-type estuaries; (3) bar-built estuaries, and (4) estuaries produced by tectonic processes. The fourth type is a catch-all term for estuaries which do not fit the other three types.

The bar-built estuary, as described by Pritchard (1967), forms when offshore barrier-sand islands and sand spits build above sea level and extend between headlands as a chain, broken by one or more inlets. The area enclosed by the barrier

6. Major geographic features, Mallacoota Inlet

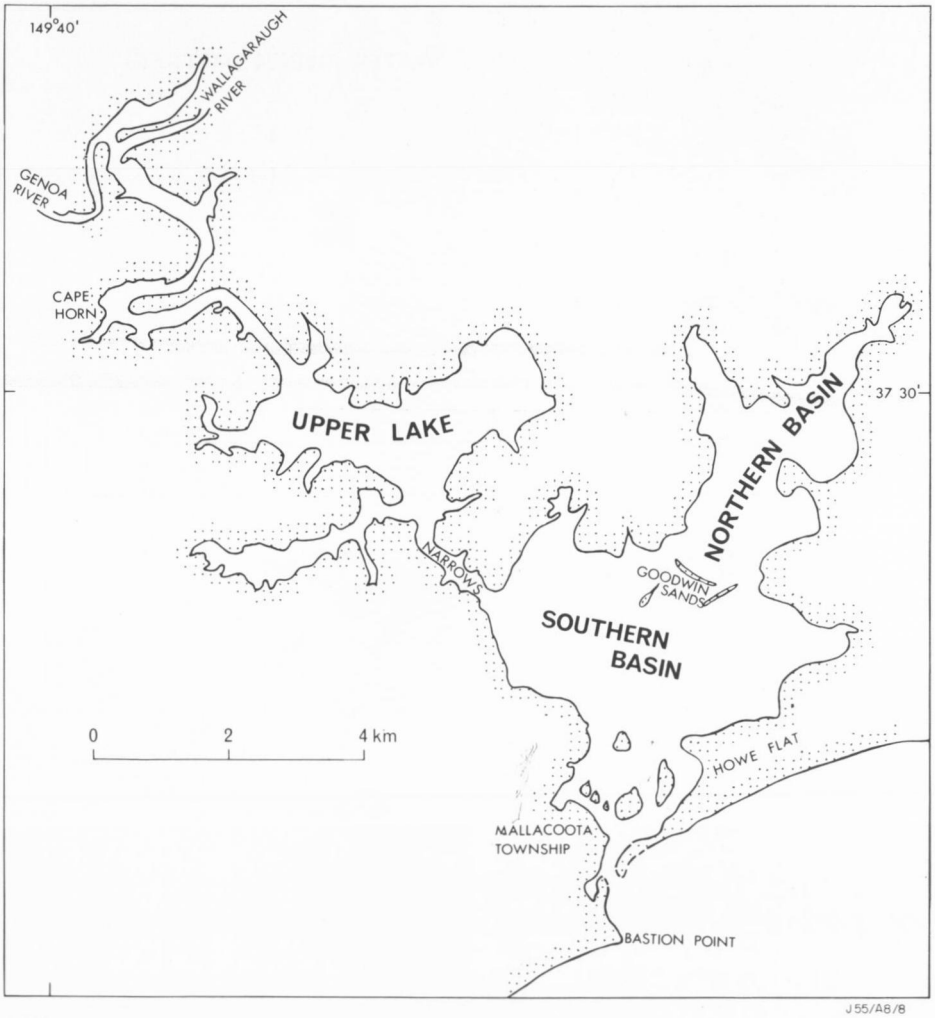

beaches is generally elongated parallel to the coastline. The bar-built estuary is often a composite system, because the lower valleys of the rivers entering it have frequently been drowned during the Holocene by rising sea level. The estuary then consists of an outer embayment partly enclosed by a barrier, and a drowned river valley or valleys. The channels connecting the bar-built estuary with the ocean are usually relatively small compared to the size of the sound within the barrier, and thus tidal action is reduced in such estuaries. Pritchard noted also that estuaries of this type are usually shallow and winds provide an important mixing mechanism.

The Genoa River estuary is a bar-built estuary, according to Pritchard's classification. It consists of an outer embayment partly enclosed by an extensive barrier-beach and dune-ridge complex, and a major drowned river valley with minor attendant ones in its upper reaches (Fig. 3). The estuary is separated into three large basins, referred to as the Northern Basin, Southern Basin and Upper Lake (Fig. 6). The three basins are interconnected by narrow passages. The basement topographic high on which the Goodwin Sands is situated isolates the Northern Basin almost completely from the Southern Basin. The Upper Lake is connected to the Southern Basin by the Narrows, a deep, narrow channel which has similar bathymetry and topography to that of the main river channel in the upper parts of the estuary (Fig. 7). This main river channel is narrow, has very irregular bedrock-controlled bottom topography, and is much deeper than the basinal areas. The water depth in the river channel is generally greater than 10 m (the deepest part is at Cape Horn, 22 m),

7. Bathymetry; datum, mean low water (modified from detailed bathymetric map compiled by P. J. Cook, BMR)

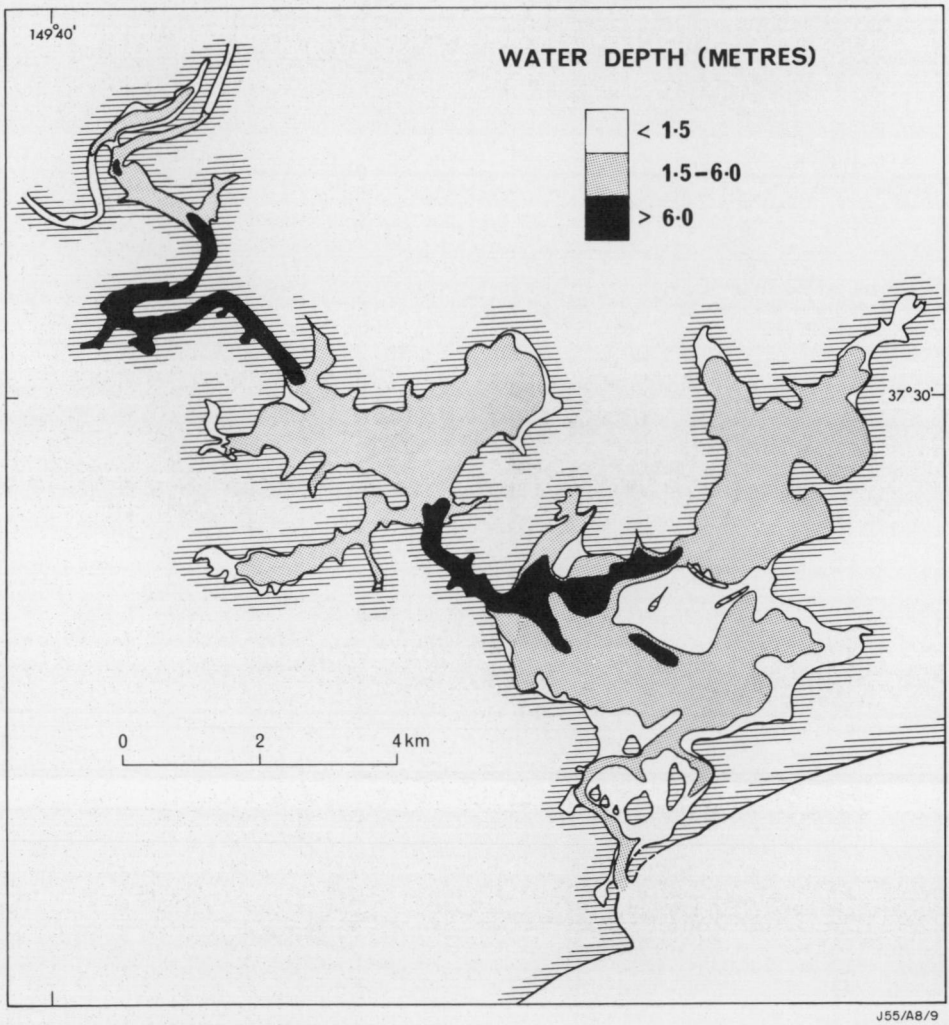

whereas the basinal areas are usually less than 6 m deep. The shallowest part of the estuary is at the seaward end where an extensive delta has formed immediately inside the entrance (cover photo) and shallow sand banks rim the inside of the coastal barrier.

Hydrography

Detailed hydrographic measurements were obtained from the estuary in order to determine the relationships between fresh water and sea water. The interaction of fresh water and sea water produces observable circulation patterns which directly and indirectly affect depositional environments and sediment distribution patterns. The dominant physical processes involved in the movement and mixing of water masses in an estuary are tides, and the inflow of river water. Bowden (1967) has discussed these two processes in detail, and has described four basic types of estuarine circulation based on the interaction of these two opposing forces. These are:

1) salt-wedge estuary, in which river discharge completely dominates the circulation;
2) two-layer flow with entrainment, in which river flow is modified somewhat by tidal currents;
3) two-layer flow with vertical mixing, in which river flow is mixed downwards and saline water upwards;
4) vertically homogeneous estuary, in which tidal currents are dominant over river flow, and there is no significant change in salinity from surface to bottom.

There are less dominant factors such as the

8. Hydrographic sampling stations. Line joining stations is location of axial profiles of salinity, temperature, and suspended sediment (Figs 9, 10, 14, 15, 16)

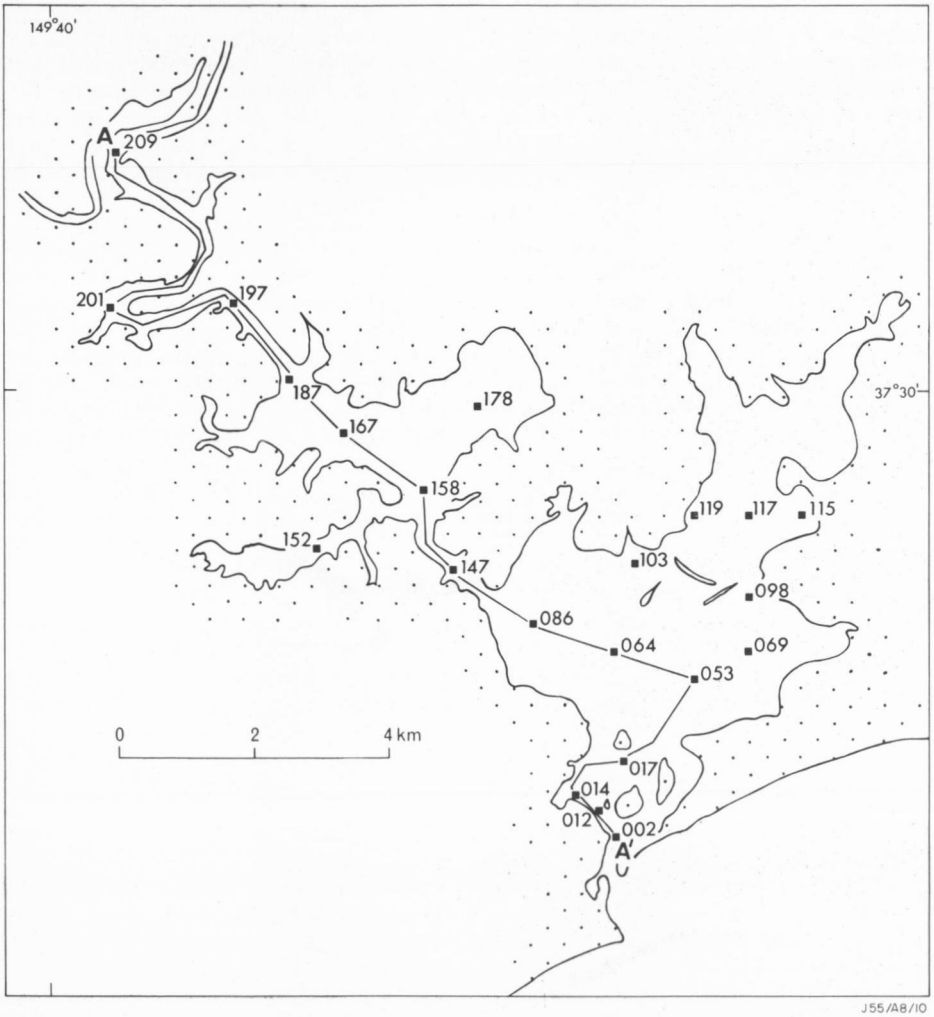

physical dimensions of the estuary, wind, and the effect of the earth's rotation represented by the Coriolis force, which affect the interaction of tidal forces and river flow to some degree (Bowden, 1967). Lateral variation in mixing of waters can also occur in an estuary and this depends largely on the size and three-dimensional shape of the estuary.

Field and laboratory methods

Hydrographic measurements were obtained during the major field season, from November 1970 to April 1971. Additional data were collected during August 1971. Twenty-two hydrographic stations were established in the estuary, and were marked by buoys or adjacent shore markers, so that they could be reoccupied from time to time (Fig. 8). During the major field season, salinity measurements were obtained by measuring the electrical conductivity of water samples which had been collected and stored in polyethylene bottles. Conductivity readings were made in a field laboratory with a Philips conductivity meter. Temperature readings were taken in situ, with a Hydrotemp thermister. In August 1971 a Beckman induction salinometer was used to measure temperature and conductivity in situ. All conductivity instruments were calibrated using standard sea water (Copenhagen water). Conductivity in micromhos was converted to salinity in parts per thousand (‰), by using graphs constructed from salinity-conductivity data in Horne (1969, p. 487). Current-velocity measurements were made with a rotation current meter of a type described by Horrer (1967). Suspended-solid concentrations were obtained by filtering one-litre water samples through 0.45 μm membrane-filters following the procedures described by Banse et al. (1963).

The initial hydrographic sampling program was set up in the estuary, to obtain a three-dimensional view of water circulation through time. This required all hydrographic stations to be occupied repeatedly, and at least some of them simultaneously, through a complete tidal cycle. Each hydrographic station was reoccupied every 2 hours over a 14-hour period, and three stations were sampled simultaneously by three field crews in small boats. The Southern Basin was sampled on 2 December, the Upper Lake on 3 December, and the upper main river channel on 4 December 1970. The hydrographic data collected over the three days were combined to give an overall picture of circulation throughout the estuary. This type of approach is similar to one described by Hartwell (1970).

Subsequent salinity, temperature, and suspended-load profiles were obtained only at high water, because the changes in stratification were not significant over a tidal cycle except near the seaward end of the estuary.

Salinity stratification and water circulation

Figure 9 depicts various profiles of the salinity stratification existing in the water column, along the axis of the main estuarine channel, over a tidal cycle. It can be seen clearly that the Genoa River estuary is well stratified and, except in the area near the estuary mouth, the water column consists of two layers throughout the tidal cycle. At high water a small salt wedge intrudes over the delta, but the two-layer stratification remains unmodified over a tidal cycle throughout most of the estuary.

The salinity profiles in Figure 9 were taken when river discharge was about 1 m^3/s at Wangarabell (E. E. Bibra, written communication), which is well below the average discharge of 3.22 m^3/s. Figure 10 shows the salinity stratification along the main axis, on 5 January 1971, when river discharge was near normal. It is evident from Figures 9 and 10 that the vertical variation in salinity becomes more pronounced, the upper fresher water layer is thicker, and the boundary between the two water masses is sharper, when river discharge is higher.

Figure 10 also shows the salinity stratification existing in the estuary in August 1971, a period of abnormally low river discharge. The two-layer flow system still exists, but the boundary across the layers is more diffuse, and more vertical mixing occurs throughout the water column.

Two extreme floods occurred during the summer of 1970-71, on 10 December 1970, and 6 February 1971. Rainfall measurements on and about these dates were the highest ever recorded for the area. This resulted in a peak river discharge at Wangarabell of 619.5 m^3/s on 10 December 1970 and a discharge of 622.4 m^3/s at half river-flood stage on 6 February 1971 (E. E. Bibra, written communication). The February flood eventually reached a height of 13 m at the gauging station. Hydrographic measurements were taken in the estuary on 10 December at about high tide, and as soon as physically possible after the February flood. Salinity profiles are plotted in Figure 10. The two-layer system still existed in the lower part of the estuary. A sea-water lens remained in the deepest parts of the lower estuary, because of the configuration of the bottom there. As the fresher-water layer increased in volume and velocity, it entrained most of the existing lower sea water, but did not remove the sea water right at the bottom of the water column.

In summary, the vertical circulation pattern consists essentially of a two-layer flow system with entrainment of salt water into the upper, seaward-moving layer. The configuration of the bottom of the estuary assists in maintaining this two-layer

system in that the intruding sea water tends to sink down slopes into topographic lows, and due to slow movement upstream, is entrained in the opposite-moving upper layer as it rises up-slope on the other side (Fig. 11). The deepest parts of the water column may remain undisturbed for periods of several months or more. The salinity of the upper fresh-water layer depends on the magnitude of discharge. When discharge is high, entrainment of lower salt water increases. When discharge is lower, the estuarine circulation pattern still resembles a two-layer flow system but vertical mixing occurs throughout the water column, especially near the seaward end of the estuary. During stages of exceptionally high river discharge, sea water is still not flushed completely from the estuary. Gross entrainment of sea water into the column of seaward-moving fresher water occurs, but because of the shape of the bottom, a small lens of salt water still remains in the Narrows and Southern Basin of the estuary.

Water circulation is shown in three dimensions in Figure 12. A complex lateral circulation pattern exists in the estuary. When sea water intrudes, it is channelled northwards owing to the physical restrictions imposed on it by the narrow entrance. Deflection by the seaward-flowing, fresher-water

9. Salinity variations, December 1970, along axis of main estuarine channel $^{o}/_{oo}$

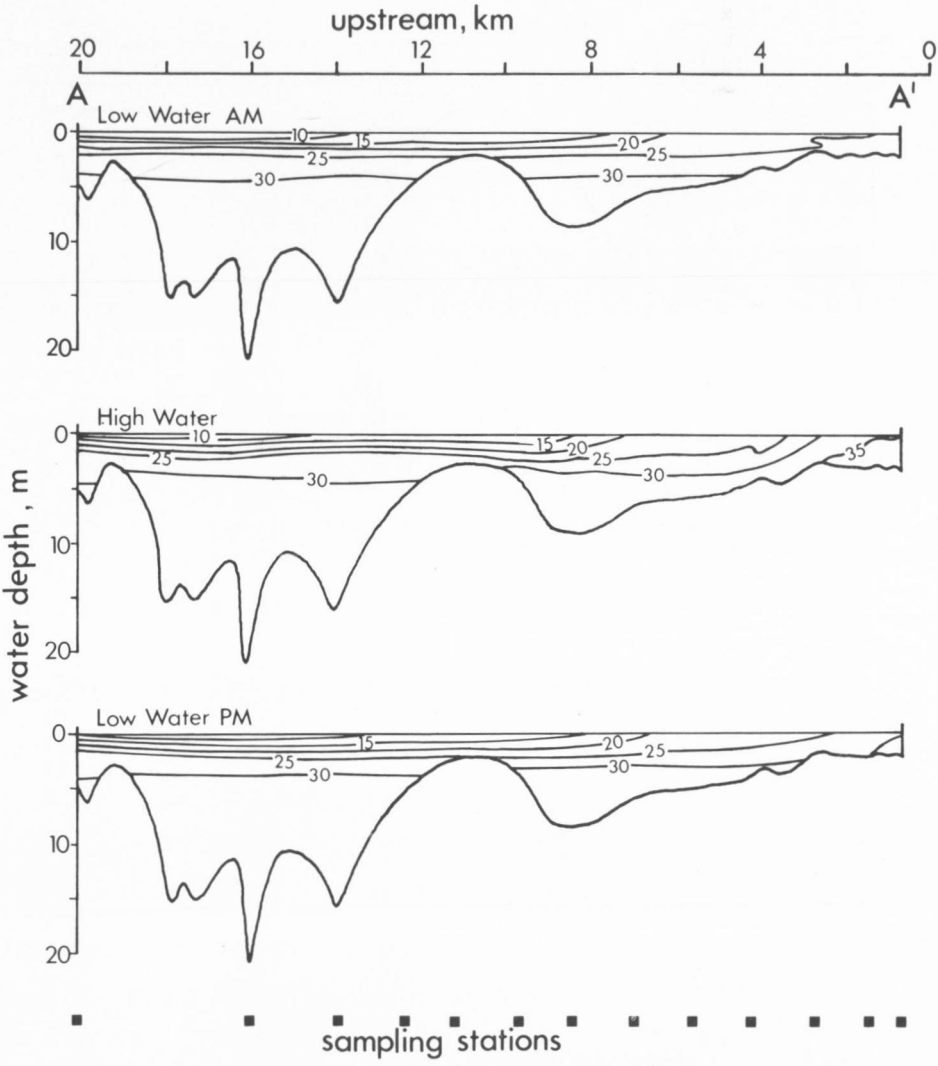

J55/A8/11

10. Salinity variations at high water, axis of main estuarine channel $^{0}/_{00}$

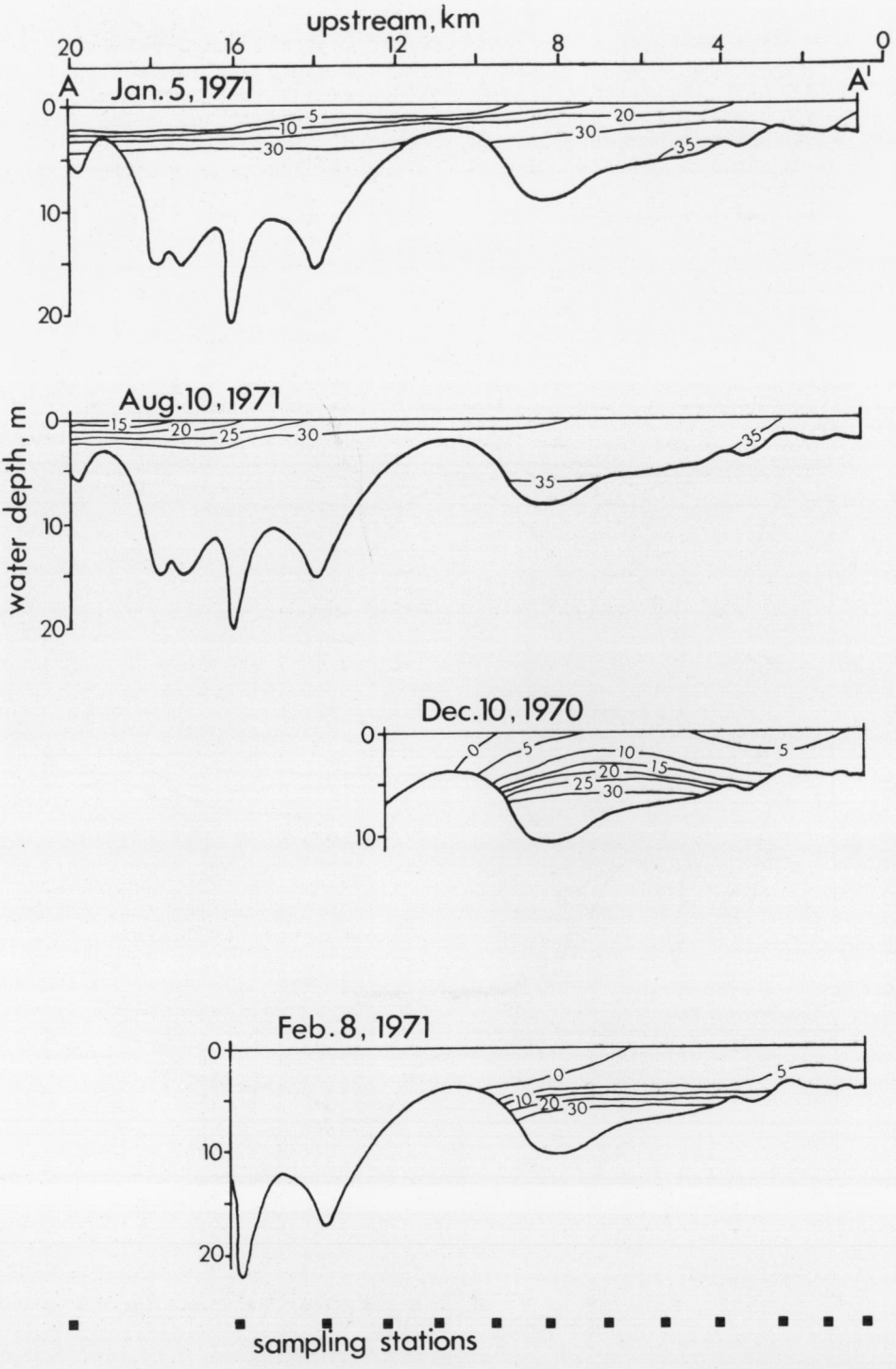

J55/A8/12

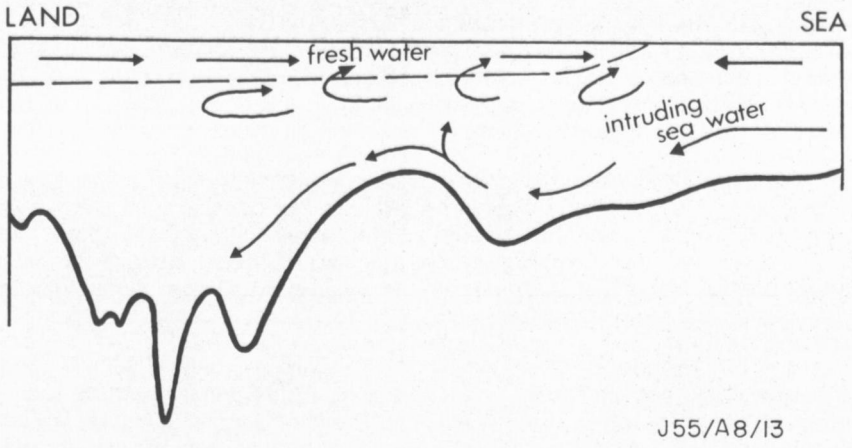

11. Schematic profile showing pattern of vertical water circulation along the axis of the principal route of water movement

12. Salinity stratification profiles, high water. Composite of data collected 2-3 December, 1970. The curved, dotted and dashed lines in the Upper Lake and Southern Basin demarcate the lateral extent respectively of saltier water at depth and fresher water near the surface

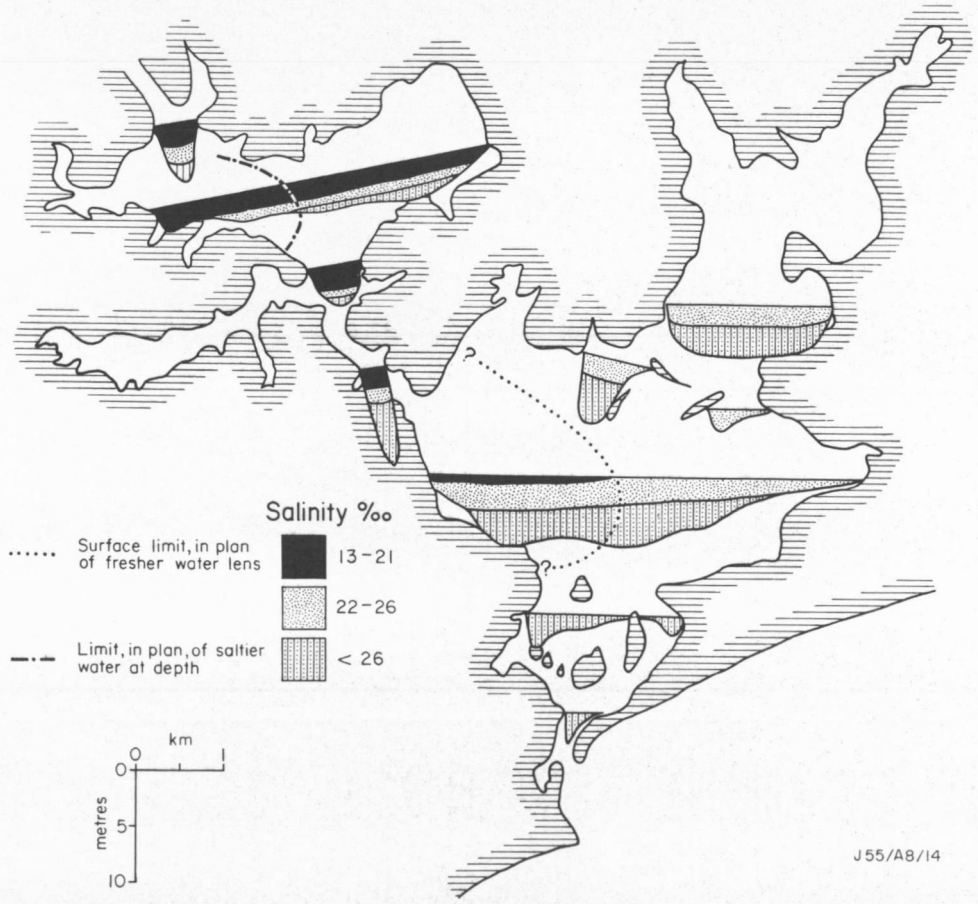

layer also occurs. The denser sea water sinks as a wedge into deeper areas, and as it forces its way farther upstream, a secondary deflection occurs in the Upper Lake. Intruding sea water is again deflected to the right side by the surface fresh water and the direction of the channel.

A similar three-dimensional view of the estuary, during the extreme runoff period of 8 February 1971, is depicted in Figure 13. This shows that the residual lens of sea water was confined to the deepest parts of the Northern Basin, Narrows and Southern Basin, while the rest of the estuary was virtually devoid of sea water.

It is evident that the Genoa River estuary is well stratified throughout the year and consists of a two-layer flow system with entrainment of salt water into the upper layer. Magnitude of river discharge governs the degree of demarcation of the two layers, and the amount of sea water entrained in the upper layer. Bottom topography, magnitude of river discharge, and physical dimensions and shape of the estuary, are the dominant factors controlling water circulation.

Water temperature

Profiles of temperature distribution in the water column along the axis of the main channel are plotted in Figures 14 and 15. In summer, the variation in temperature over a tidal cycle is negligible except near the entrance to the estuary, where there is intrusion of colder sea water at high tide (Fig. 14). The temperature decreases down the water column, reflecting the salinity stratification, with warmer fresher water at the top and colder more saline water below. In mid to late afternoon, surface waters become warmer due to solar heating.

The winter profile (Fig. 15) illustrates the seasonal variation in temperature of both the fresh water and sea water in this area. The intruding sea water is warmer than the existing waters in the lower half of the estuary, and in the upper half

13. Salinity stratification, high water, 8 February 1971, showing effect of an extreme flood in the catchment area

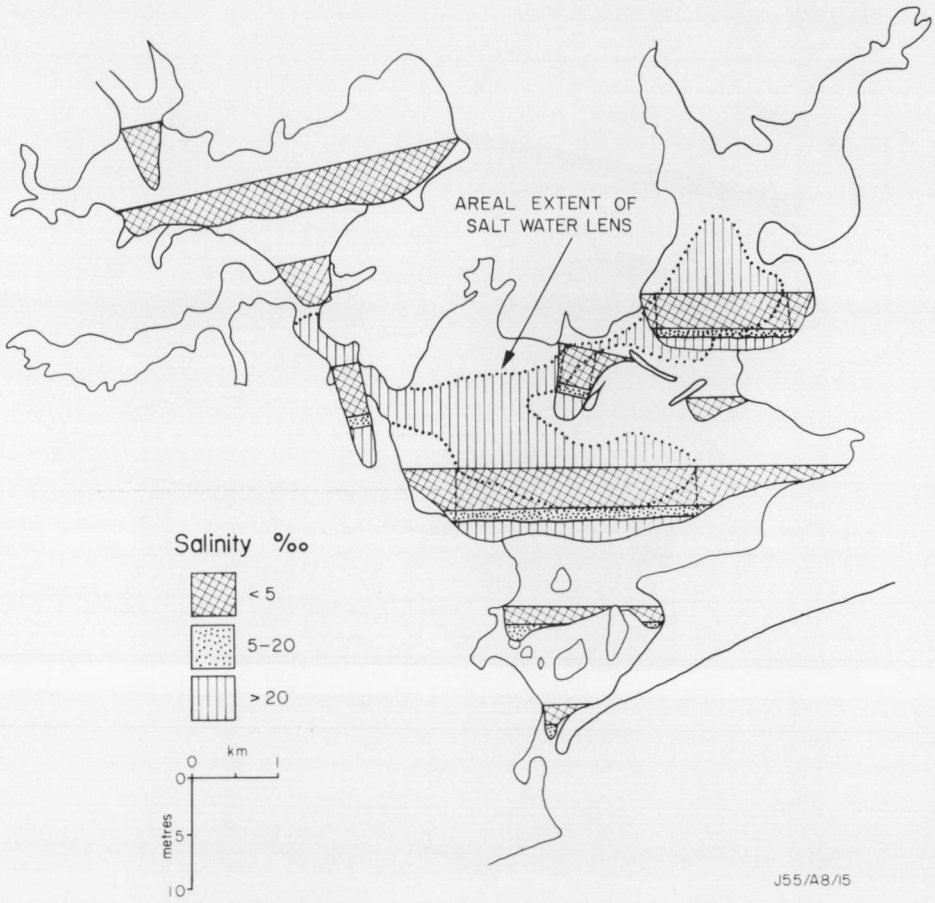

there is no significant change in temperature throughout the water column. It appears that some of the thermal energy of the upper part of the water column, in the seaward half of the estuary, may be lost to the colder atmosphere, while in the lower part, heat is stored.

The temperature distribution essentially reflects the salinity stratification.

Suspended sediment

Suspended sediment data obtained over a tidal cycle (Fig. 16) show that sea water is relatively low in suspended solids relative to fresh water. The profile of 5 January 1971 also substantiates this (Fig. 15). Intruding sea water has concentrations in the order of 2 mg/l, whereas fresh water carries up to 35 mg/l during periods of normal discharge.

Variations in concentrations of suspended solids appear to be negligible over a tidal cycle, except near the entrance, where sea water intrudes. Relatively high concentrations of suspended material occur in the deepest parts of the main channel (Fig. 16), but this may be due to contamination caused by disturbance of bottom sediment at time of sampling. It was difficult to

14. Distribution and fluctuations of temperature (°C) over a tidal cycle, 2-4 December 1970, along axis of main channel (Fig.8)

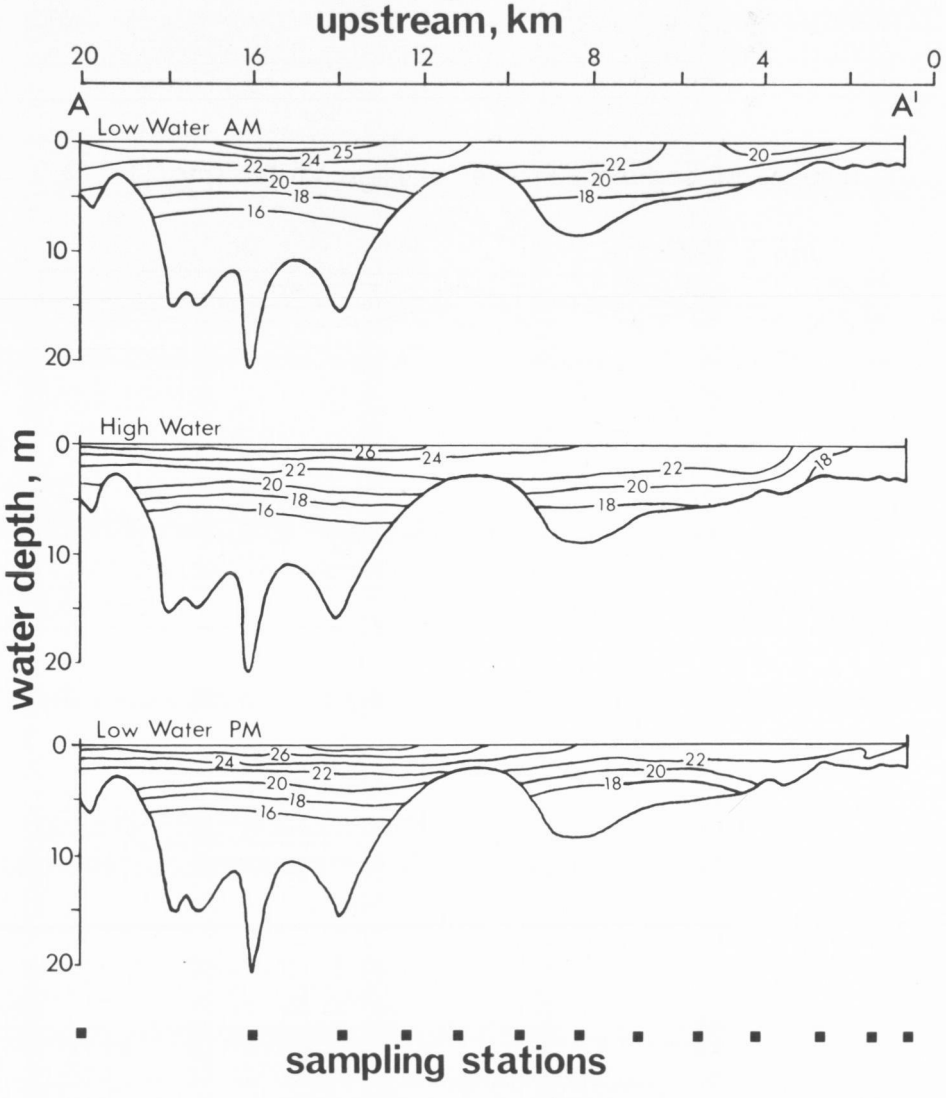

J55/A8/16

15. Winter temperature profile and summer suspended-sediment profiles, along axis of main channel (Fig. 8)

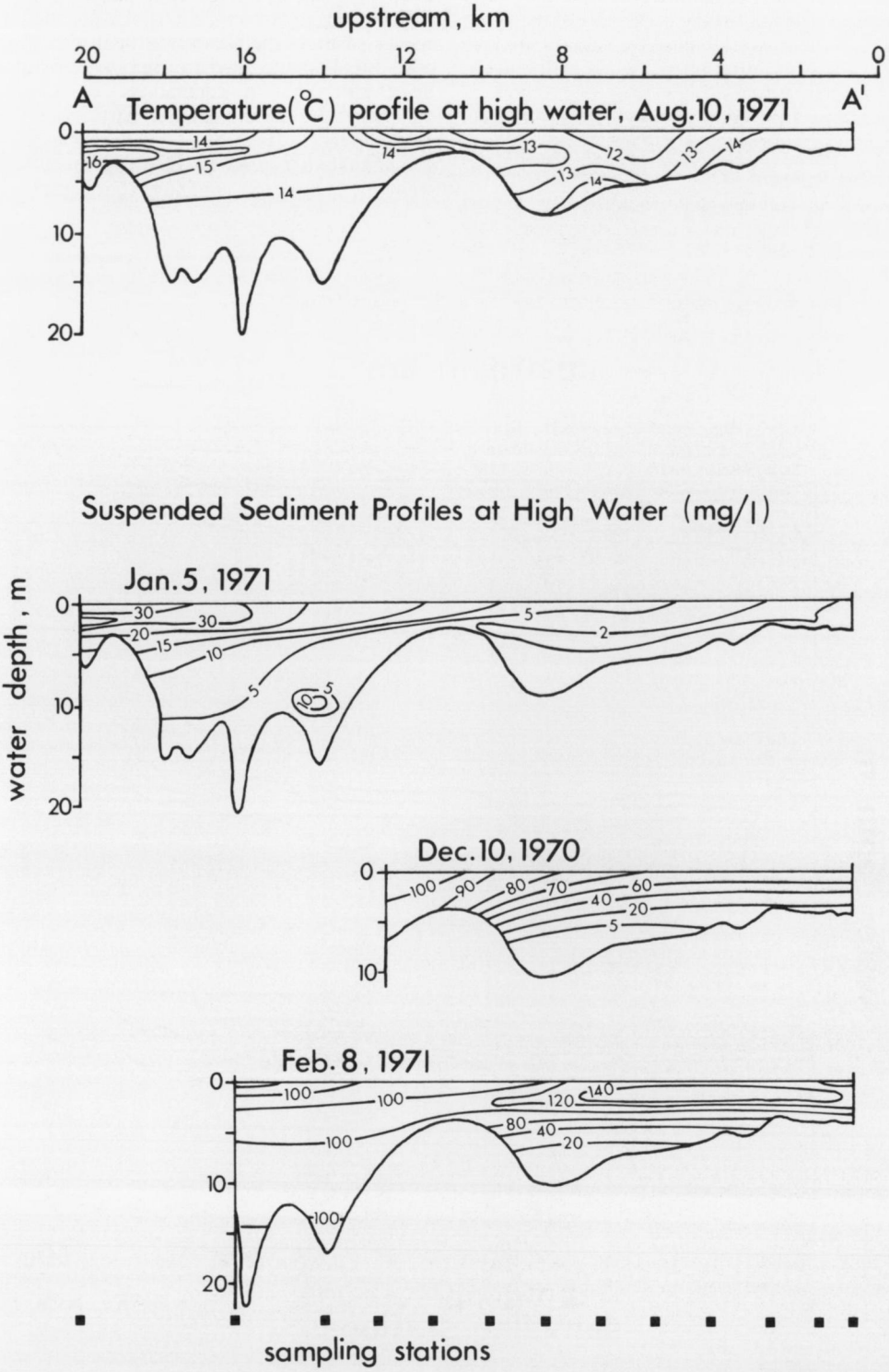

J55/A8/17

lower the sampling device without disturbing the bottom in the physically restricted 'deeps'.

The suspended sediment profiles of 10 December 1970 and 8 February 1971 (Fig. 15) emphasize the effects of extreme fresh-water discharge throughout the entire estuary. The suspended load concentrations at this time were more than five times normal. However, the residual lens of sea water is clearly delineated by the abrupt decrease in suspended solids in the lower part of the water column.

In general, the suspended-sediment profiles correspond to the well stratified horizontal two-layer water system existing in the estuary, as depicted by both salinity and temperature measurements.

Velocity and direction of water currents

Current velocities were too low to measure in many parts of the estuary, particularly in the extensive basinal areas. In the narrow channel-

16. Distribution and fluctuations in suspended sediment (mg/l) over tidal cycle, 2-4 December 1970, along axis of main channel

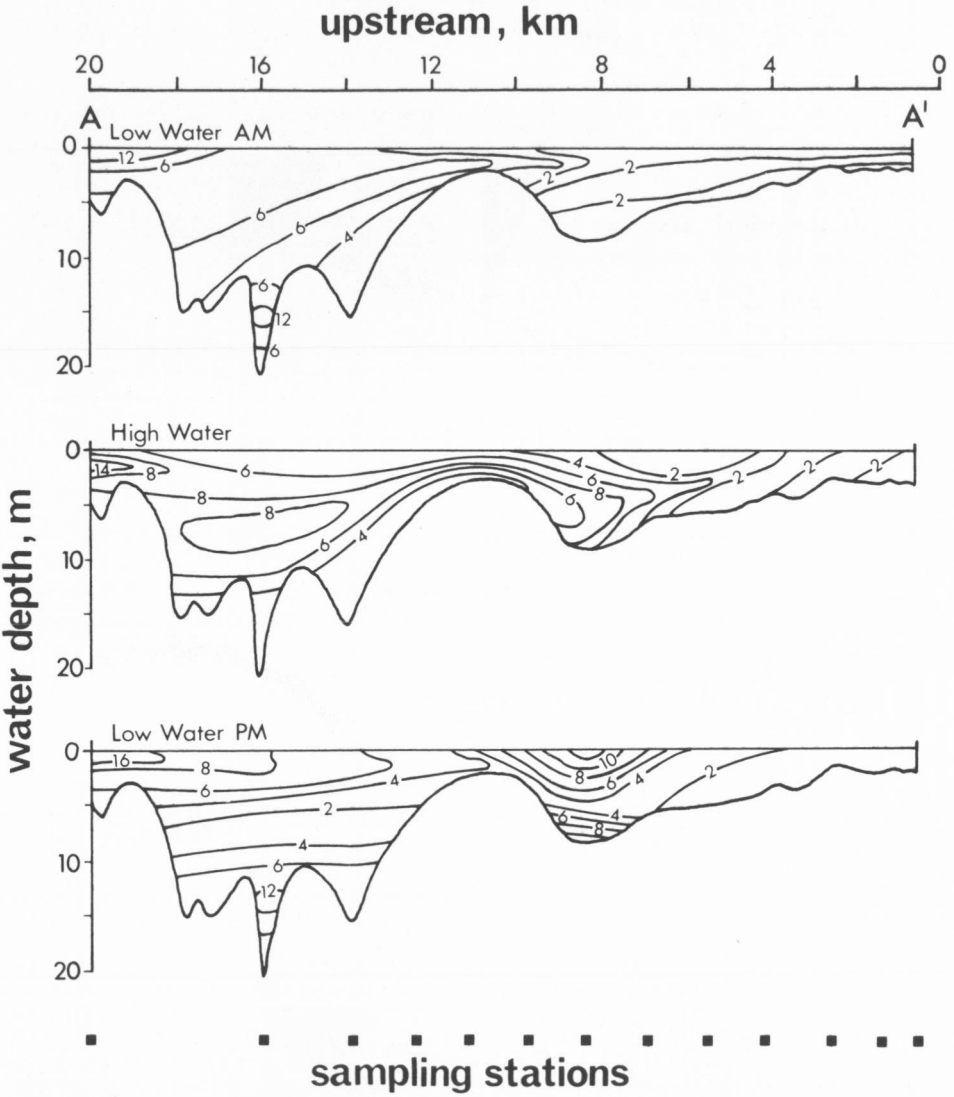

J55/A8/18

17. **Current velocities at various depths over a tidal cycle in the Narrows (147), in the Southern Basin (053), and on the delta (012). Figure 8 shows location of sampling stations**

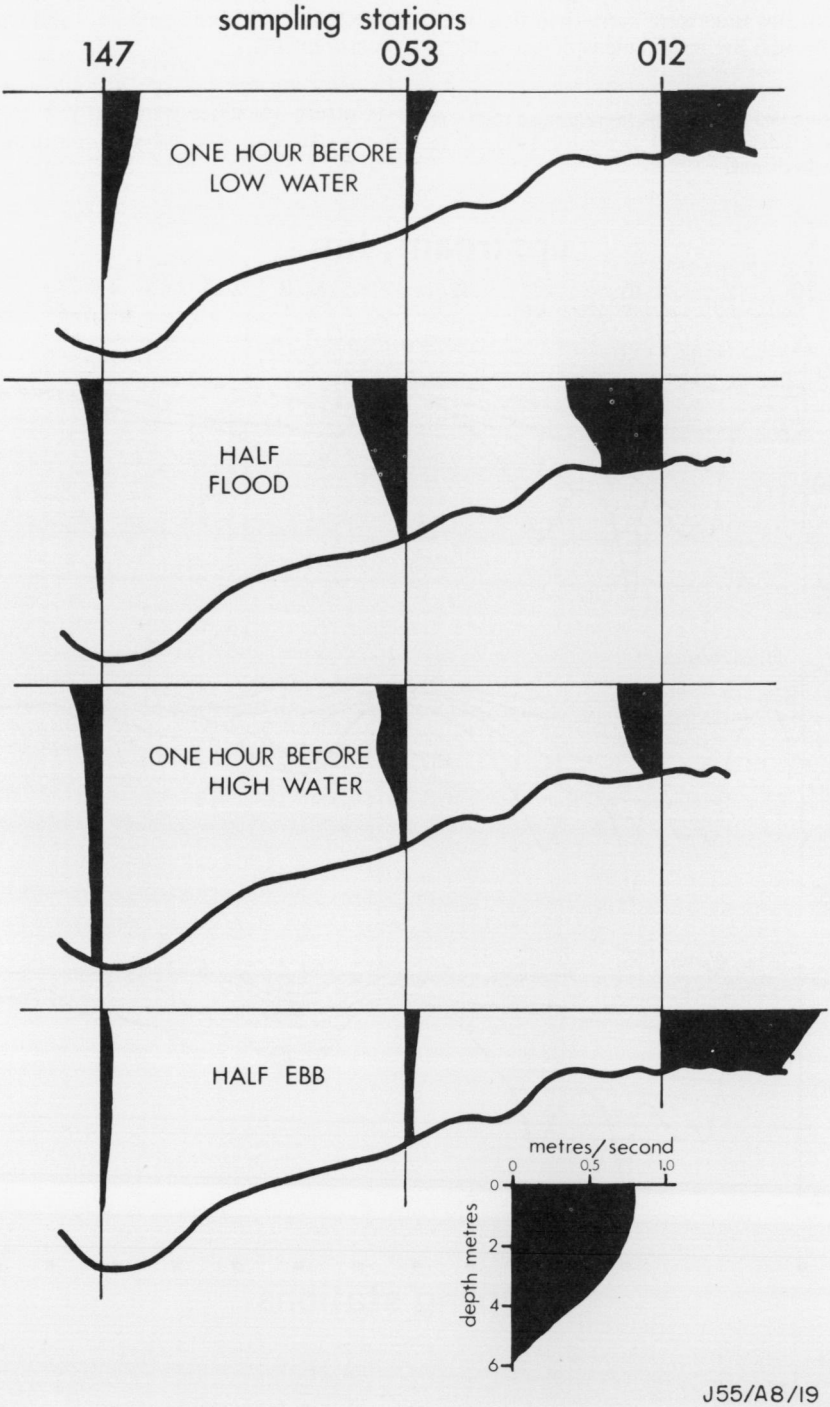

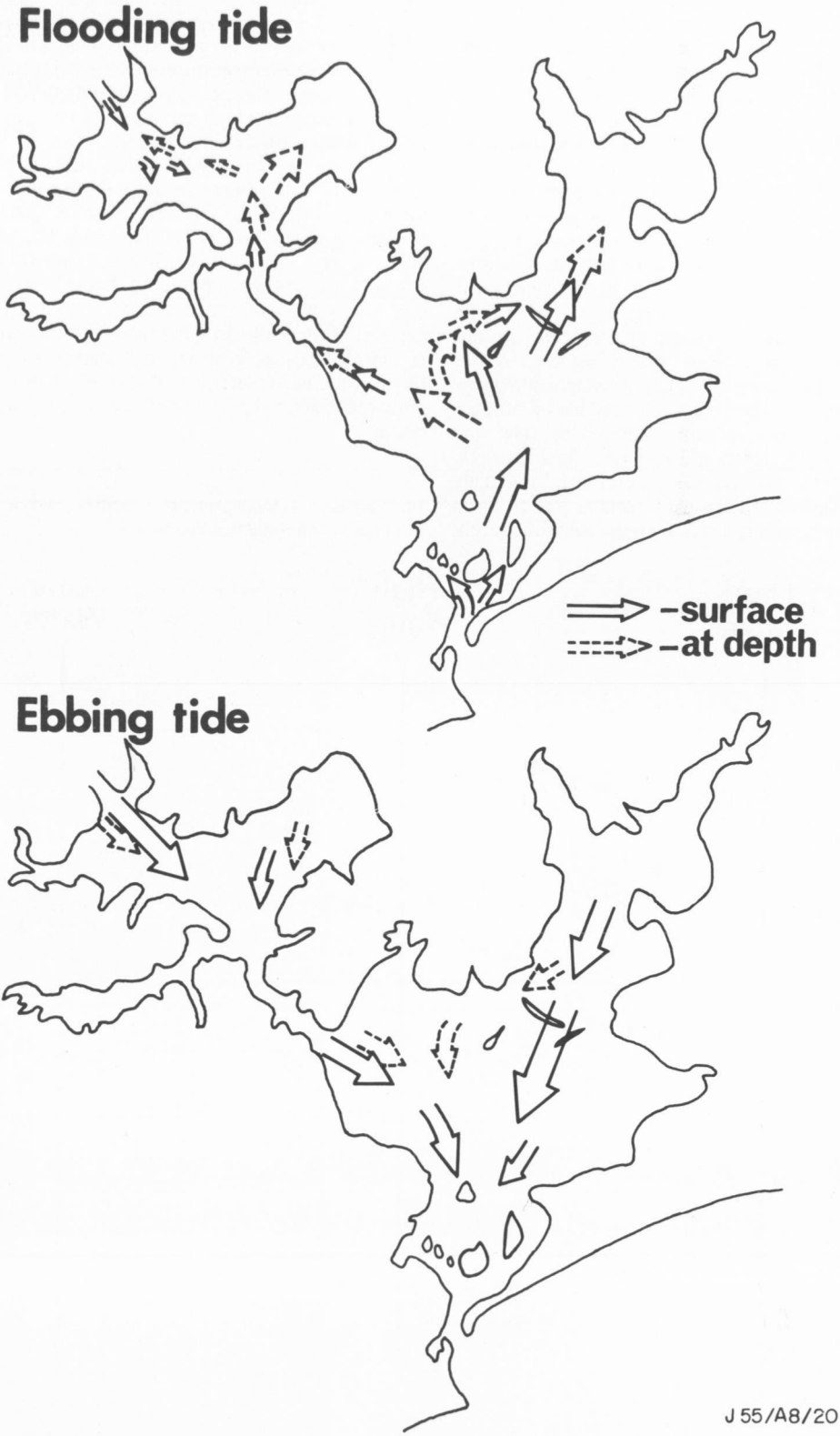

18. Current directions during flood and ebb tides (derived from daily observations of surface waters, current-meter readings, aerial photographs, salinity and temperature data)

ways, velocities are higher, and significant variations can be measured. Figure 17 shows the variation in current velocity through a tidal cycle from three stations along the main axis of water movement. Tide poles were read at each station, so that comparison could be made of the currents at each station during the same phase in the tidal cycle. These profiles indicate how tidal currents generate motion and are dissipated upstream.

The velocity of water is highest in the delta area where tidal influence is greatest. In the deeper parts of the estuary most of the water movement occurs near the top of the water column, and in this respect, vertical current-velocity patterns reflect the same two-layer stratification system shown by salinity, temperature and suspended-load profiles.

Directions of currents generated by tidal and river-discharge forces are illustrated in Figure 18. This current pattern was determined from daily observations of the estuary surface waters, from directional readings taken with the rotation current meter, from various aerial photographs, and from the salinity and temperature data. Distribution of textural types, carbonate and light minerals in the bottom sediments (which are discussed later) reflect this circulation pattern.

Currents in the delta area are slightly asymmetric with respect to time, during the tidal cycle (Fig. 19). Flood current velocities rise to a maximum about one hour after mid-tide, when most of the intertidal sands are covered. Ebb currents are strongest about 1.5 hours after mid-ebb, when most of the intertidal sand areas are exposed. This results in a net landward movement of marine detritus, which is reflected in the bed-forms (discussed later), and accounts for the observed shallowing of the seaward end of the estuary.

19. Time-asymmetry of current velocities, over a tidal cycle at two stations in the estuary

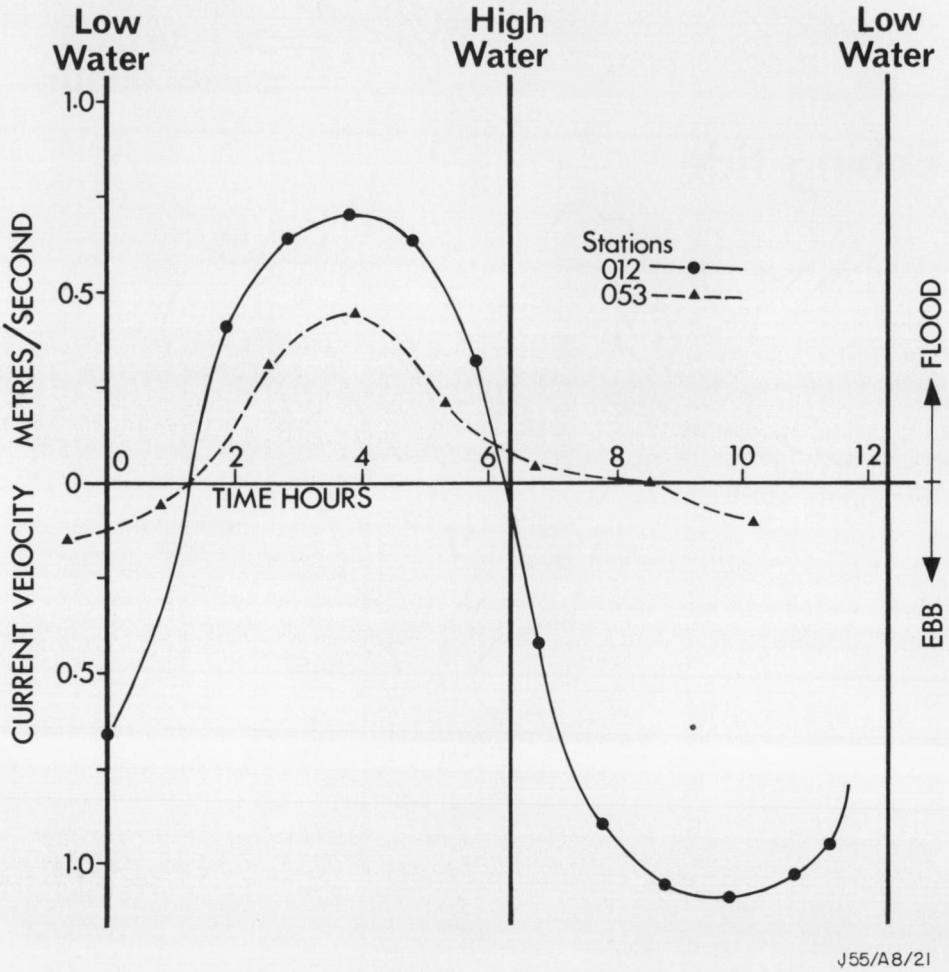

Maximum current velocity in the delta region of the estuary is considerably higher during the ebb phase than during the flood phase (Fig. 19). This can be accounted for by the fact that tidal currents and river runoff are opposed during the flood phase, but in harmony during the ebb phase. Also, ebb currents are confined gradually to the channels during continued drop in water level, whereas flood-waters become unrestricted as the water level rises.

DESCRIPTIVE MORPHOLOGY AND SEDIMENTARY ENVIRONMENTS

Five major sedimentary environments are recognized within the Genoa River estuarine system: deep channel, basin, shallow-bank, flood-tidal delta, and coastal barrier (Fig. 20). It has been shown previously that the hydrology of the estuary is controlled to a large extent by its physiography. Both hydrology and physiography control the distribution of sedimentary environments. This chapter deals with the major surface features and gross sedimentary aspects of each environment. The physical characteristics of sediments from each environment are summarized in Table 1.

Basinal area and Deep channel

The basinal and deep channel environments dominate in the estuary and are characterized by muddy sediments, as opposed to the sandy sediments of the other environments. They are abritrarily separated on the basis of water depth and submarine topography. Deep, linear, geomorphologically restricted areas of the estuary are considered as separate environments from the relatively shallow and unrestricted basinal areas.

There are three separate basins in the estuary, all of which are connected by narrow passages (Fig. 6). The Northern Basin is partly separated from the Southern Basin by the Goodwin Sands, and the Upper Lake is connected to the Southern Basin only by the Narrows, a deep, narrow channel which is the most seaward example of the deep-channel environment.

20. Main depositional environments of the estuary

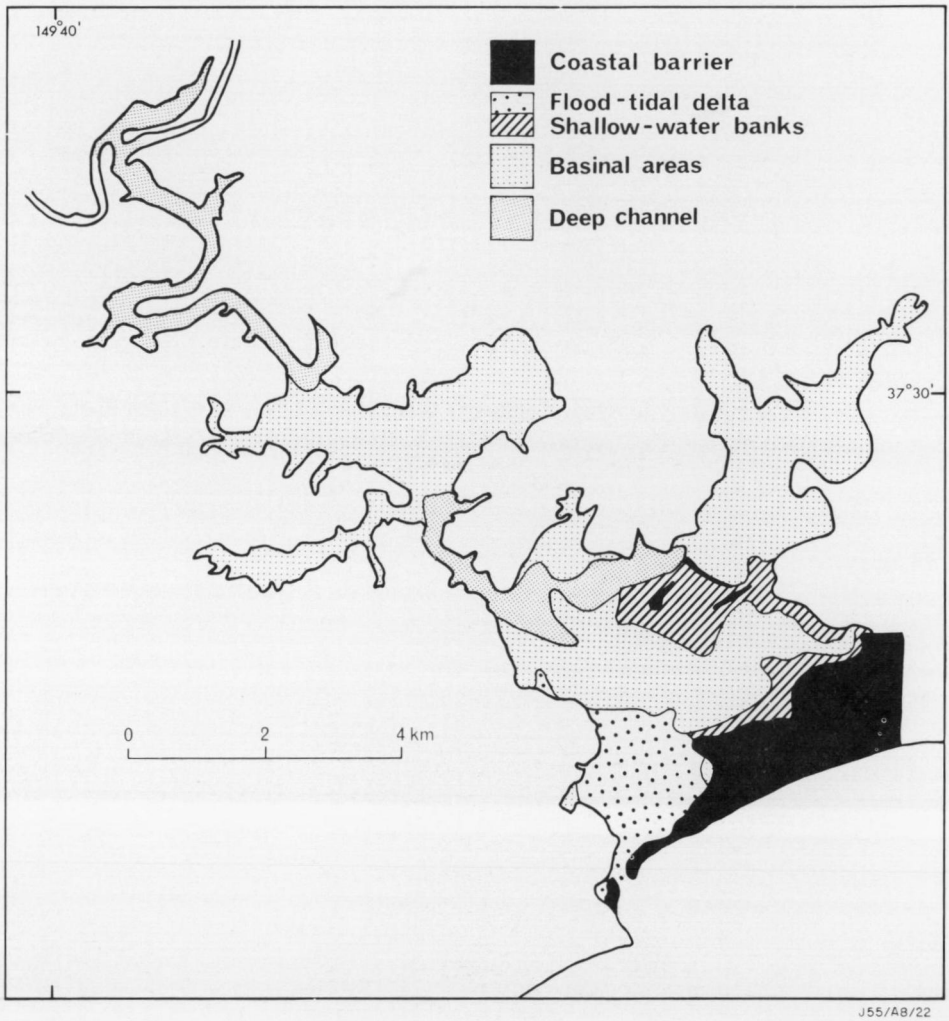

Shallow Bank

Shallow sand banks rim the estuarine side of the coastal barrier complex, and extend around the shore to the Goodwin Sands. The boundary between the sand bank and basinal mud environments is marked by dense sea grass vegetation, which terminates abruptly in the deeper mud environment. The sea grass apparently acts as a baffle for the sandy sediment, minimizing the zone of mixing between sand and mud.

Large-scale ripple bedforms with wave lengths greater than 6 m are present on these banks, and their slip-faces are oriented in a northward direction. This suggests that the sand is of marine and aeolian (coastal dune) origin, and is migrating along the inner shore through the influence of wind-generated surface waves and flood-tidal currents.

The Goodwin Sands are a shallow sand bank, rimmed by small sand ridges rising above high-water mark. The bank is not situated in a high-energy area of the estuary, and its northwestern and northern sides are steeply dipping (Fig. 7). It is likely that the Goodwin Sands are a reflection of an underlying bedrock feature, and their position suggests they are a submerged extension of the headland to the northeast.

A thin veneer of sand is present on this 'basement' (pre-Holocene rocks) topographic high, and is mainly of marine-aeolian origin. However, some sand grains are coarse and well-rounded, and are believed to be locally derived, possibly from underlying Tertiary sediments. Fragmented crusts of semi-indurated dark reddish-brown rock ('sand rock') are present within the modern sediments on the Goodwin Sands (Fig. 21). The coarse-grained constituents of this sand rock are similar to those in the indurated Tertiary strata capping some of the hills surrounding the estuary. This sand rock is also similar to the 'coffee rock' found on the eroded inner shore of the coastal barrier complex. The possibility exists that the Goodwin Sands was once covered entirely by a soil layer, and has since been partly covered by water, leaving rims of the exposed former land surface which form the linear

21. Sand rock, Goodwin Sands. Coin is 2 cm across (BMR Neg. No. M/1504)

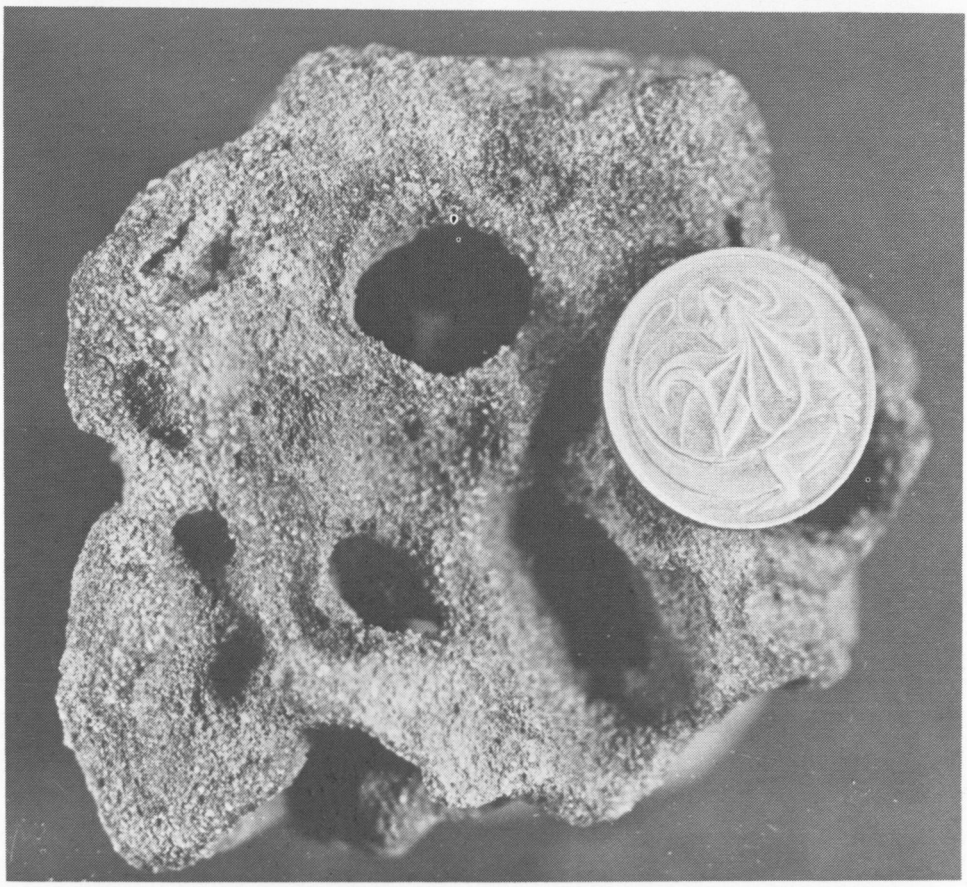

islands. If this is so, then the semi-indurated crusts may represent the remains of the B horizon of a palaeosol. This is discussed in detail in a later chapter.

Flood-Tidal Delta

The term 'flood-tidal delta', as used here, is defined as, 'sediment accumulation formed inside an inlet by flood-tidal currents' (Coastal Research Group, University of Massachusetts, 1969, p. 456). Three elements make up the Mallacoota flood-tidal delta (Fig. 22 and cover photo): subtidal channels and entrance; islands; and intertidal sand accumulations.

The main subtidal channel through the delta has maintained its present position throughout the 20th century. However, the position of the entrance changes frequently, migrating northward during low runoff periods, and southward during high runoff. The entrance is maintained by tidal currents and river discharge, and during drought periods its water depth decreases to 0.5 m.

A secondary subtidal channel exists on the eastern side of the flood-tidal delta, adjacent to the ancient barrier complex. This channel is presently terminated at its seaward end by the barrier-bar. The small niche in the barrier-bar in this area (cover photo), is the remnant of a secondary entrance which formed during the extreme floods of February 1971. This entrance was rapidly closed by longshore drift.

The small islands inside the entrance to the estuary may be the result of the permanent build-up of sand banks above water level. Alternatively, they may be elevated remnants of the coastal barrier complex, which at one time may have extended across to the bedrock headlands. These islands appear to be actively growing on their landward sides. Grasses, salt bush, tea-tree, and other forms of vegetation help to stabilize and increase the size of these exposed areas. Soils are forming on the higher and drier parts of these islands.

22. Location of sand bodies on flood-tidal delta, 5-7 March 1971

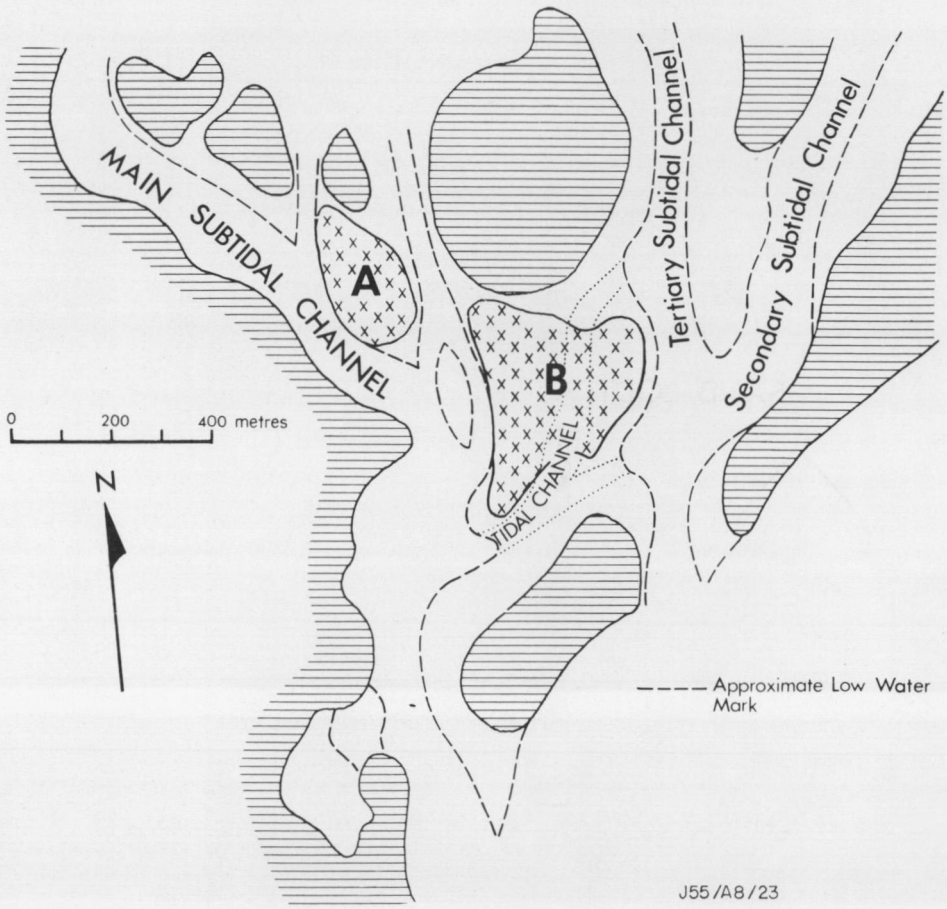

The net movement of marine detritus appears to be landward. This may be indicated by the predominance of a flood-tidal delta relative to its ebb-tidal counterpart, although the absence of an ebb-tidal delta may be largely due to longshore drift. The intertidal sand bodies of the delta display numerous sedimentary bedforms. These bedforms reflect the hydrological conditions under which they were deposited, and provide evidence for the dominant landward movement of marine detritus.

23. Slip-face azimuths of ripples and megaripples, Sand Body A at low water, 5-7 March 1971

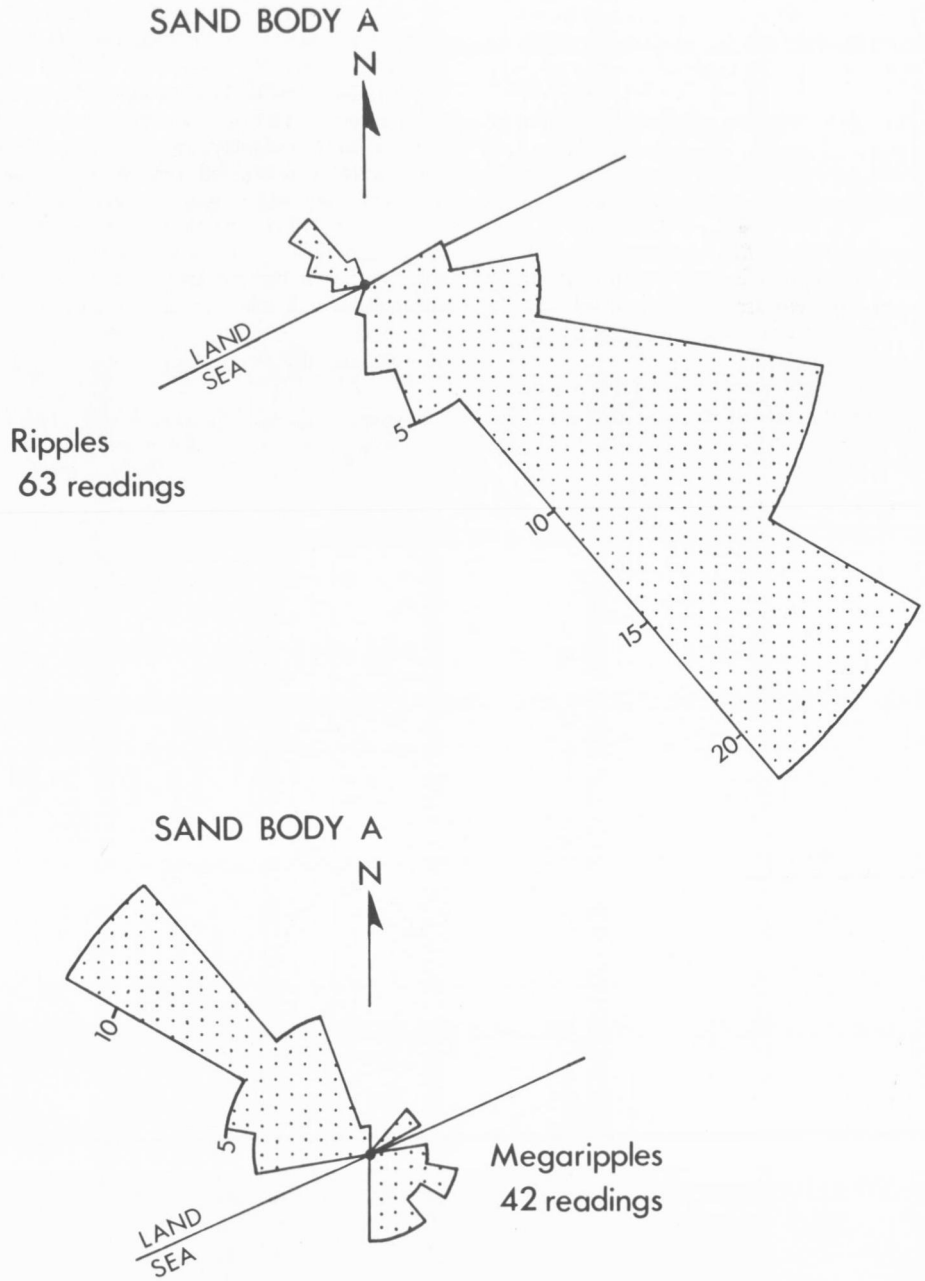

J55/A8/24

Sedimentary bedforms

The sedimentary bedforms on two intertidal sand bodies (Fig. 22) of the flood-tidal delta system, were studied in detail. The two intertidal sand bodies were visited over three consecutive days at low tide, and bedform azimuths and wavelengths were recorded. Two east-west traverse lines were established across each sand body at low tide. Readings of the small-scale bedforms were taken every 2 m along the lines, and of the large bedforms every time one was encountered along the lines. When this phase of the field work was being undertaken, two entrances existed to the estuary (Fig. 22). Soon after, however, the eastern one became completely sealed up.

Sedimentary bedforms and associated features encountered on the flood-tidal delta are defined according to the classification of the University of Massachusetts Coastal Research Group (1969, p. 456) and are as follows:

Ripples — Asymmetric bedforms formed by unidirectional flow.

Wavelength less than 2 feet (0.6 m).

Lunate-linguoid ripples — Asymmetric bedforms with both slip-faces and scour pits concave down-current.

Sand-waves — Asymmetric bedforms formed by unidirectional flow.

Wavelength greater than 20 feet (6 m).

Megaripples — Asymmetric bedforms formed by unidirectional flow.

Wavelength between 2 and 20 feet (0.6 and 6 m).

Scour megaripples — Megaripples with undulatory to cuspate crests, and well-developed scour pits in front of the slip-faces.

Of the two sand bodies examined, Sand Body A is characterized by ripples and megaripples, whereas Sand Body B displays ripples and sand waves. Sand Body A is located next to the main subtidal channel where ebb-current velocities are greatest, and where water movements in general are greatest (Fig. 22). Sand Body B is situated between the main entrance and the temporary entrance, is subjected to less restricted channel flow, and is more affected by water currents with variable flow directions.

24. Looking seaward at ebb-oriented ripples superimposed on flood-oriented megaripples, low water, Sand Body A. (BMR Neg. No. M/1220)

Figure 23 shows the distribution of azimuths of slip-faces of ripples and megaripples on Sand Body A. The slip-faces of megaripples are predominantly flood-oriented in a northwest direction, whereas ripples are almost entirely ebb-oriented in a southeast direction. This suggests that the dominant sediment movement, on Sand Body A, is in the flood-tidal direction. As the flood water rises, flood currents increase in velocity, and linear and scour megaripples are formed on the sand body. During early ebb tide, currents are low, and ebb-oriented ripples are superimposed on the flood-oriented megaripples (Figs. 24, 25, 26). This is the only major modification of flood-oriented bedforms that occurs on Sand Body A, because when ebb-currents are greatest, water level is lower, and the sand bank is exposed. Maximum ebb-currents are confined to the channels and the flood-oriented megaripples are preserved on the banks.

On the southeastern edge of Sand Body A, flood-oriented ripples are superimposed on flood-oriented megaripples (Fig. 27). The ripples are modified by ebb-currents to some extent but their flood-orientation remains. These ripples form when flood-currents are waning just before the tide turns. By the time ebb-currents become fast enough to modify these ripples significantly, water is no longer flowing over this area. The few ebb-oriented megaripples observed are on the western edge of Sand Body A, beside the main subtidal channel. These megaripples form from flood-oriented megaripples as a result of intense modification of the crests of the megaripples during early ebb-channel flow.

The bedform orientations on Sand Body A are essentially unidirectional: flood-oriented megaripples form in an opposite direction to ebb-oriented ripples.

Rose diagrams of ripple and sand-wave orientations from Sand Body B are shown in Figure 28. Sand waves are entirely flood-oriented to the northwest whereas ripples display four directions, two flood-oriented populations, and two ebb-oriented populations. Sand waves appear to have been formed by flood-currents acting through the temporary inlet, during rising tide (Fig. 29). Flood-oriented ripples are formed by currents directed through both inlets as indicated by the two

25. Different view of ripples, etc., in Figure 24. The ocean is to the right. (BMR Neg. No. M/1220)

dominant flood-oriented directions. As the water rises and the sand body is covered late in the tidal cycle, flood-currents from two directions flow over this bar, creating ripples oriented between north-northwest and north-northeast. Variations in the small bedforms, such as ladder-back ripples and rhomboid marks (Coastal Research Group, 1969, p. 441) are present on Sand Body B. These types of ripples are indicative of interference during changes in current direction.

Figure 30 is an enlarged plan-view of the distribution of bedforms on Sand Body B. A small tidal channel cuts the sand body into two sand-wave fields. This channel is covered by ebb-oriented ripples at low tide. No ebb-oriented bedforms are present on the sand-wave fields. However, interference ripples and partly destroyed bedforms occur near the edges of the sand-wave fields. Numerous flood-oriented ripples on the sand waves have nipped crests (Fig. 31), due to modification by weak ebb-currents during the early ebb-tidal phase.

During the early ebb-tidal phase, water flows seaward over Sand Body B and creates ebb-oriented ripples which display two dominant orientations, one parallel to the main subtidal channel through the delta, the other parallel to the tidal channel running through the bar (Fig. 30). As ebb-currents increase, and the water level drops, flow is confined to subtidal channels. Thus, flood-oriented bedforms are preserved on the higher parts of Sand Body B, and ebb-oriented bedforms are confined to the lower and perimeter areas.

26. Ebb-oriented ripples superimposed on flood-oriented megaripples, low water, Sand Body A. View looking seaward. (BMR Neg. No. M/1220)

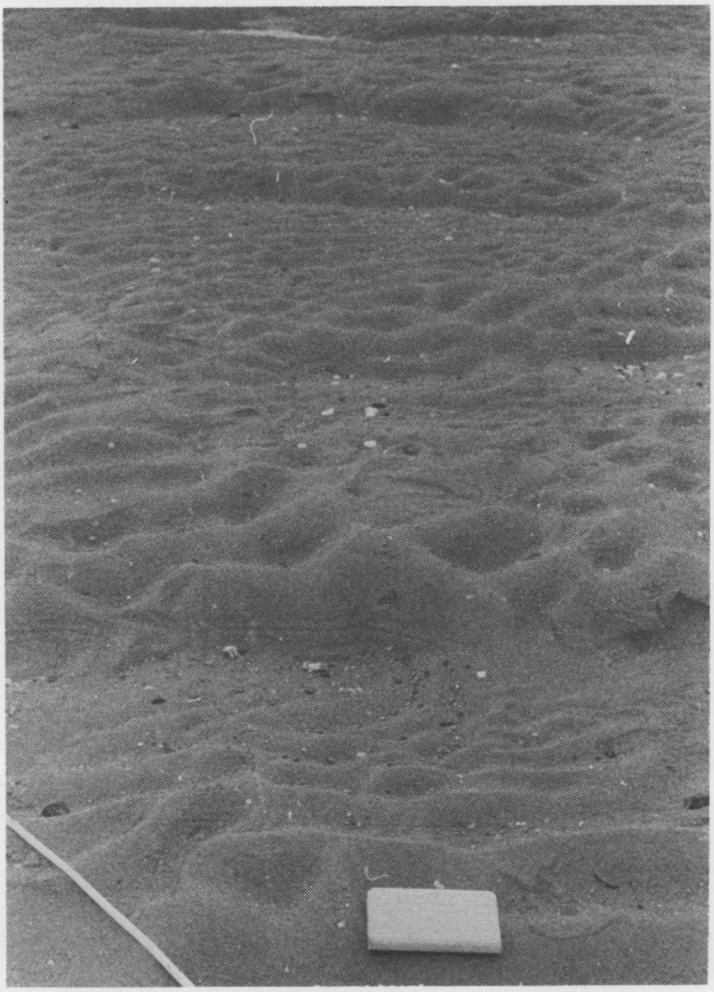

Coastal barrier

The term 'coastal barrier' as used here is defined by Bird (1964) as a 'strip of depositional land extending above high-tide level, and standing offshore or across the mouths of inlets and embayments'. A large coastal barrier complex extends from Bastion Point northeastward to Gabo Island, and is broken only by the entrance to the estuary (Figs. 1 and 3). This type of barrier, in which two headlands are connected by sand deposits of Late Quaternary age with an embayment behind, is very common on the New South Wales coast (Langford-Smith & Thom, 1969; Thom, 1965).

The Mallacoota barrier complex consists of two major tracts:

1) The modern barrier consisting of the present ocean beach backed by a parallel foredune ridge. This complex forms the present coastline. It is a linear, actively-changing tract situated in front of the ancient barrier.

27. Looking seaward at flood-oriented ripples superimposed on flood-oriented megaripples, low water, Sand Body A. (BMR Neg. No. M/1217)

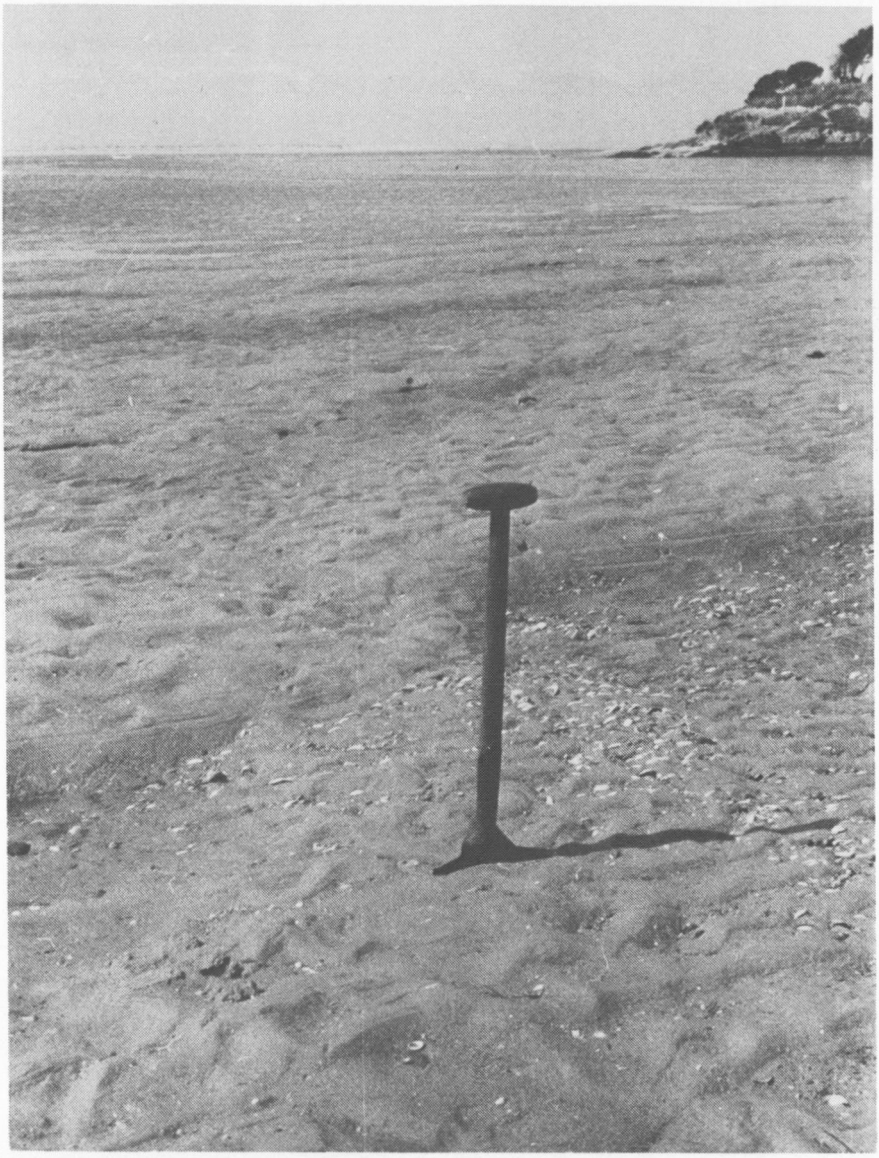

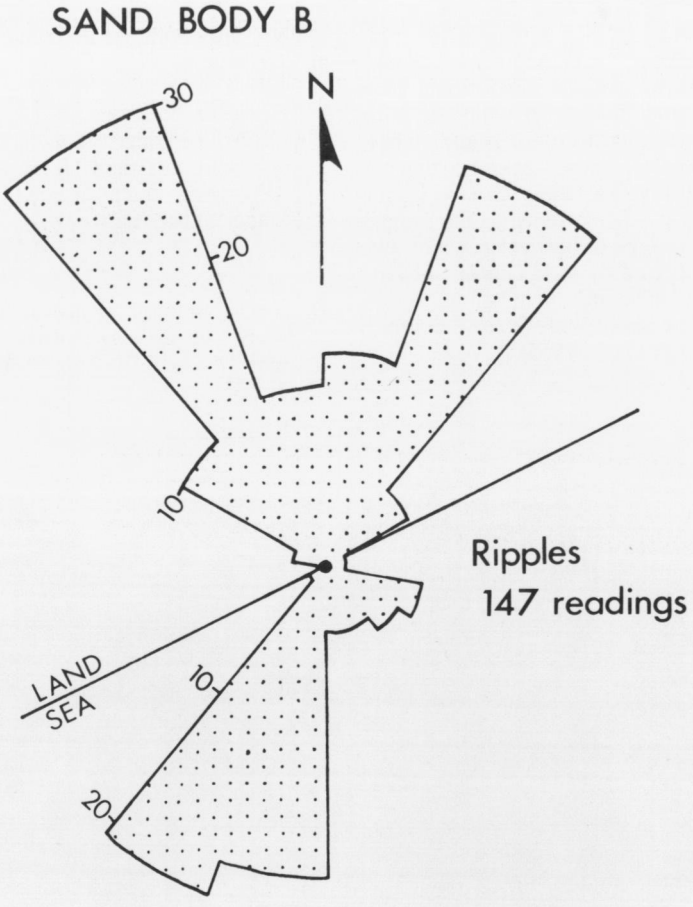

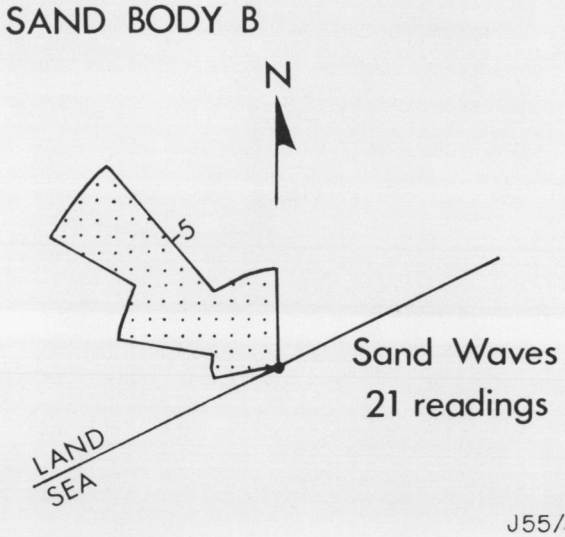

J55/A8/25

28. Slip-face azimuths of ripples and sand waves, Sand Body B, low water, 5-7 March 1971

2) The ancient barrier is a broad plain (Howe Flat) with relatively low relief compared to the modern barrier. It is a densely vegetated area made up of a series of parallel ridges, separated by marsh, swamp, and grassy flatland.

Coastal foredune and beach

The beach is a long curvilinear tract averaging 30 m in width, backed by a foredune belt for most of its length. The foredune belt rises to about 25 m above the beach foreshore, and is frequently cut by parabolic dunes and blowout troughs. Although the continuity of the foredune is modified somewhat by the blowouts and parabolic dunes, it is in general stabilized by strong growth of grasses such as *Festuca, Spinifex* and Marram grass. Thick scrub vegetation abounds on the landward side of the foredune belt. The long-axes of parabolic dunes and blowouts are oriented north to northeast. This general direction corresponds to the dominant wind directions of southwest and northeast recorded at Gabo Island (Fig. 4). The seaward side of the foredune belt is often cliffed and unvegetated, as a result of being cut back by present-day marine erosion.

The beach profile varies somewhat along its length. At the southwest end, near the estuary entrance, the beach is backed by a berm, on which incipient foredunes have been formed by the accretion of wind-blown sand from the beach foreshore (Fig. 32). Growth of Marram and *Spinifex* grasses has helped to consolidate this progradation. The incipient foredune tract is separated from the main foredune belt by a small swale zone, barren of vegetation (Fig. 33). The incipient foredune gradually pinches out eastwards along the coastal tract, and the berm ridge becomes nipped, forming a cliff-like face (Fig. 34). Halfway between Bastion Point and Tullaberga Island, accretionary features are absent, and the back-beach zone abuts against the main foredune belt (Fig. 35). Here, the foredune is truncated, by erosion of its seaward face. Locally, remnant beach ridges and incipient foredunes occur in front of the truncated foredune face, but in general large-scale progradation has ceased at the present time. Bird (1965, p. 24) noted a similar cessation of progradation on the Ninety-Mile Beach of East Gippsland.

29. Sand-wave field, Sand Body B, low water, 5 March 1971. View looking west. (BMR Neg. No. M/1220)

Ridges, marsh-swamp, flatland

Howe Flat is characterized by an older-established sequence of parallel sand ridges, between which marsh, swamp and dry flatlands have developed. The ridges have subdued relief compared to the present coastal foredune barrier. They are low-angle ridges with a maximum height of 7 m above the surrounding marsh and flatland.

The ridges are marked by thick, sandy heath vegetation and woodland. According to Willis (1969) some of the shrubs present are sedges, rope rushes, and various forms of sclerophyll shrubs such as *Leptospermum laevigatum* (coastal tea-tree), and *Hakea*. Coastal species of *Eucalyptus* and *Banksia* dominate the woodland vegetation. The swampy, water-logged areas support thickets and scrubs dominated by *Melaleuca ericifolia*. Various forms of salt bush, such as *Salicornia*, swamp grasses and reeds are abundant. The dry flatlands support *Spinifex* and other forms of grasses. Details of the species of vegetation types on Howe Flat are discussed by Willis (1969).

Loamy soils are extensively developed on the innermost sand ridges. The sand in the upper soil

30. Bedform characteristics of Sand Body B at low water, 5-7 March, 1971

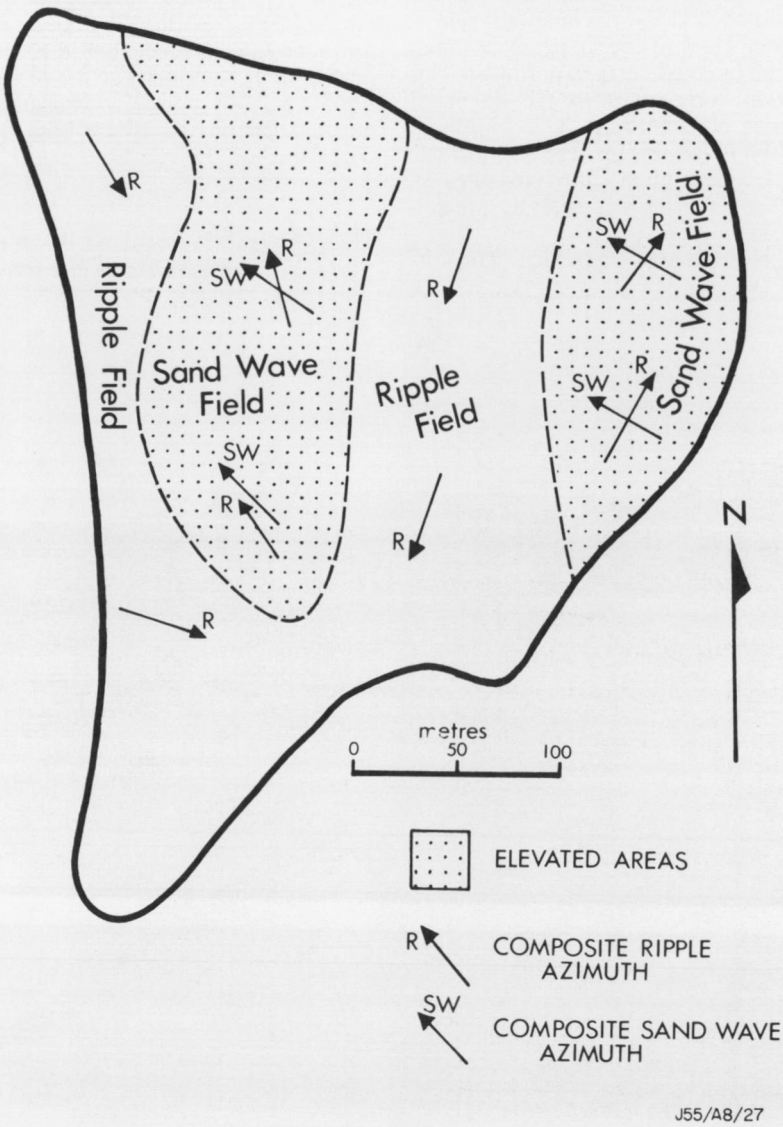

J55/A8/27

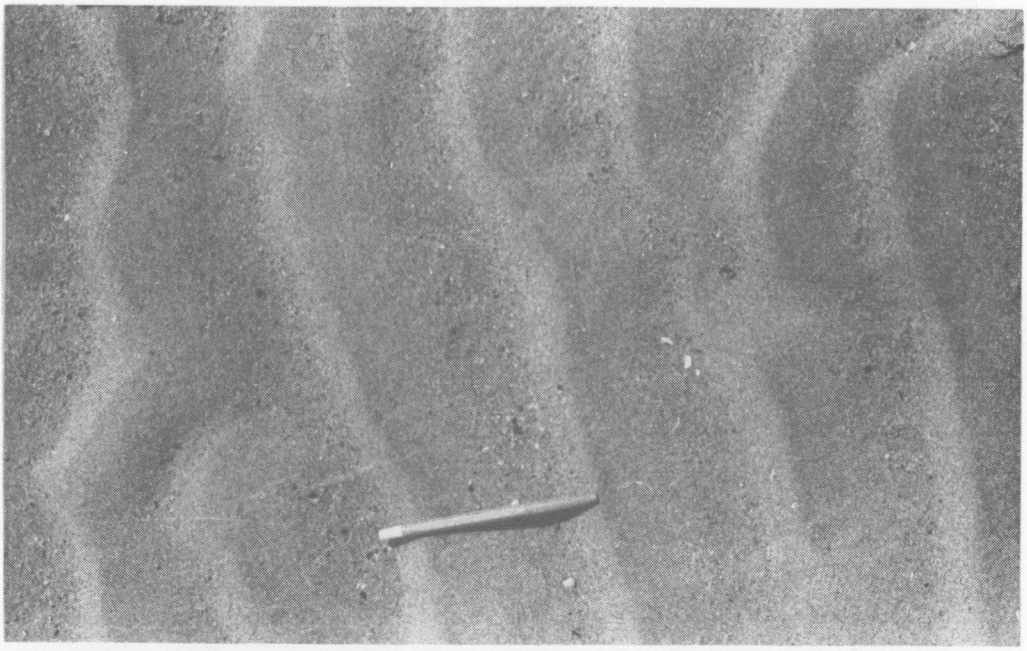

31. Flood-oriented ripples with nipped crests due to modification by weak ebb currents. Ebb direction is from left to right. (BMR Neg. No. M/1220)

32. Ocean beach and foredune near entrance to estuary. Looking northeast. (BMR Neg. No. M/2031)

33. Incipient foredune separated from main foredune belt by swale zone. (BMR Neg. No. M/2031)

34. Ocean beach and foredune belt seen from the southwest. Incipient foredune is pinching out, due to erosion, towards the northeast. (BMR Neg. No. M/2031)

zone is bleached to a greyish-white colour, indicating intense leaching has occurred.

A number of the innermost ridges appear to be truncated by the present estuary shoreline, suggesting that active erosion of the ancient barrier is occurring from within. The estuary, therefore, appears to be encroaching on to the rim of the ancient barrier.

A layer (≃20 cm) of semi-indurated sand rock is exposed within the loose sand sequence just below high water, along the inner shoreline of the barrier complex (Fig. 36). This rock is dark reddish-brown, and consists of well-sorted quartzose sand, cemented by iron oxides and organic matter. It is similar to the 'coffee rock' B horizon of ground-water podzols formed on ancient dunes in other parts of the east coast of Australia (Bird, 1964; Thom, 1965; Langford-Smith & Thom, 1969). Its possible origin and significance are discussed in the next chapter.

35. Main foredune belt and ocean beach lacking incipient foredune; back-beach abuts against eroded seaward face of main foredune belt. (BMR Neg. No. M/2031)

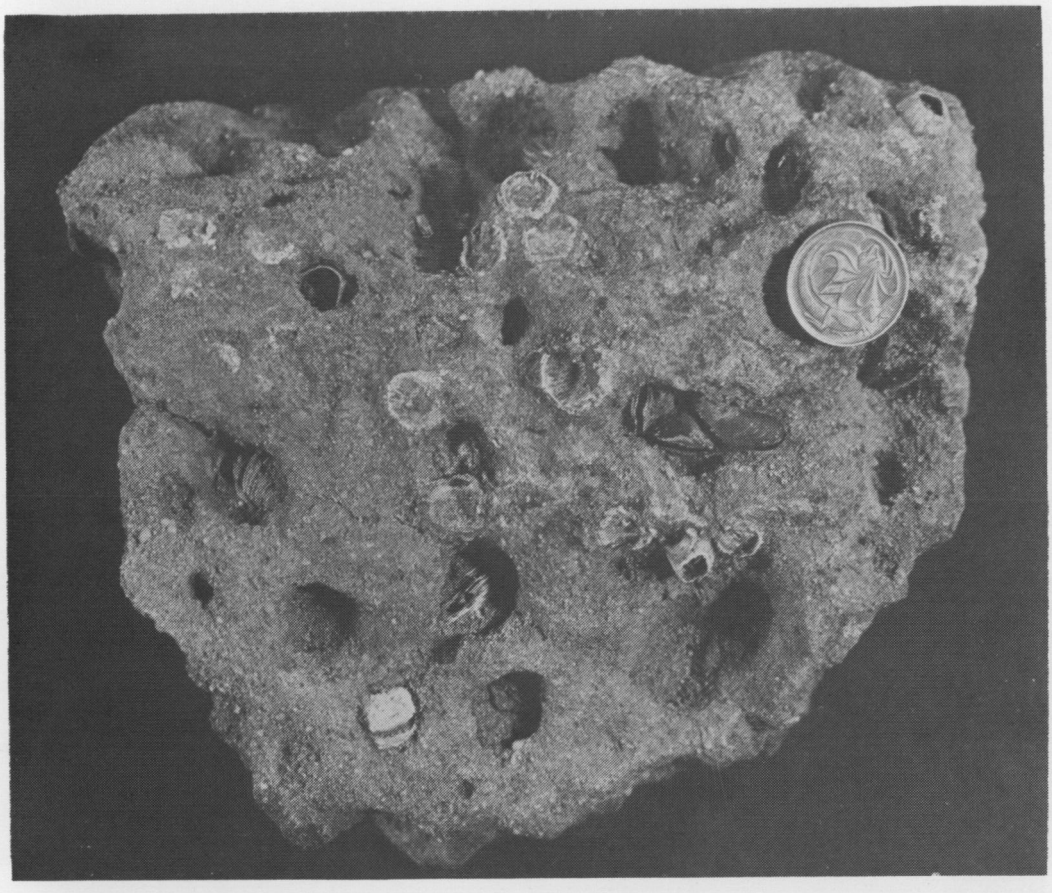

36. Sand rock, inner shore of coastal barrier. Coin is 2 cm across. (BMR Neg. No. M/1504)

Barrier development on the east Australian coast

As mentioned previously, the coast of New South Wales is characterized by gently-curving barrier-beach complexes, terminated at both ends by headlands. Langford-Smith & Thom (1969) report that these barrier systems are highly variable in length, from 90 m to 50 km or more, and in width from a few metres to 8 km. The barrier systems may be represented by a single foredune ridge, a series of beach ridges, a complex dune system, or a combination of these three situations.

Two separate barrier systems are recognized (Langford-Smith & Thom, 1969), according to their position relative to the hinterland: an older inner barrier and a younger outer barrier. The outer barriers are generally separated from the inner barriers by lagoons and swamps, but sands of the outer barriers are commonly superimposed on inner barrier ridges. According to Langford-Smith & Thom, outer barriers occur on most parts of the coast but inner barriers are scarce south of Newcastle. They suggest that topography governs this distribution: the flatter the topography, the better developed the inner barrier. Most of the coast south of Sydney consists of steep-sided drowned river valleys enclosed by arcuate outer barriers of Holocene age. Examples of well-developed dual barrier systems on the New South Wales North Coast are at Newcastle Bight and Myall Lakes (Thom, 1965). On the far South Coast, such as at Disaster Bay (40 km north of Mallacoota), outer barrier-ridge formation is extensive, but inner barrier features appear to be absent.

A characteristic feature of the inner barrier systems is the presence of a semi-indurated sand-rock horizon below the leached podzol soil profiles of ridges and swales (Langford-Smith & Thom, 1969; Thom, 1965; Hails & Hoyt, 1968). According to the workers mentioned above, this sand rock is composed of quartzose sand cemented by carbonaceous matter (humates) and iron-oxides. The equivalent swamp deposits are indurated sandy peats. Such deposits are often dissected by present-day streams and extend above and below present sea level. In areas of major coastal recession, such as at Evans Head, parts of the inner barrier have been destroyed and sand rock is exposed as cliffs along the beach backshore (Langford-Smith & Thom, 1969).

37. Coastal barrier. Locations of cores and cross sections (Figs 39, 40)

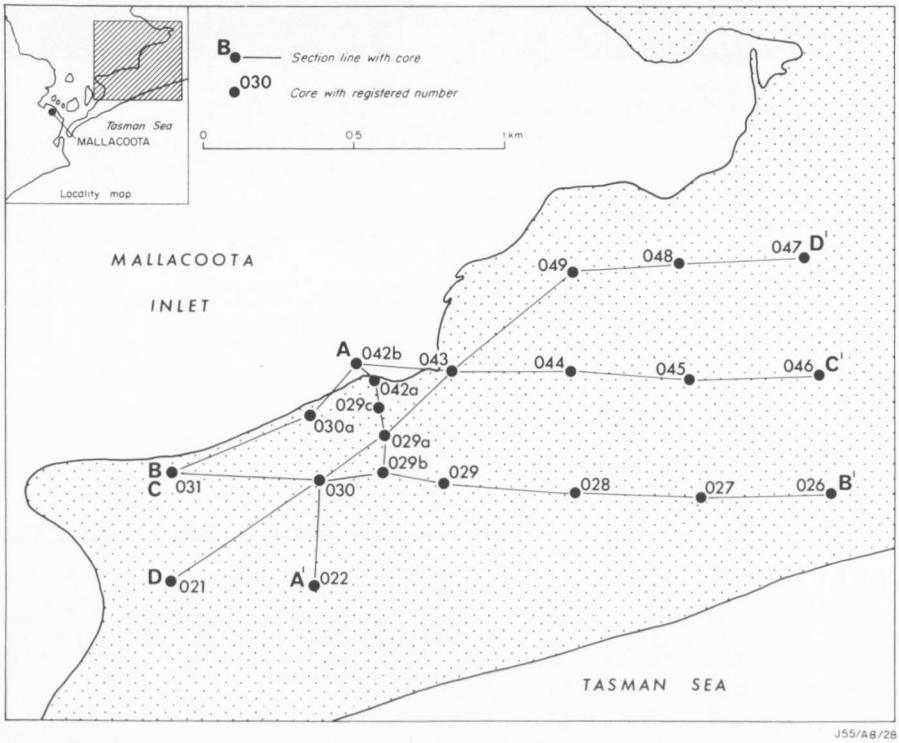

The inner barrier is considered by Langford-Smith & Thom (1969), to be of Pleistocene age and the outer barrier of Holocene age. They suggest that sea level rose rapidly after the last glacial, during the period from about 17 000 to 6000 years B.P. and then more slowly to 3000 years B.P., when it reached its present level. They consider that outer barrier formation occurred during the last 3000 to 6000 years. On the New South Wales North Coast, sand rock and peats associated with the inner barrier at Jerusalem Creek (south of Evans Head) and at Broadwater Beach have been dated at 25 900 ± 1100, 15 530 ± 650, and 12 150 ± 230 years. These dates, along with morphological evidence indicating a time break between inner and outer barrier development (such as the presence of an interbarrier lagoon, the higher elevation of the inner barrier relative to the outer barrier, and the deep incision of the inner barrier by streams), suggest to Langford-Smith and Thom that the inner barrier formation is related to a late Pleistocene interstade.

Barrier development in the Mallacoota area

General stratigraphic sequence and relationships

A reconnaissance study of the Quaternary stratigraphy of the coastal barrier was undertaken in March 1971. Twenty-three cores were obtained from Howe Flat (Fig. 37) and seven cores from the Goodwin Sands. All the cores are less than 1.5 m long, because no suitable coring device was available, and the cores had to be obtained manually with plastic tubing. These short cores are inadequate for determining the Quaternary stratigraphy in detail. However, they do point to a complex history for the development of the coastal barrier, and to the need for a comprehensive coring program on Howe Flat, and a related detailed Quaternary study in this region.

An idealized stratigraphic column of the near-surface sequence of Holocene deposits on Howe Flat is shown in Figure 38, and cross-sections, based solely on core data, are given in Figures 39 and 40. The surface deposits are variable, depending on whether they are situated in marsh swamp areas or on ridges. On ridges the surface deposits are sandy brown soils consisting of a thin organic-bound A zone, underlain by aeolian sands of variable thickness. This unit appears to thicken seaward, and often contains more than one cycle of dune-sand deposition and incipient soil formation. In the wet marsh swamp areas the surface deposits consist of up to 25 cm of black peat-like material. The dune-sand unit is usually absent in these areas, and the peat is developed on the shallow-bank sand facies. The shallow-bank unit directly overlies, and is gradational with, the estuarine sand facies, a grey coarse, shelly marine sand. The Estuarine sand unit disconformably overlies a semi-indurated sand-rock unit. Where the estuarine sand unit is absent, shallow-bank sands directly overlie this basal unit. The upper 20 cm of the sand-rock unit is more consolidated than the underlying section, especially where the unit crops out at low water mark on the estuary-barrier shoreline. However, where the unit is buried by sand deposits, it remains semi-indurated throughout its cored length.

The short cores taken from the Goodwin Sands reveal that only two of the units are present here.

38. Idealized stratigraphic column, near-surface sequence of coastal barrier

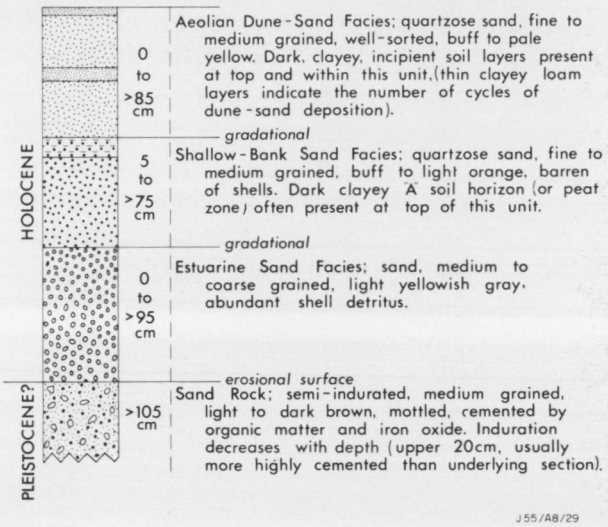

Shallow-bank sands lie directly on the irregular top of the sand-rock unit which in places protrudes through the contemporary sand cover. It is suggested that the sand rock on the Goodwin Sands may be stratigraphically equivalent to the sand-rock unit encountered on the coastal barrier. Both are at about the same elevation relative to present sea level, and are very similar in appearance (Figs. 21 and 36).

It is possible that this sand-rock unit is related to the Pleistocene inner barrier deposits described previously. Undoubtedly, the unit is part of a different cycle of deposition from the unconsolidated Holocene sand sequence which disconformably overlies it.

Formation of the coastal barrier

The barrier system at Mallacoota may be the composite of dual barriers of the type described by Langford-Smith & Thom (1969). The orientation of the ancient beach ridges suggests that the present inner shoreline of the barrier is the result of the landward progradation of the barrier during the late Holocene. Seaward progradation appears to have been less important in the formation of the Mallacoota barrier's present width, than at Disaster Bay, about 40 km to the north, where a continuous series of ridges and swales has prograded about 2 km in a seaward direction during the Holocene (Langford-Smith & Thom, 1969, plate 4).

A hypothetical progression of the growth of the coastal barrier at Mallacoota is presented in Figure 41. It is suggested that remnants of the inundated Pleistocene(?) inner barrier existed as topographic highs up to about 6000 years B.P. Subsequent Holocene deposits formed on top of remnants of

39. Cores of Holocene and late Pleistocene(?) deposits, Howe Flat (Fig. 37 shows locations of cores and cross sections)

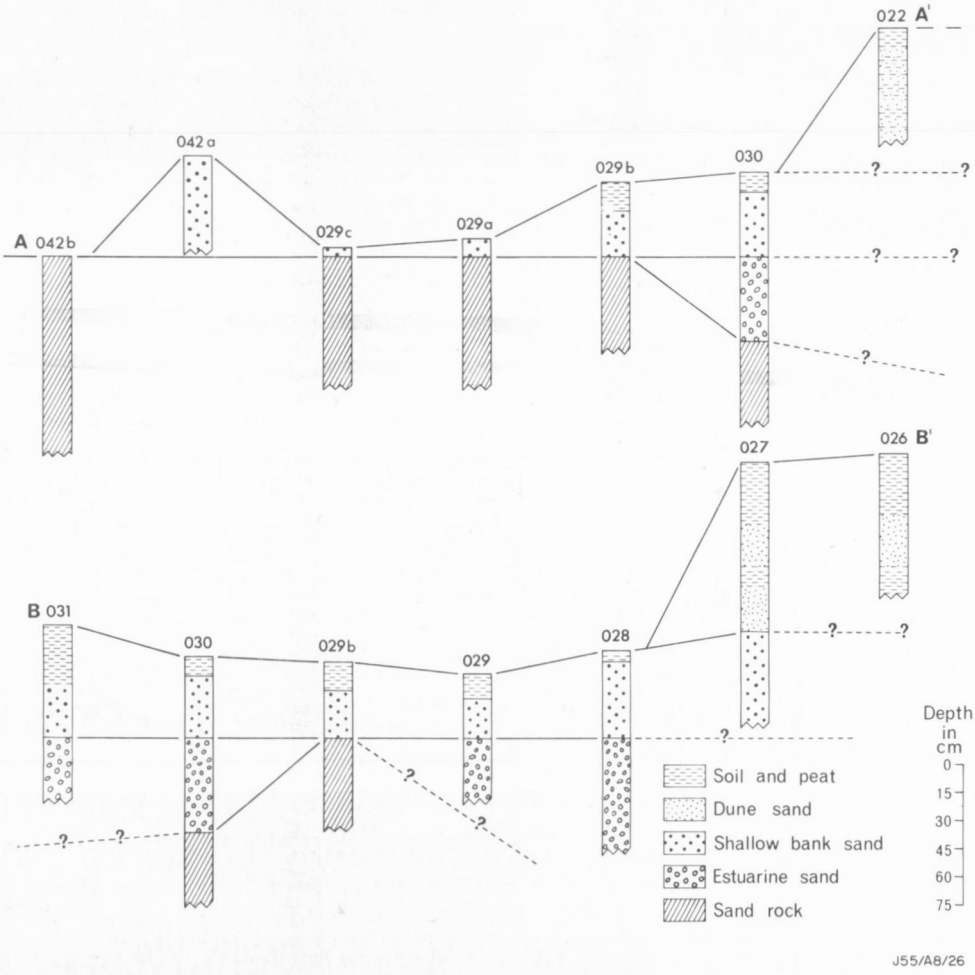

the inner barrier during the last 6000 years producing the present configuration of the coastal barrier. There is some evidence to suggest that the coastal barrier has remained relatively stable during the late Holocene. Large-scale progradation appears to have ceased, and some erosion appears to be occurring at present, on both the seaward and the estuarine side of the barrier.

40. Cores of Holocene and late Pleistocene(?) deposits, Howe Flat. Same reference and scale as Figure 39

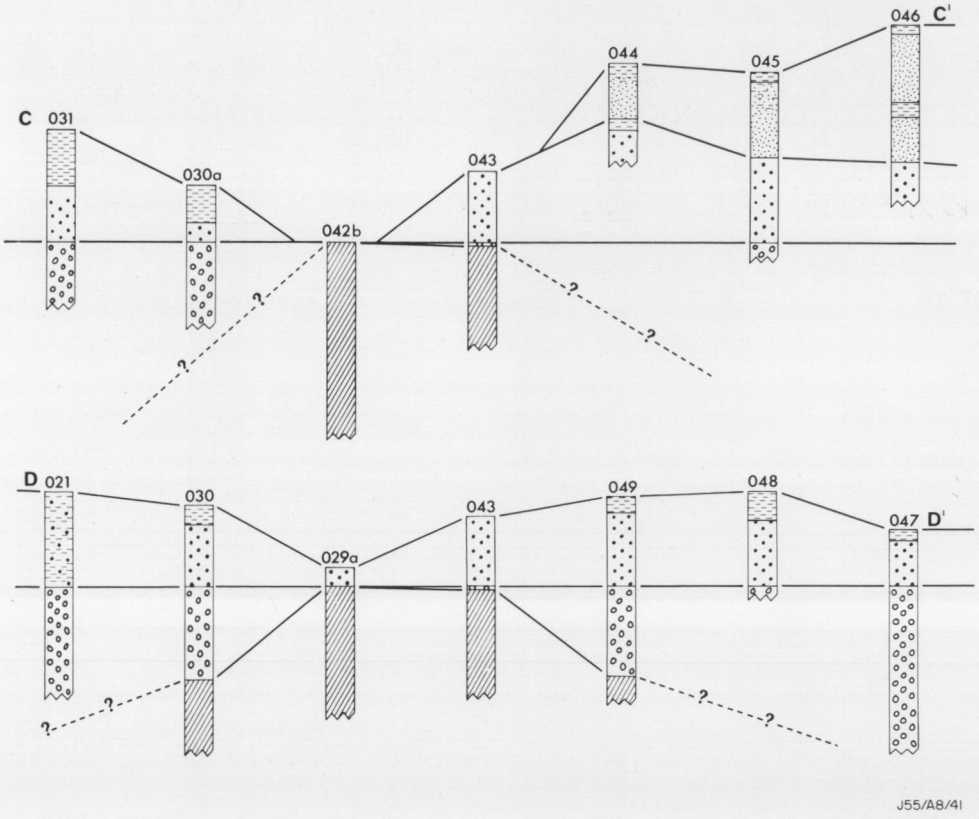

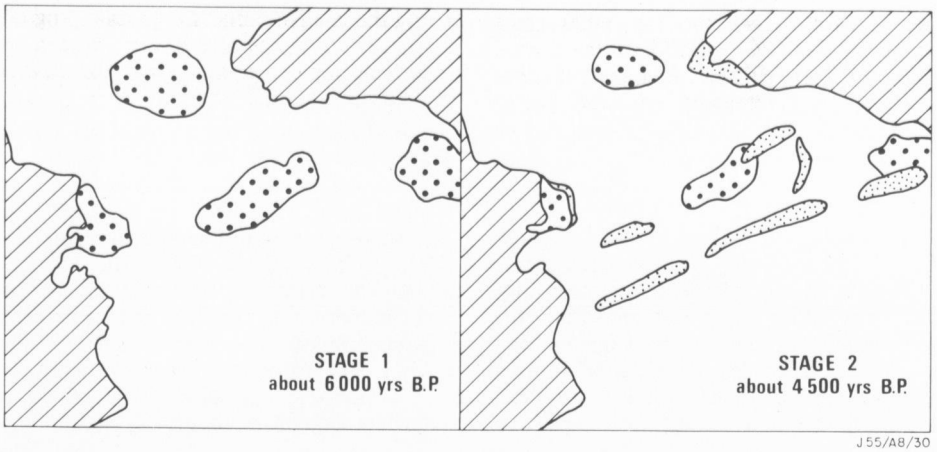

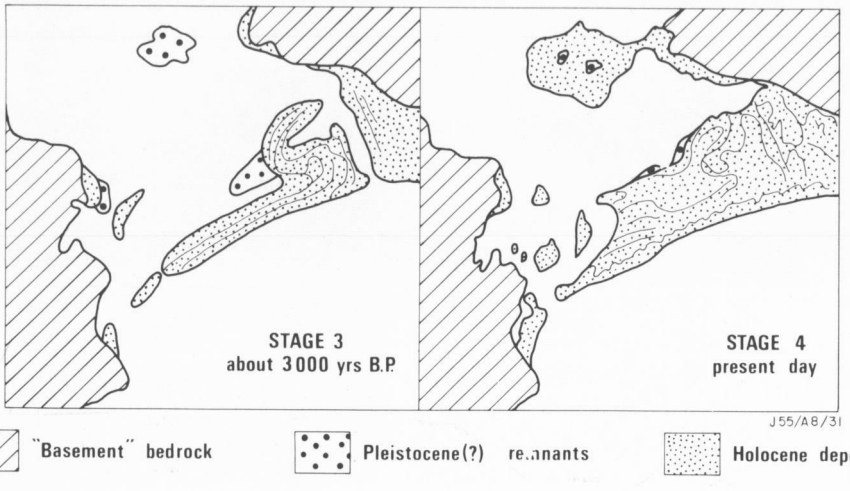

41. Hypothetical progression of growth of the coastal barrier

ESTUARINE SEDIMENTS

Samples of sediment were collected from 295 locations in the estuary and adjacent ocean. Figure 42 shows the locations of samples analysed. A sample-station grid was set up using theodolites, and buoys and shoreline markers were placed along each grid line to provide an accurate and easy method of locating sample positions. The samples were collected from a 4-m aluminium dinghy, using a small conical steel dredge fitted with an interchangeable bag which could accommodate a few kilograms of sediment and allow water to drain from the sample. In shallow intertidal or subaerial areas, samples were collected with a small shovel. Colour and odour were recorded for each sample at the time of sampling, and then the sample was placed in a polyethylene bag. The samples were later transferred to large glass jars to be stored for future analysis.

Techniques for preparation of the samples, and procedures used in textural, mineralogical and chemical analysis of the samples, are outlined in Appendix 1. In this study the major grain-size fractions are defined as follows: *gravel*, larger than 2000 μm, *sand*, 63 to 2000 μm; *silt*, 2 to 63 μm, and *clay*, smaller than 2 μm. Gravel plus sand are considered as the coarse fraction of the sediment, and silt plus clay as the mud fraction of the sediment.

A summary of the physical characteristics of the sediments found in each environment is given in Table 1, and Appendix 2 lists these parameters for each sample. The physical characteristics of the sediments from two additional environments —

42. Locations of surface sediment samples (samples represent the top 10 cm or so of the sediment column)

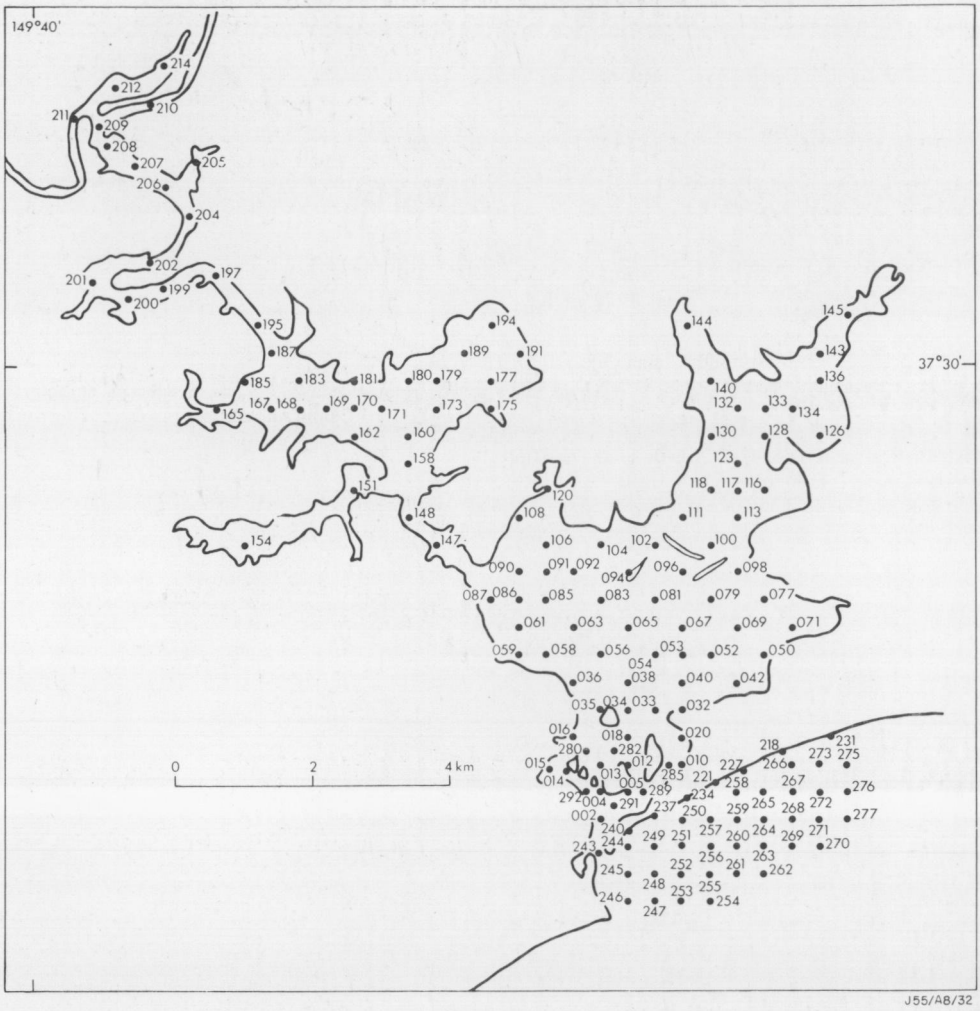

TABLE 1 PHYSICAL CHARACTERISTICS OF SEDIMENTS

	Environment	*Texture*	*Gravel Fraction*	*Carbonate (%)*	*Colour and Odour*	*Primary Structures*
SUBAERIAL Coastal barrier	DUNE	sand; fine to medium-grained well-sorted	none	0	sandy, no odour	laminations; heavy mineral laminae, aeolian cross-bedding
	ISLANDS	sand to gravelly sand, dirty where soil developed	shell debris	0 to 5	sandy, no odour	planar bedding
	SWAMP-MARSH, RIDGE, FLATS	sand to muddy sand, soil developed locally	none	0	variable, depending on soil and mud content	none on surface except large-scale concentric sand ridges
INTERTIDAL, very shallow water	OCEAN BEACH	sand to gravelly sand	shell debris and terrigenous material	0 to 5	sandy, no odour	laminations; planar bedding, ridge-and-runnel systems, ripples, swash marks, grain lineations, pebble scour marks
	FLOOD-TIDAL DELTA	sandy gravel to sand	shells and shell fragments; lesser amount of terrigenous material	5 to 27	sandy, no odour	various ripples, mega-ripples and sandwaves; cross-bedding, planar laminations, grain lineations, pebble scour marks
	SHALLOW-WATER BANKS	sand to gravelly muddy sand; clean sand dominant	largely shell debris Goodwin Sands; well-rounded terri-genous material	0 to 2	sandy, no odour	wave-generated ripples and megaripples
SUBTIDAL, BASINAL	UPPER LAKE	dominantly mud, some muddy sand and gravelly muddy sand	shell debris, coarse terrigenous material	0 to 5; local shell accumulation 15	olive grey to olive black, faint to strong H_2S odour; all samples have odour	colour laminations in mud
	NORTH-ERN BASIN	mud to gravelly mud dominant	shells, shell fragments	1 to 20; local shell accumulation 40	olive black, faint to strong H_2S odour; all samples have odour	faint colour laminations in mud
	SOUTH-ERN BASIN	muddy sand to sandy mud to mud	gravel fraction minor; largely shell debris	generally 0 to 6; local shell accumulation 25	brownish grey to olive black; faint to strong H_2S odour; only some samples have odour	colour laminations in mud
SUBTIDAL, CHANNEL	UPPER RIVER CHANNEL	sand, gravelly sand, muddy sand, sandy mud, mud	largely coarse terrigenous material	0 to 1	variable-sandy colour, brown to olive-grey, olive-black	colour laminations in mud
	NARROWS	mud	none	0	olive grey to dark grey; odorous	colour laminations in mud

subaerial and ocean beach — are outlined in Table 1, but are not considered in further detail in this study.

Textural classification of sediments

The textural classification used here is that of Folk (1968). The distribution of sediment types is shown in Figure 43. The variations in distribution of textural types correspond closely with the various depositional environments.

The shallow-water bank and flood-tidal delta environments are characterized by sand to gravelly sand.

The three basinal environments are dominated by muddy sediments but each basin has its own distinguishing textural features. The sediments in the Northern Basin are almost exclusively mud to gravelly mud, and those in the Southern Basin range from mud to muddy sand. The Upper Lake is characterized by mud, with small areas of sandy mud.

Sediments of the river channel range from gravelly sand to mud; sandy sediments predominate in the upper reaches of the estuary, with an increase in mud content in a seaward direction. The Narrows is floored entirely by mud.

Calcium carbonate

Calcium carbonate has a significant influence on the texture of the sediments. Carbonate content of the sediments is exclusively in the form of shell detritus, and is contained almost entirely in the coarse fraction. The gravel-size fraction of muddy

43. Distribution of surface sediment by textural type. Classification scheme after Folk (1968)

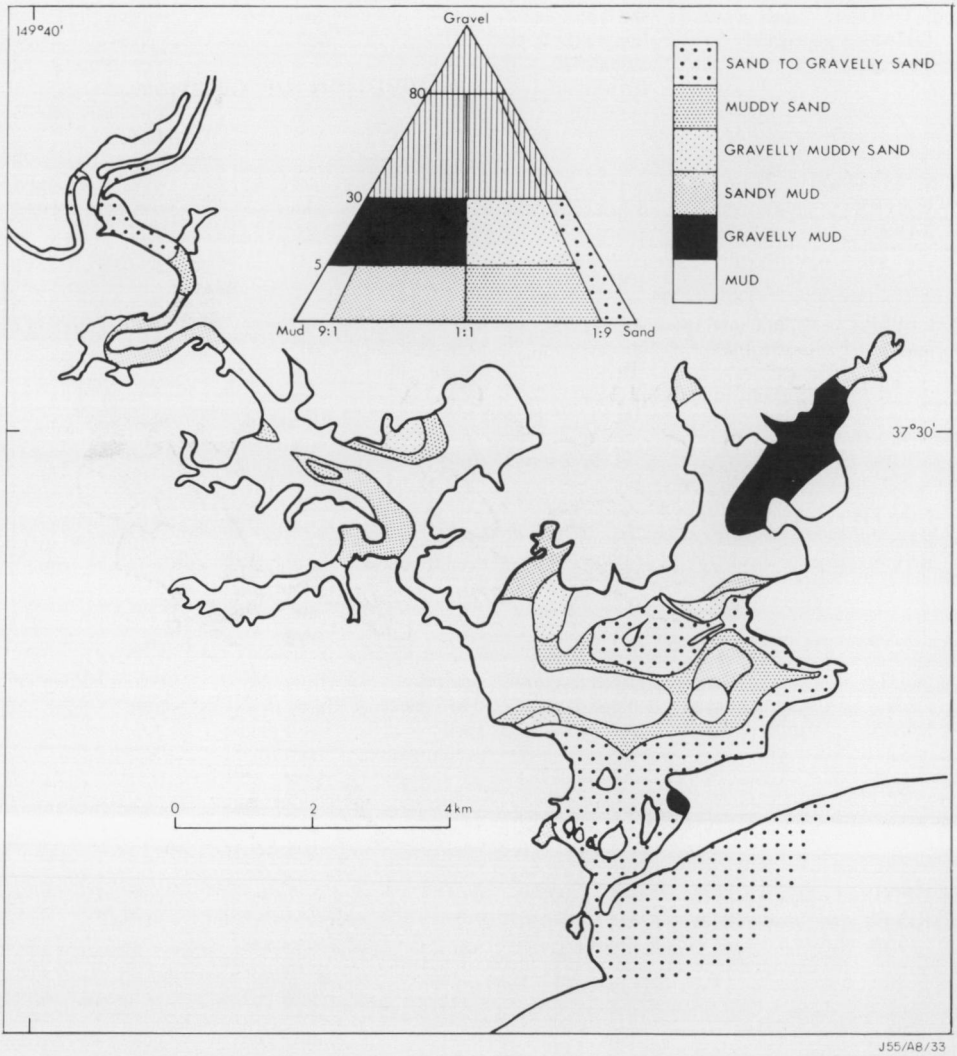

sediments is dominantly shell debris, and this is reflected in the distribution of textural types in the basinal environments (Fig. 43).

Carbonate forms nowhere less than 5 percent of the sediments of the flood-tidal delta (Fig. 44). The carbonate debris consists of remains of bivalves, gastropods, echinoids, forams and polyzoans, brought in to the delta areas from the beach and nearshore zone by tidal currents.

The shallow-water banks consist of sand which has a very low carbonate content (Fig. 44). The paucity of carbonate debris points to the predominant aeolian origin of the well-sorted sands in this nearshore environment. The sediments on the Goodwin Sands are also devoid of carbonate detritus.

The sediments of the Northern Basin have a higher carbonate content than any of the other basinal environments (Fig. 44). The sediments here are shelly muds, and the gravelly mud (depicted in Figure 43) is a reflection of the high content of shell debris in these sediments. The Southern Basin sediments generally have less than 5 percent carbonate, although locally they contain up to 25 percent. Most of the Upper Lake sediments have carbonate contents of less than 1 percent, although the nearshore areas have up to 3 percent carbonate. In this basin, there is also a local near-shore accumulation of coarse sediment which contains up to 15 percent carbonate.

Carbonates in the basinal environments consist largely of broken shells of thin-shelled bivalves. The presence of carbonate debris of this type only in the nearshore zone of the Upper Lake, and in the Northern Basin, suggests that this carbonate debris

44. Distribution of $CaCo_3$ (percent by weight of total sediment)

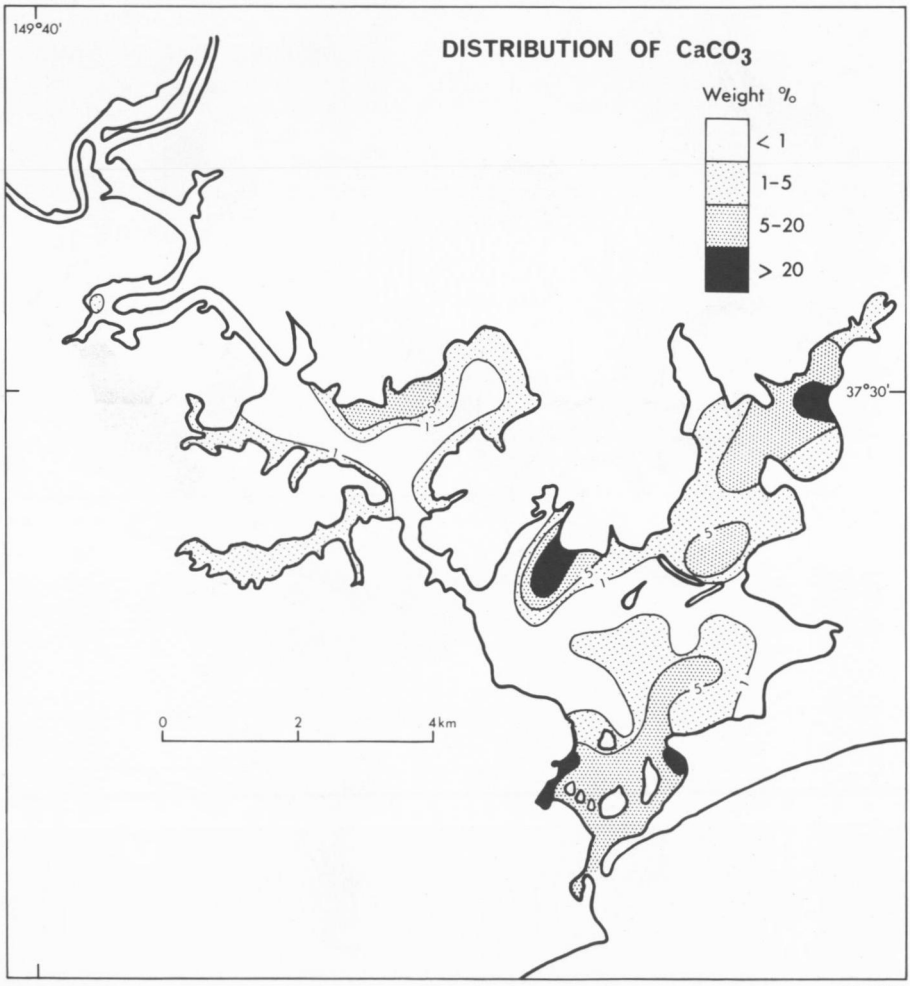

is autochthonous, derived from bivalves living in the quiet-water, muddy environments.

The river channel sediments are virtually devoid of carbonate.

Distribution of sand, silt and clay

Distribution maps of the three major size fractions — sand, silt, and clay — are given in Figures 45, 46 and 47.

Sand is the major size fraction in the flood-tidal delta and shallow-water bank environments. Except for the accumulation of sand in the uppermost reaches of the river channel, and minor accumulations in the Upper Lake, sediments with a high sand content are restricted to the seaward end of the estuary.

The basinal and river-channel environments, which comprise most of the estuary, are characterized by high silt and clay content. The river-channel environment increases in silt and clay content in a seaward direction. Silt is the most abundant of the three size-fractions in the upper river channel, whereas clay dominates in the lower river channel. The three basinal areas can be distinguished on the basis of the most abundant size-fraction contained in their sediments: the Northern Basin has a very high clay-content (>60 percent), whereas silty muds predominate in the Upper Lake. The basinal area in the Southern Basin is characterized by a mixture of silt and clay.

Colour and odour

Colour of the sediments was determined at time of sampling with the Rock Color Chart (Geological Society of America, 1951). Intensity of odour (H_2S) was recorded qualitatively at time of sampling.

45. Distribution of sand (percent by weight of organic-free sediment)

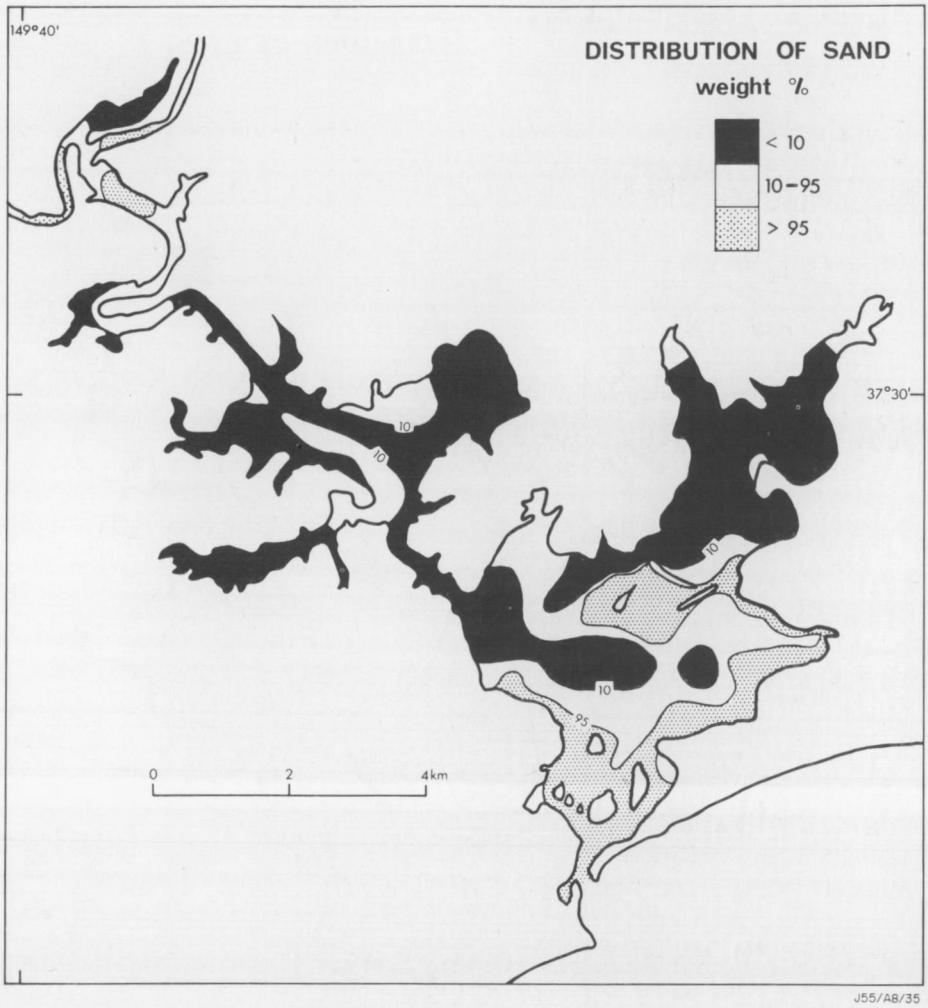

The sediments which consist predominantly of clean sand, such as in the flood-tidal delta and shallow-water bank environments, are yellowish-orange to yellowish-brown in colour. The muddy sands range from brown, to brownish-grey, to olive-grey, depending on their mud content. The sediments which are predominantly mud, range in colour from olive-grey to olive-black to black. Hydrogen sulphide was detected in most of these fine-grained sediments at the time of sampling. Colour laminations were observed in the fine-grained samples; these consisted of alternating olive-grey and olive-black layers. On exposure to air, the muddy sediments rapidly turned a reddish-brown colour, indicating the presence of the ferrous form of iron in the unaltered sediment.

Mineralogy of the sand fraction

The mineralogical composition of the fine to medium sand-size fraction (63-to-500 μm) of 113 samples is given in Appendix 3.

Quartz, feldspar and mica are the main constituents of this fraction. Rock fragments are absent except in the coarse sandy environment of the upper river channel, where there are some granitic rock fragments in the 63-to-500 μm fraction. These, however, constitute less than 1 percent of the total grains counted, and are recorded according to the minerals that formed them. Heavy minerals generally constitute less than 1 percent of the grains counted, and consist almost entirely of hornblende and epidote. Hornblende and epidote grains are generally elongate, jagged, and angular. Opaque minerals are rare in the sediments of the estuary, except at the seaward

46. Distribution of silt (percent by weight of organic-free sediment)

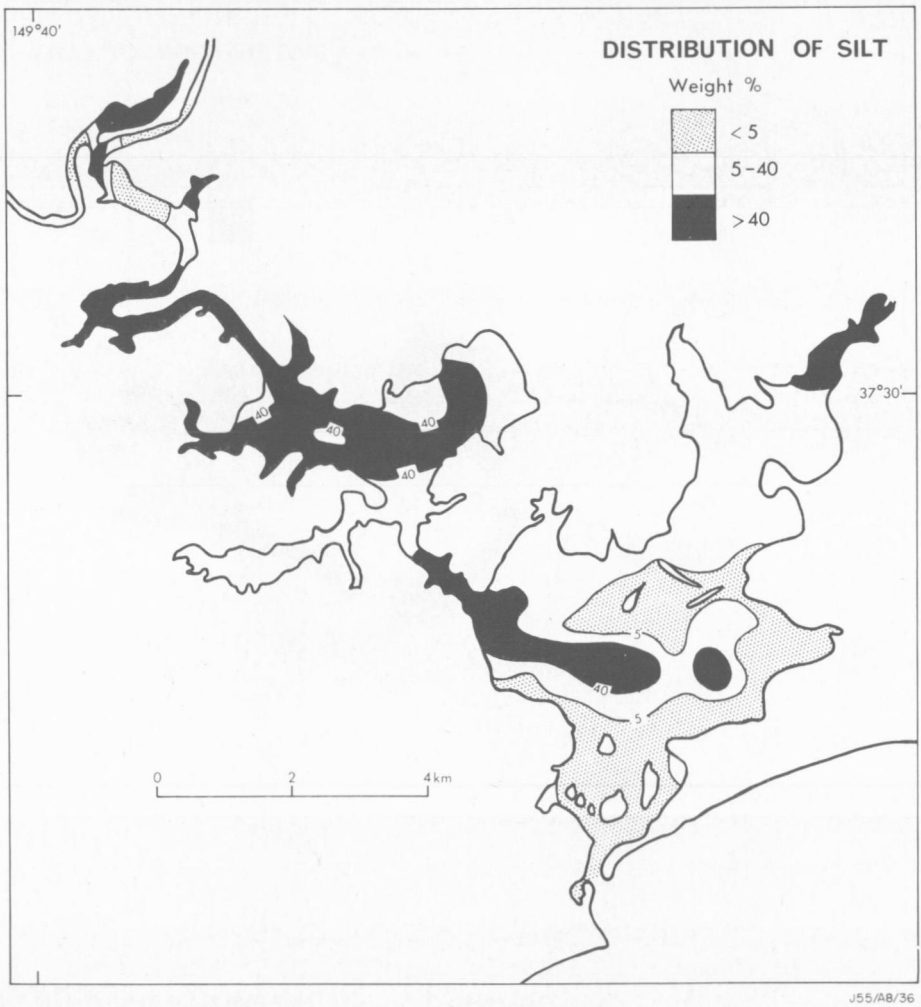

end, where they are well-rounded and polished. Of the minerals in the sand-size fraction, quartz, feldspar and mica are of primary concern, and are discussed below.

Quartz

Quartz makes up the bulk of the sand-size fraction in every sample. Colourless and transparent quartz grains are most abundant — milky varieties and composite grains are less common. Most grains are angular to subangular throughout much of the estuary. At the seaward end and in the Northern Basin, well-rounded and polished quartz grains are abundant, and in the Southern Basin are mixed with angular quartz.

The distribution of quartz in the 63-to-500 μm fraction of the sediments is depicted in Figure 48. The percentage of quartz decreases generally in an upstream direction, indicating the increasing influence of other terrigenous material towards the source area. The highest concentration of quartz occurs on the east side of the estuary (including the Northern Basin). This pattern coincides with the lateral water circulation pattern (Fig. 12), and is believed to be caused by it. The higher proportion of quartz in the northeast part of the estuary results from quartz-rich sands being blown into the southeast margin of the estuary. These aeolian sands, along with marine sands from the delta area, are transported northward by tidal and wind-generated currents. Some of this sand is carried over the Goodwin Sands into the Northern Basin. Fluvial quartz detritus is brought down along the axis of the estuary to the Southern Basin, where limited mixing of quartz from the fluvial and marine sources occurs.

47. Distribution of clay (percent by weight of organic-free sediment)

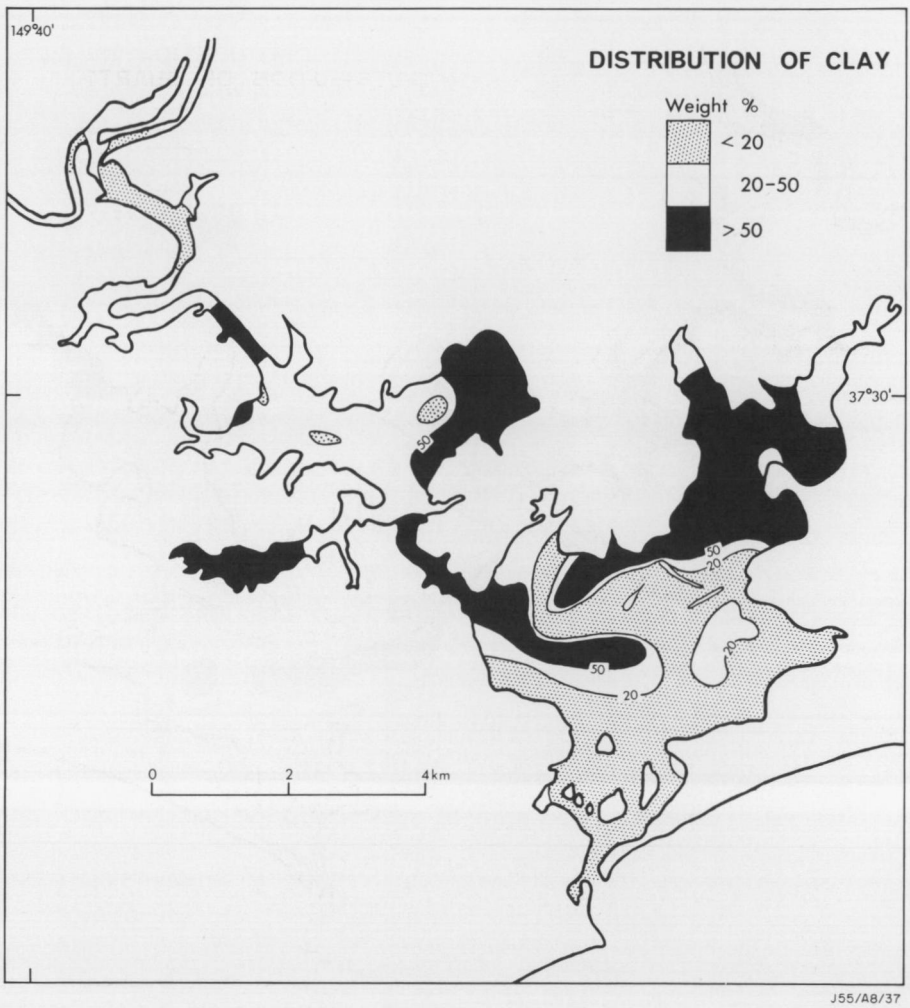

Feldspar

Plagioclase and K-feldspar were not differentiated in this study. Most of the feldspar grains are angular and are most abundant in sediments which are rich in angular quartz.

The distribution of feldspar in the 63-to-500 μm fraction of the sediments is shown in Figure 49. Feldspar content decreases in a downstream direction, emphasizing its fluvial source. The sand-size sediments of the northeastern part of the estuary have the lowest feldspar content. As with quartz, the distribution of feldspar reflects the lateral water circulation pattern existing in the estuary. The feldspar content is lowest in that part of the estuary where sea water dominates the hydrological system, and is highest where fresh-water discharge makes a significant contribution.

48. Distribution of quartz (percent by number in 63-500 μm fraction of carbonate-free sediment)

Mica

Mica grains are generally platy and angular. Colourless, brown and light-green varieties are present. The brown and green grains are probably bleached biotite, while some colourless ones may be muscovite.

The distribution of mica in the 63-to-500 μm fraction of the sediments is shown in Figure 50. Mica increases in abundance upstream, reflecting its fluvial source. The part of the estuary which experiences the highest fresh-water discharge is delineated by the distribution of mica. As with quartz and feldspar, the distribution of mica reflects the hydrological pattern existing in the estuary.

Significance of distribution patterns

In general, the water circulation pattern of the estuary is reflected in the distribution of textural types and coarse-fraction mineralogy of the

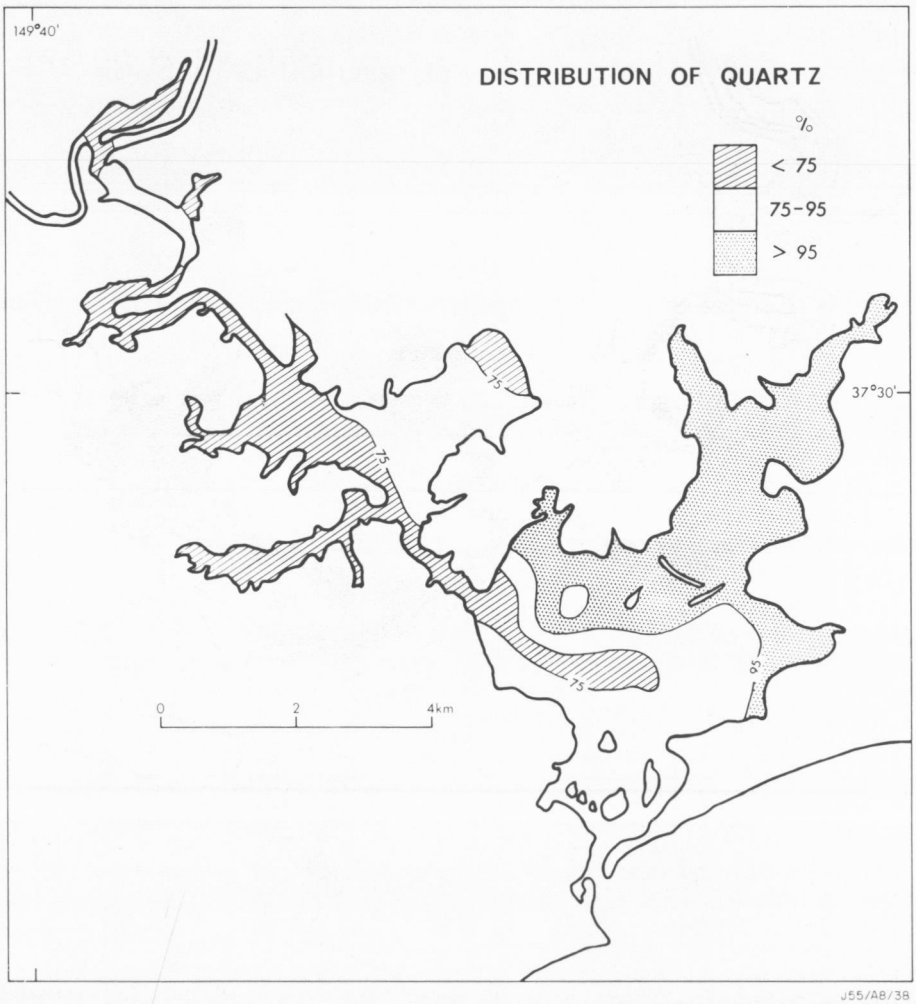

sediments. This is borne out by the following observations:

1) Sandy sediments at the seaward end of the estuary are situated in the shallowest parts of the estuary where water currents are greatest.

2) Sediments in the basins and river channel are mainly mud, because maximum flow in these areas is confined to the top of the water column, and currents are very weak at depth.

3) The accumulation of sand in the Upper Lake corresponds roughly with the area where river water and intruding sea water meet (Figs. 45 and 12). Sand concentrations are higher in the southwest half of the Upper Lake than in the northeast half.

4) Carbonate concentrations are higher in the eastern part, or seaward half of the estuary (including Northern Basin), than in the western part (Fig. 44). The eastern part of the estuary is subjected to a greater influence of sea-water circulation than the western part, as shown in Figures 12 and 18.

5) The relative abundance of the three constituents, quartz, feldspar and mica in the coarse fraction of the sediments changes rapidly across the postulated freshwater-seawater boundary (Figs. 12, 48, 49, 50). There is a preponderance of mica and feldspar on the 'fresh-water side' of the estuary, and of quartz on the 'sea-water side'.

These distributions suggest that fresh water is ponded, by intruding sea water, in the southwest part of the Southern Basin. When fresh-water

49. Distribution of feldspar (percent by number in 63-500 μm fraction of carbonate-free sediment)

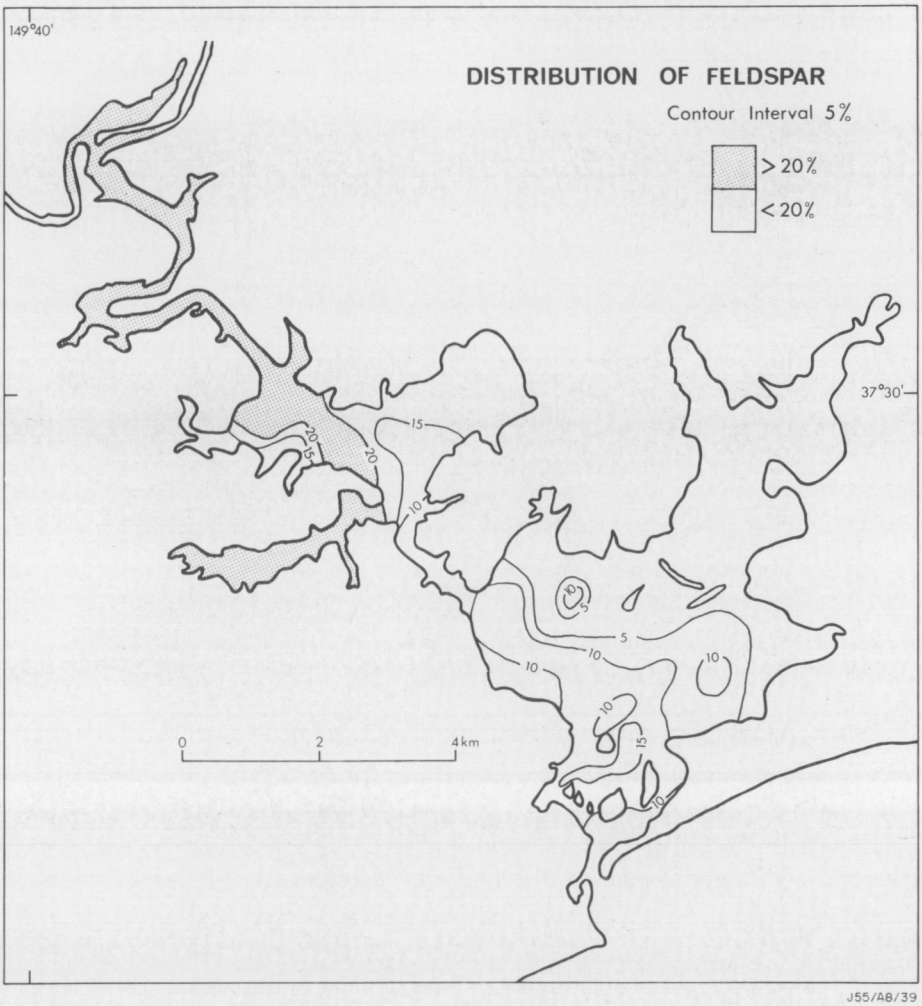

discharge is impeded, its sediment load is deposited, accounting for the high content of mica and feldspar in the sand of this area. A similar situation evidently occurs in the Upper Lake. The capacity of water to transport mica is higher than its capacity to transport other light, but less platy, minerals of similar size. Hence its distribution in the sand fraction of sediments is modified to some extent, and its concentration is almost as high in the Southern Basin as it is in the upper main river channel.

The sources of the principal components of the coarse fraction of the sediments in the estuary are suggested in Figure 51. This diagram is based purely on characteristics (texture, carbonate content, mineralogy) of the coarse fraction (63 μm) of the sediments. It can be viewed as depicting the dominant provenance of the coarse sediments in different parts of the estuary, and the differences in the sediments of similar depositional environments. For instance, the three basinal environments are obviously different with regard to the source of their coarse sediment. The Northern Basin is dominated by marine processes, and characterized by sediments with a coarse fraction high in carbonate and quartz, and low in mica and feldspar. The Upper Lake is characterized by sediments which are low in carbonate and have a coarse fraction which is high in mica and feldspar, but relatively low in quartz. This indicates that the coarse fraction of the sediments of the Upper Lake is controlled by material from a fluvial source. The Southern Basin is characterized by sediments in which the coarse fraction is influenced by material derived from both fluvial and marine sources.

50. Distribution of mica (percent by number in 63-500 μm fraction of carbonate-free sediment)

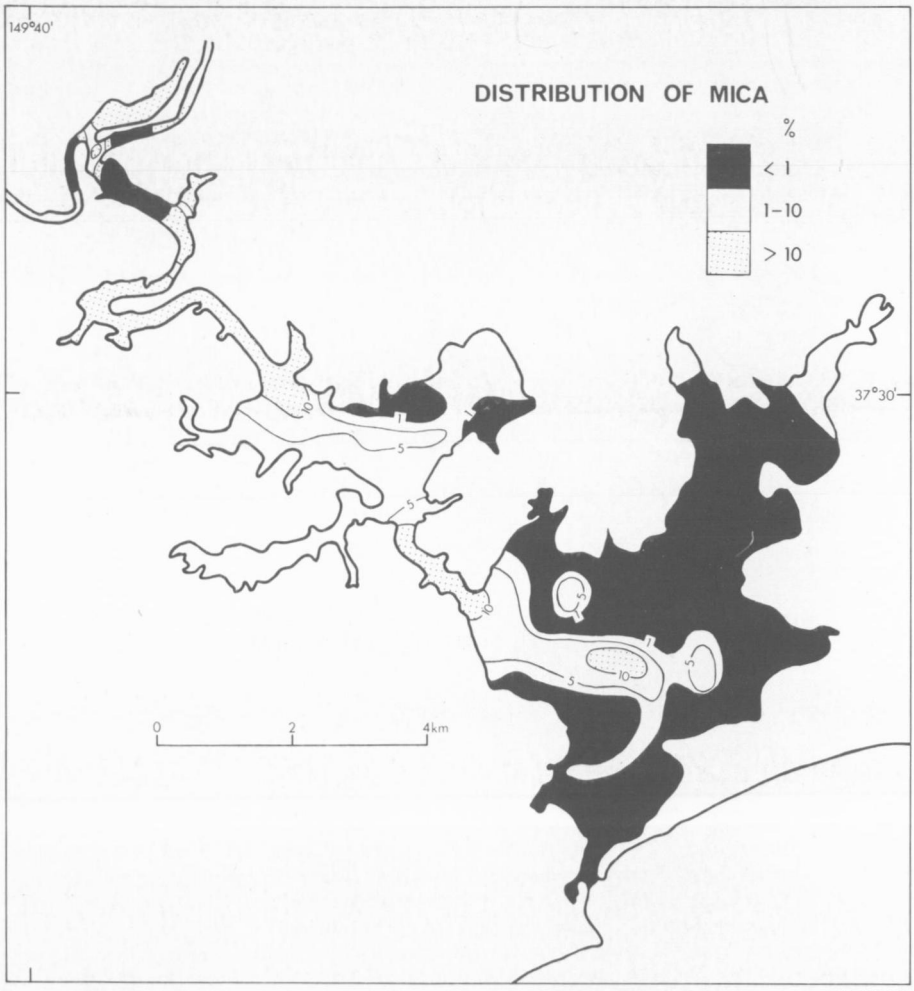

Mineralogy of the mud fraction

Silt-size fraction (2·63 μm)

The mineralogy of the silt-size fraction of 45 samples, which is given in Table 2, was determined by X-ray diffraction analysis (Appendix 1). The locations of these samples are shown in Figure 52. The objective of this analysis was to obtain comparative mineralogical compositions of the silt-size fractions in order to delineate any relative changes occurring in groups of samples from different environments. The three main groups of minerals in the silt-size fraction of the sediments are quartz, feldspar, and clay minerals. Plagioclase is dominant over K-feldspar but the two were not estimated individually. Illite is the most abundant clay-mineral group in the silt-size fraction.

51. Depositional realms, based on texture and coarse fraction mineralogy of the sediments

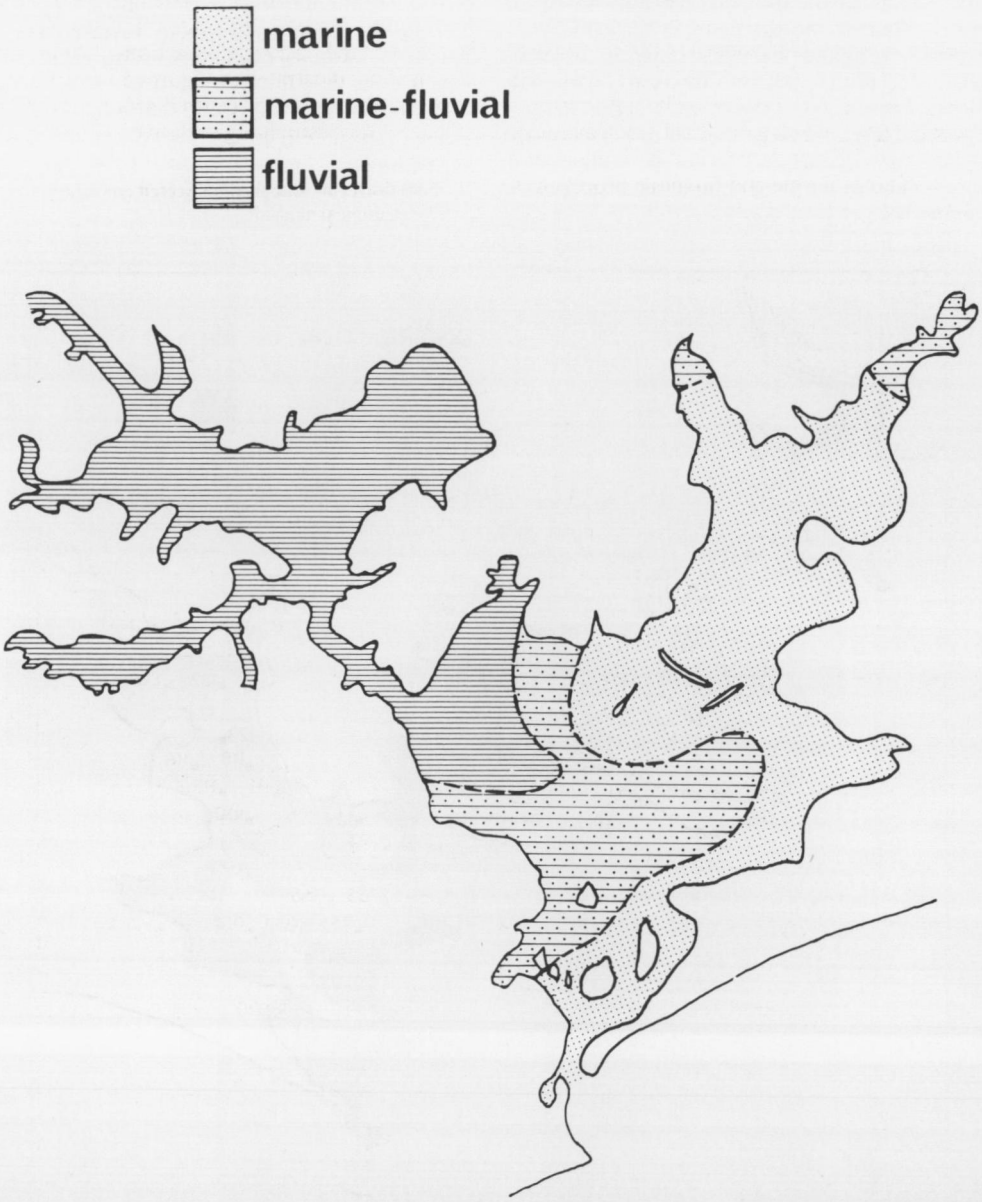

It is evident from Table 2 that there are considerable differences between groups of samples. There is a paucity of feldspar in the silt-size fraction of sediments of the Northern Basin. In addition, this basin has a much higher content of clay minerals in the silt fraction relative to the other basins and the river channel.

In general, the distribution of minerals in the silt fraction indicates the areas most influenced by coarser fluvial material (Fig. 51). The Upper Lake and main river channel have a higher quartz and feldspar content in the silt fraction of their sediments than the Southern and Northern Basins. Conversely, clay-mineral content of the silt fraction is much higher in the seaward part than the landward part of the estuary. The intermediate values of feldspar and clay in the silt-size fraction of the Southern Basin indicate that it is under the influence of both marine and fluviatile processes of sedimentation.

Clay-size fraction (smaller than 2 μm)

The clay-size fractions of 48 samples distributed throughout the estuary (Fig. 52) were analysed by X-ray diffraction, using the technique described in Appendix 1. Identification of the clay minerals in the samples was based on the X-ray diffraction characteristics of untreated, glycolated, and heat-treated mounts. Standard diffraction criteria were used to identify the main groups of clay minerals (Brown, 1961; Grim, 1968). The clay-minerals present in the estuary samples are illite, kaolinite, a mineral with a 14-Å basal spacing termed 'vermiculite', and mixed-layer clays. Typical diffractograms of the clay-size fractions of estuarine sediment are illustrated in Figures 53 and 54.

Much discussion has centred around the various schemes for estimating relative abundance of

52. Locations of samples subjected to clay and silt mineralogical analysis

TABLE 2 MINERALOGY OF SILT-SIZE FRACTION OF SEDIMENTS (%)

Sample Number	*Quartz*	*Feldspar*	*Clay Minerals*
Main river channel and Upper Lake			
214	41	24	35
212	38	23	39
209	41	21	38
205	44	24	32
202	38	24	38
201	37	15	48
199	38	38	24
197	38	17	45
195	31	23	46
183	41	35	24
167	36	21	43
169	48	37	15
171	39	21	40
194	30	16	54
189	39	20	41
177	28	20	52
173	38	21	41
160	38	24	38
158	41	23	36
165	43	21	36
147	32	18	50
Southern Basin			
106	24	5	71
090	32	17	51
087	38	21	41
061	43	26	31
063	33	24	43
056	33	20	47
065	29	13	58
054	25	7	68
079	39	17	44
052	25	9	66
038	37	22	41
085	38	27	35
Northern Basin			
145	43	4	53
143	42	5	53
140	38	3	59
134	39	5	56
132	29	3	68
123	30	5	65
118	25	9	66
116	26	10	64
113	27	5	68
111	30	12	58
104	35	11	54
092	28	17	55

individual clay minerals in a clay-mineral assemblage. Pierce & Siegel (1969) compared some of the weighting methods, and demonstrated that gross changes in apparent quantity of clay minerals may occur using the different methods devised. Gibbs (1967) outlined the most reliable method for obtaining accurate quantitative estimates of clay minerals; that is, by preparing standards of clay minerals extracted from the samples to be analysed. However, this method was precluded because of lack of time and facilities for undertaking such a procedure, and because of the complexity of the clay-mineral phases present in the samples.

Areal and vertical changes in clay-mineral assemblages of sediments can be adequately depicted by using the semi-quantitative techniques of Biscaye (1965), or Scafe & Kunze (1971). The method of Scafe & Kunze was utilized, using peak areas rather than peak heights. Peak areas were measured in triplicate on the untreated diffractograms with a polar planimeter.

Details of the weighting methods used are as follows: the area of the 14-Å peak was compared to 3 times the area of the 10-Å peak, the area of the 17-Å peak was compared to 4 times the 10-Å peak, the area of the 7-Å peak was compared to 2.5 times the 10-Å peak, and the area of the 12-Å peak was compared to 2 times the illite peak. Weighted percentages of each clay mineral were calculated from the sum of these four ratios.

Following the suggestion of Pierce & Siegel (1969), each actual peak area is also reported as a percentage of the total area of all measured clay-mineral peaks (Table 3). This makes it easier to compare the data with other clay-mineral studies, and the weighted percentages with actual percentages in this study.

The clay minerals of the estuarine sediments are present in roughly the same proportions as those found in the bottom and suspended sediments of the streams flowing into the estuary (Reinson, 1973). In general, illite and kaolinite display the same characteristics in the estuarine clays as they do in the soil and stream-sediment clays. The only difference is that the illite peak in the estuarine clays is always strong and well-resolved from the background, whereas in the soil and stream sediment, the illite peak, when present, is often broad and diffuse.

The major difference between the fresh-water and soil clays, and the estuarine clays, is in the characteristics which the 14-Å vermiculitic mineral displays on diffractograms. In the soil and stream-sediments the vermiculitic mineral displays a sharp, well-defined diffraction maximum at 14 Å on both the untreated and glycolated diffractometer trace. It collapses on heating at 450°C, to the area of 10 to 12 Å. The vermiculitic mineral in the estuarine samples displays a sharp 14-Å peak on the untreated sample, but on glycolation this peak partially expands in such a manner that it becomes broad and diffuse, and at times it appears only as a hump against the background (Figs. 53 and 54). On heating to 450°C, the peak collapses to 10Å, and not to 11 to 12 Å as happens in some of the clay-size samples of the soil and stream sediment.

The mixed-layer component in the estuarine clays is also different to that of the soil and stream-

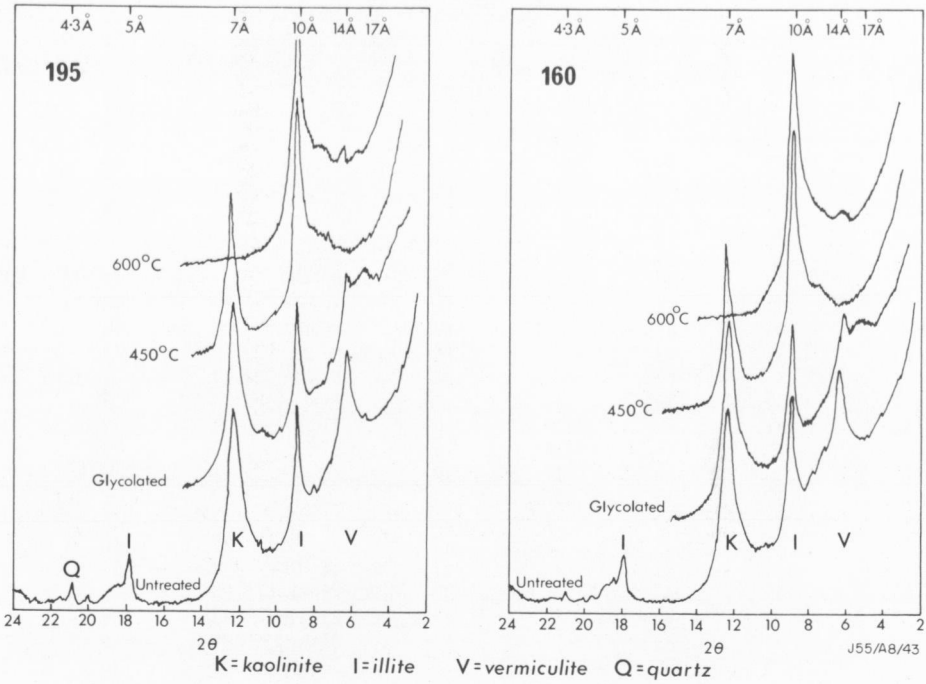

53. Typical diffractograms, clay fraction. River channel and Upper Lake

54. Typical diffractograms, clay fraction. Southern and Northern Basins

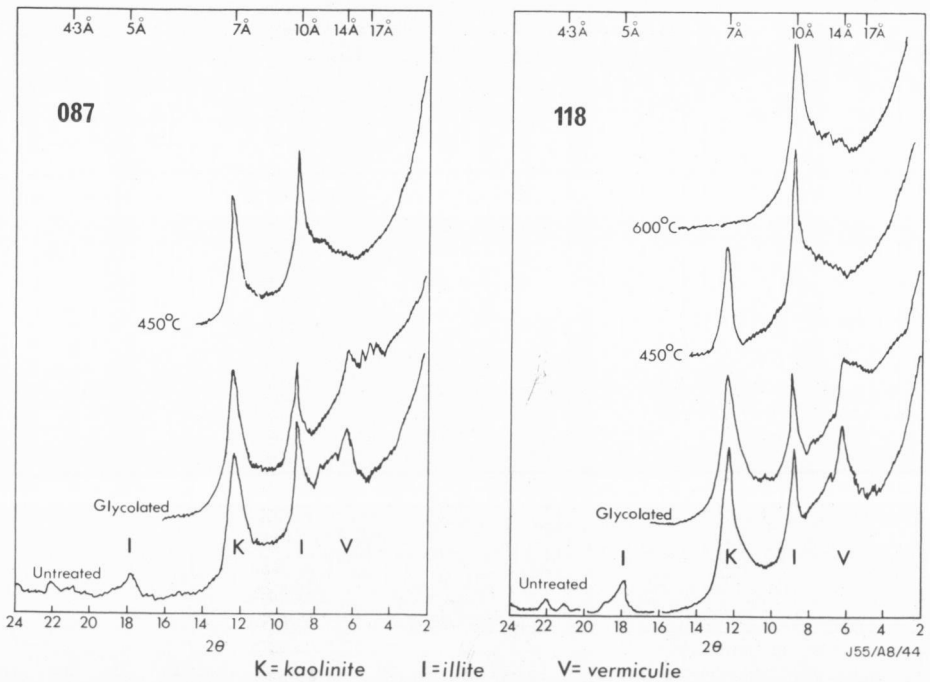

TABLE 3 CLAY MINERALOGY OF SEDIMENTS

Sample Number	*Kaolinite*		*Illite*		*Vermiculite*		*Mixed-Layer*	
	W	*S*	*W*	*S*	*W*	*S*	*W*	*S*
Main river channel and Upper Lake								
214	27	39	45	26	14	19	14	16
212	33	40	33	16	24	36	10	8
209	30	38	37	19	19	28	14	15
205	31	41	38	20	16	25	15	14
204	28	36	36	17	28	40	8	7
202	29	39	42	23	17	27	12	11
201	39	48	30	14	21	29	10	9
199	33	41	38	19	15	25	14	15
197	35	43	32	16	19	29	14	12
195	36	47	45	24	19	29	trace	
183	32	39	36	17	25	36	7	8
167	31	37	29	14	23	33	17	16
169	37	48	33	15	23	30	7	7
171	30	38	37	19	22	31	11	12
194	37	45	37	18	26	37	trace	
189	33	42	37	20	15	23	15	15
177	37	45	31	15	22	32	10	8
173	29	35	36	17	24	28	11	10
160	35	44	40	20	18	28	7	8
158	33	41	37	18	23	33	7	8
148	40	49	30	13	21	30	9	8
147	28	35	34	17	28	39	10	9
Southern Basin								
106	32	42	36	18	23	30	9	10
090	40	47	28	12	24	34	8	7
087	30	41	50	28	10	19	10	13
061	32	40	32	16	30	40	6	4
063	37	47	37	17	26	36	trace	
056	36	44	40	19	16	26	8	11
065	35	41	32	15	26	38	7	6
054	32	38	32	15	26	33	10	14
079	36	44	40	21	13	21	11	14
052	37	46	37	18	26	36	0	0
038	44	50	28	13	28	37	trace	
033	29	36	42	21	17	29	12	14
020	36	47	45	22	19	31	0	0
015	35	47	44	23	13	23	8	7
Northern Basin								
143	35	43	35	17	20	31	10	9
140	34	41	34	16	21	31	11	12
134	30	36	37	18	22	34	11	12
132	30	42	43	23	14	23	13	12
118	29	38	36	18	21	31	14	13
116	36	43	36	18	21	32	7	7
113	38	47	34	17	21	29	7	7
111	38	45	31	15	22	32	9	8
104	25	32	42	23	21	32	12	13
100	38	47	41	22	13	22	8	9
092	36	45	40	20	16	27	8	8
*123a	37	47	33	17	20	28	10	8
b	39	47	30	15	24	32	7	7
c	38	47	35	17	21	29	6	7
d	35	43	38	19	19	31	8	7
e	42	49	32	16	19	28	7	7
f	41	50	37	18	18	28	4	4

W — Weighted peak-area percentages (after Scafe & Kunze, 1971)
S — Actual peak-area percentages
* — Replicate analysis of sample on separate clay-mounts

sediment clays. It is identified by a broad reflection or band between 10 and 14 Å on the untreated diffractograms. On glycolation this reflection completely disappears. There is no evidence of any regular integral order of spacing, such as a higher order reflection at approximately 24 Å, which occurs in the soil clays. This suggests a random interlayering of 10-Å illitic material and 14-Å expandable material. The mixed-layer clays of soil and stream sediment seem to be regularly interstratified, and consist of 10-Å material and 14-Å material that has an expanding structure in some samples, but in most samples tends not to expand.

No crystalline hydroxide or oxide phase was identified in any of the samples. Amorphous material probably exists but in relatively minor amounts, as the clay-mineral diffraction maxima are usually clearly resolved from the background radiation (Figs. 53 and 54).

Quartz is ubiquitous but minor in the clay-size fraction of all samples. The strongest quartz reflection corresponds to the third-order reflection of illite at 3.3 Å, and thus the intensity of this reflection is enhanced in most samples.

It appears, then, that the clay-mineral assemblage of the estuarine sediments is very similar to the clay-mineral assemblage of the soils and stream sediment. Since there is no evidence for formation of any significantly different clay mineral in the estuarine environment, it is safe to assume that the estuarine clay-mineral assemblage is essentially of detrital origin.

Lateral variations in estuarine clay minerals

There is much discussion in the literature on whether clay minerals undergo extensive structural transformation upon entry into marine environments. Studies on Recent oceanic and deep sea clays (Biscaye, 1965; Naidu et al. 1971; Venkatarathnam & Ryan, 1971; Stoffers & Muller, 1972) have shown that the lateral and vertical variations in the clay-mineral assemblages can be attributed largely to the supply of different clay minerals from differing continental source-areas.

Various studies on estuarine clays have shown that diagenetic changes occur in estuarine clay minerals as a result of the seaward increase in water salinity. Griffin & Ingram (1955) observed that kaolinite decreased, and 'vermiculitic chlorite' and illite increased, in the downstream direction in the Neuse River estuary of North Carolina. Powers (1957) considered that chlorite-like and vermiculite clays are forming in estuaries along the Atlantic coast of the United States from the alteration of weathered illite and montmorillonite-like clays. Nelson (1960, 1963) studied the clay minerals in bottom sediments of the Rappahannock River estuary in Virginia, and found a decrease in kaolinite and dioctahedral vermiculite downstream, with a corresponding increase in illite and the appearance of a thermally stable chlorite. Nelson suggested that thermally stable chlorite is generated in the saline environment, probably from vermiculite.

Grim & Loughnan (1962) studied the clay minerals of Sydney Harbour, and found that illite increased in abundance in the outer part of the harbour relative to the inner part. They also observed a decrease in abundance of 10-Å and 14-Å mixed-layer clays in the harbour compared to mixed-layer clay abundance in the rivers draining into it. Grim & Loughnan found that the content of vermiculitic mineral decreased sharply downstream in the rivers entering the harbour. They suggested that illite develops from ferrous vermiculite. They considered that some of the Fe^{3+} present in land-derived ferric vermiculite was reduced to the Fe^{2+} form on passage from the fresh-water into the marine environment. The Fe^{2+} in the degraded vermiculite was then replaced by K^{+}, forming illite. They considered the development of illite was a slow process because of the relatively low concentration of K in marine waters, and because of the abundance of Fe^{2+} and Fe^{3+} in the bottom muds, which impeded fixation of K.

The data in Table 3, and the diffractograms of all samples analysed, suggest there is no significant areal variation in the clay mineralogy of bottom sediments throughout the Genoa River estuary. The clay-mineral assemblage in all the environments is essentially the same. The only change that is evident is the possible decrease in abundance of the mixed-layer clay mineral towards the open sea. However, this observation is tenuous, since the mixed-layer clay mineral is the least abundant of all the clay-mineral phases present, and thus the error in measurement of relative abundance is much greater.

All the previously mentioned estuaries (Neuse River, Rappahannock River, Sydney Harbour) which display lateral variation in clay-mineral assemblages in a downstream direction, have a lateral (as distinct from vertical) salinity gradient. That is, the salinity of the largest part of the water column increases laterally downstream from 0‰ to up to 25‰ and 35‰. This salinity gradient occurs gradually over the length of these estuaries. This is not the case in the Genoa River estuary, where the water column is essentially in two layers. The salinity of the largest part of the water column in the Genoa River estuary is usually 20‰ or more throughout the entire estuary. The lateral fresh water/sea water boundary is abrupt, and a significant lateral salinity gradient does not occur. Land-derived clay minerals encounter highly saline water rather abruptly, as they are transported into the estuarine realm. It is suggested that this lack of

a pronounced lateral salinity gradient in the Genoa River estuary is the dominant factor in restricting lateral variation in clay-mineral assemblages.

The land-derived clays, on passage from the fresh-water to the estuarine realm in the Genoa River estuary, have undergone very early diagenetic changes. These aspects are discussed below.

Halmyrolysis and early diagenesis of clay minerals

Since only dredge samples were obtained of the bottom sediment, and not cores, the changes occurring in the land-derived clays are documented only for the period of time from when the clays first encountered estuarine saline water until they became buried by a few centimetres of sediment. Chemical interaction between land-derived clays and sea water must proceed rapidly upon contact, because the sea-water environment is markedly different chemically from stream-water and river-water environments. Russell (1970) and Berner (1971, p. 176) apply the term 'halmyrolysis' to these rapid reactions between clay minerals and sea water. Berner used the term 'early diagenesis' for the reactions taking place in the top few metres of sediment. Using this terminology, then, both halmyrolytic changes and early diagenetic changes are represented in the clay minerals examined from the Genoa River estuary.

The estuarine clay-mineral studies previously mentioned showed that progressive changes in the clay minerals do occur from fresh-water to sea-water environments, even though these changes may not be gross in terms of large-scale structural transformations. If the theory is accepted that the oceans have remained chemically stable through time, then according to Mackenzie & Garrels (1966a, b), these clay mineral changes must occur in order that the oceans maintain this steady state. For this to happen, dissolved ionic constituents that are supplied by streams must be removed from the ocean as rapidly as they enter it (Mackenzie & Garrels, 1966a, b). Mackenzie & Garrels contend that reaction between clay and sea water to remove cations occurs immediately upon entry of land-derived clays into the marine environment and before burial. They suggest also that the clay minerals carried to the oceans by streams may not be markedly altered chemically or structurally upon entering the marine realm, but that a small part of the clay minerals, the 'amorphous alumino-silicates', react with cations and silica to form new clay minerals.

In two complementary studies of the Rio Ameca in Mexico, Russell (1970) and Drever (1971) examined the changes which occur in clay minerals when they come in contact with sea water. Russell (1970) found that the number of equivalents of cations is the same in the river clay as in the marine clay, disproving any rapid reaction between clay and sea water to remove cation alkalinity. He found that ion exchange was the only halmyrolytic reaction that occurs, and cation ratios were adjusted only to the extent of the cation-exchange capacity of the clays. Russell stated also that the clay of the Rio Ameca did not show any evidence of reaction with amorphous material which would add cation alkalinity to the clays. He found that experimental soaking of montmorillonite in sea water removed Mg, which was accompanied by a decrease in alkalinity of the solution. He suggested that montmorillonitic clay can lower the pH of a limited volume of sea water by the mechanism of $Mg(OH)_2$ adsorption, and that the $Mg(OH)_2$ may enter the montmorillonite structure to form a brucite-like interlayer of a chloritic nature. Russell considered that this reaction could be a mechanism for the removal of excess alkalinity from the ocean without invoking wholesale clay transformation or crystallization of new clay minerals from amorphous material.

Drever (1971), in a study of Banderas Bay in the Rio Ameca area, found that apart from initial cation exchange there was no general uptake of Na or K by land-derived clays in the top metre of sediment. He also proposed a mass-balance model for the ocean which did not require extensive clay-mineral transformation or synthesis of clay minerals from an amorphous starting material.

More pertinent to the present study, Drever (1971) found that the clay mineralogy did not vary significantly among the different environments in Banderas Bay. He found that the clay-size fraction, which is largely montmorillonite, has a higher content of non-exchangeable Mg, and a lower Fe content in sediments from strongly reducing environments, than in similar sediments from less reducing environments. Drever suggested that Fe leaves the montmorillonite structure to form a sulphide in the strongly reducing environments, and Mg enters the same sites, by diffusion from the overlying seawater and interstitial fluids; thus the gross clay mineralogy remains unchanged. Berner (1964) suggested that reduction with H_2S will extract Fe from chlorite, and Drever (1971) proposed it was reasonable to assume the same process may extract Fe from poorly-crystallized montmorillonite. Thus Drever, in effect, suggested that mass balance of cation alkalinity could be achieved by removal of Mg from sea water, just as Russell (1970) suggested, but that Mg was exchanged for reduced Fe in the montmorillonite structure, rather than by simple adsorption of Mg in interlayers of the clays in the hydroxide form.

In the Mallacoota study it was suggested that the vermiculite mineral derived from weathering processes formed as a result of interlayer filling, between mica-unit layers, by ferric-hydroxide and

aluminium-hydroxide complexes (Reinson, 1973). It is suggested here that on passage into the estuarine realm some of the Fe may be reduced by the same process postulated by Grim & Loughnan (1962) and Drever (1971), and Mg may be replacing some of it. This would explain why the 14-Å mineral partially expands upon entry into the estuary. It may also account for the change in the typed of mixed-layer mineral, from regularly interstratified 10-Å layers and 14-Å non-expandable layers in the soil clays, to a randomly interstratified mineral with an expandable 14-Å clay component in the estuarine clays. The sediments (basinal and deep-channel) are H_2S-rich, and black to olive-black. Upon exposure of part of the samples to the atmosphere, the Fe oxidizes rapidly, and the samples turn a rusty colour. This suggests that some Fe is present in the ferrous form in the bottom sediments.

In the estuarine clays, a trace of chloritic material may be present, because on diffractometer traces of a few 600°C heat-treated samples, a small faint peak persists at 14 Å (Fig. 53). A small amount of the vermiculitic material may be absorbing a sufficient amount of Mg in the hydroxide form, to give a brucite-like interlayer to the clay.

No significant increase in illite is evident in the estuarine clays relative to the continental clays of the Genoa River drainage basin. Berner (1971, p. 184) considers that the wholesale conversion of montmorillonitic clays to illite (and chlorite) should be observed during halmyrolysis and early diagenesis. The presence of abundant Fe^{2+} may

55. Distribution of organic carbon (percent by weight of total sediment)

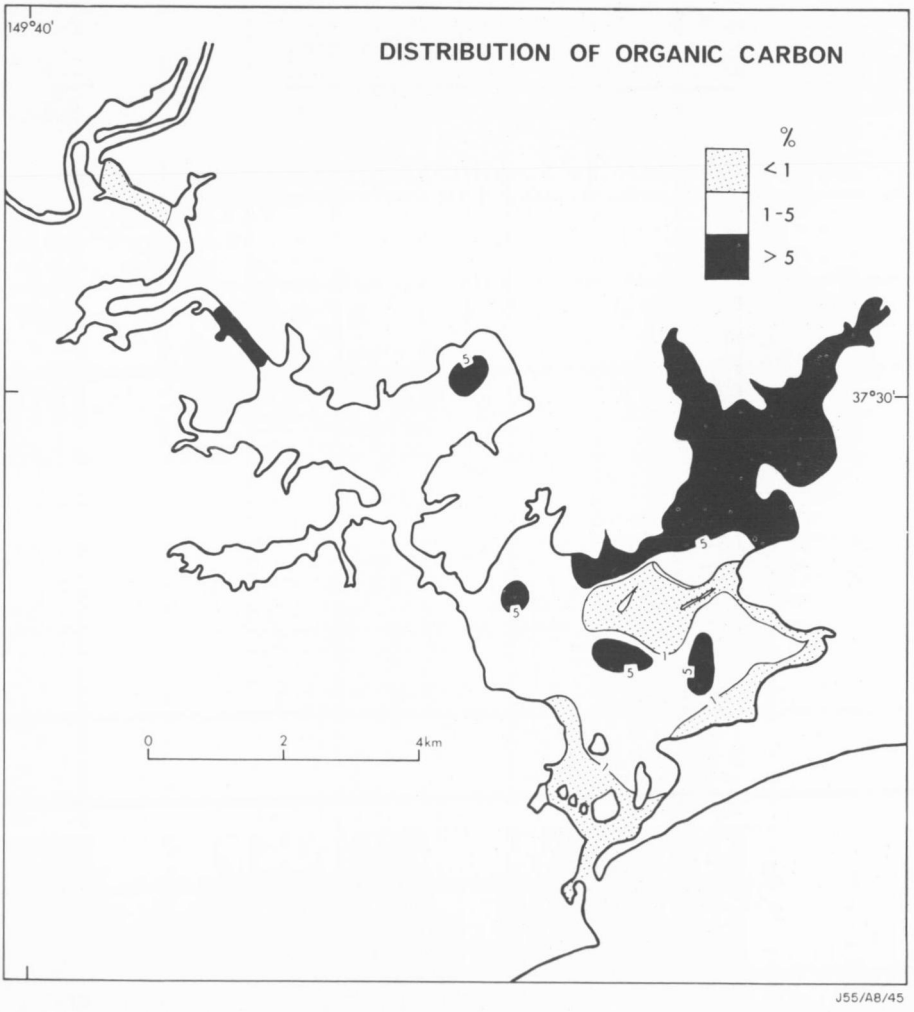

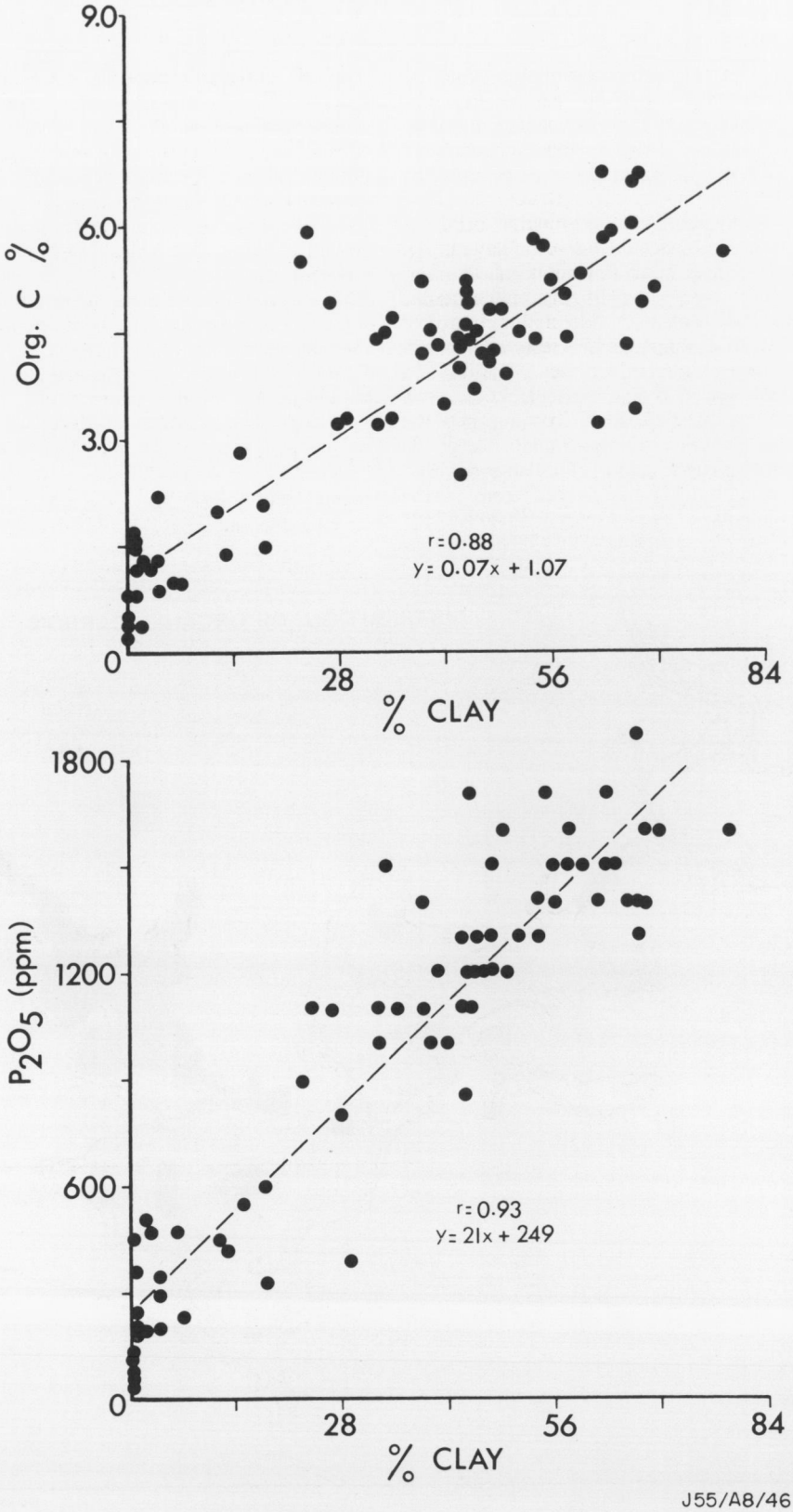

56. Relationships between organic carbon and clay content, and between phosphate and clay content

retard the fixation of K^+ (Grim & Loughnan, 1962). Alternatively, dissolved organic materials in the pore waters of bottom sediments may block interlayer sites in clays, and inhibit transformation (Berner, 1971, p. 184-185).

In conclusion, no major structural transformation of land-derived clay minerals occurs in the estuary, and the observed clay-mineral assemblage is largely a reflection of the clay minerals generated by weathering and erosional processes in the source areas. The minor changes in the land-derived clays when released to the estuarine environment, can be explained by halmyrolytic and early diagenetic reactions with sea water, as documented in the previous discussion.

GEOCHEMISTRY

Distribution of organic carbon, phosphate and transition metals

Seventy-seven bulk-sediment samples were analysed for organic carbon, P_2O_5, Ti, V, Cr, Mn, Fe, Co, Ni, Cu and Zn. The results of these analyses are given in Appendix 4. Organic carbon concentration provides a means of depicting the organic-matter component of the sediments, and is discussed along with the transition metals and P_2O_5, because it is invariably associated with certain of these chemical elements in the natural environment.

The distribution of organic carbon is shown in Figure 55 and the relationship of organic carbon to the clay-size fraction of the sediments is shown in Figure 56. Organic carbon concentrations are highest in the sediments of the Northern Basin and a few isolated areas of the Southern Basin and main river channel, and are lowest in the sand environments of the flood-tidal delta and shallow-water banks. The positive linear relationship of organic carbon with clay (Fig. 56), is further emphasized by

57. Distribution of P_2O_5 (content of total sediment)

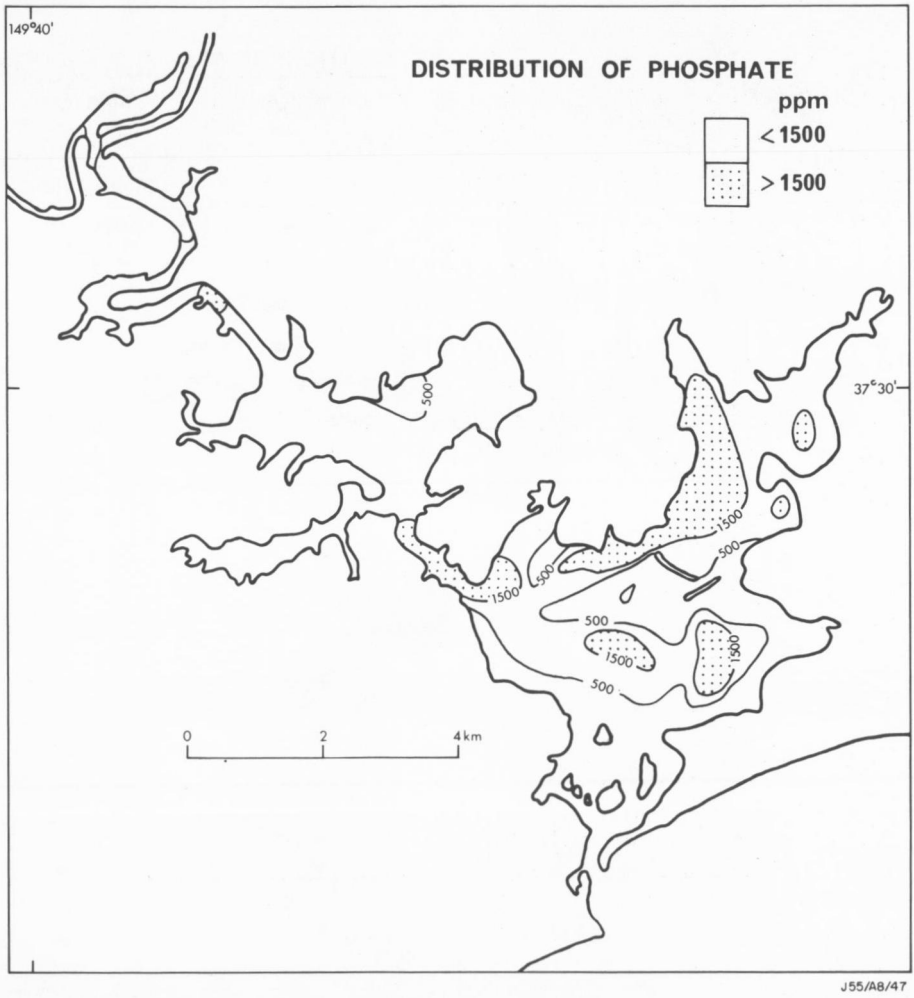

the similarity of areal distribution of high concentrations of organic carbon with high concentrations of clay (Fig. 47).

The distribution of P_2O_5 is depicted in Figure 57, and its relationship with the clay-size fraction of the sediments is shown graphically in Figure 56. The P_2O_5 distribution is similar to that of organic carbon, in that areas with high concentrations of P_2O_5 correspond to areas of high clay content. Lowest concentrations of P_2O_5 occur in the sandy sediments of the flood-tidal delta and shallow-water banks.

The distribution of the transition metals is shown in Figures 58 to 66. It is evident from these distributions that all transition metals are highly concentrated in the muddy sediments of the basinal and deep-channel environments, relative to the sandy sediments of the flood-tidal delta and shallow-water bank environments.

There are also differences between the three basinal environments and the deep-channel environment in terms of transition-metal, P_2O_5, and organic-carbon content of their sediments (Fig. 58 to 66). If average concentrations are calculated separately for the muds of each of these environments, then these differences are readily apparent (Table 4). To separate the samples which represent muddy environments from those which represent sandy environments, an arbitrary cut-off was chosen at a coarse-fraction (> 63 μm) content of 15 percent by weight (Fig. 67). Highest Fe, V, Cr, Ni, Zn, Cu, P_2O_5 and organic carbon concentrations occur in the areas where clay-size sediment is most abundant, such as the Northern Basin, the Narrows, and deeper parts of the Southern Basin.

58. Distribution of titanium in bulk-sediment samples

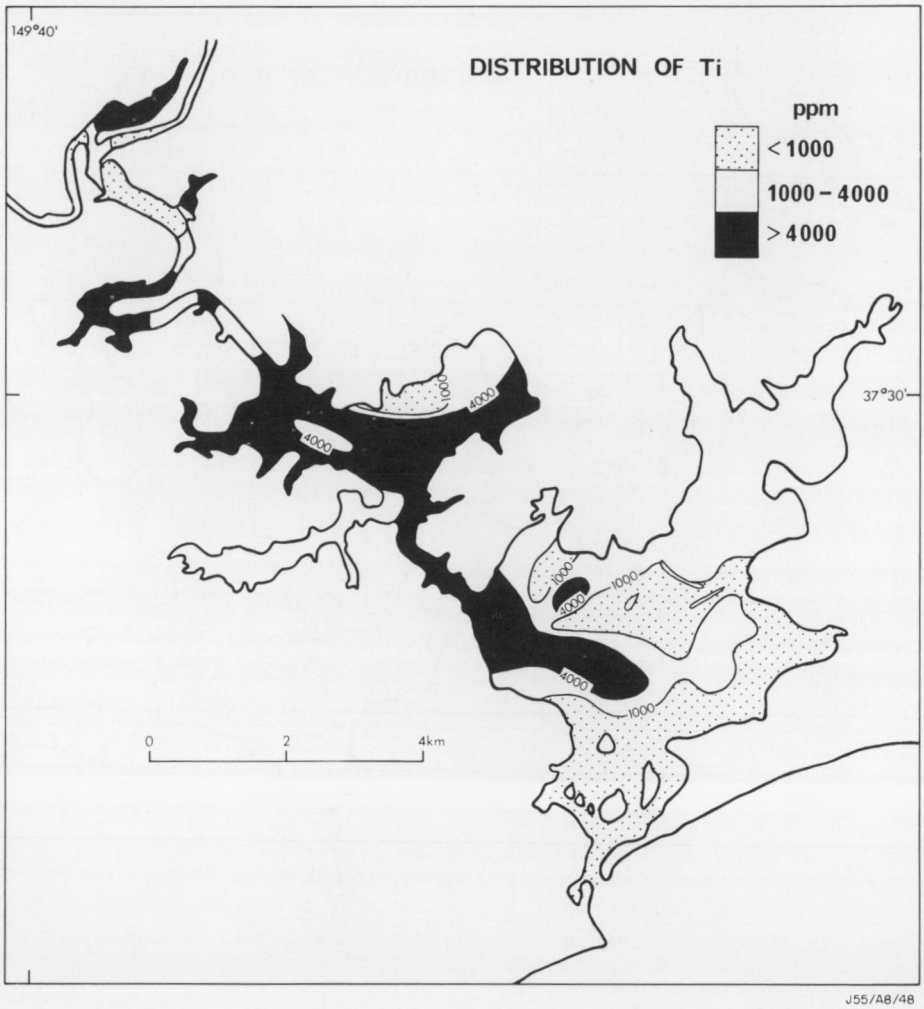

Table 4 Average concentrations of organic carbon, P_2O_5, and transition metals in mud sediments of basinal and deep-channel environments of Genoa River Estuary, in sediments of other marine basins, and in black shales (ppm except where stated).

	Upper River Channel		*Upper Lake*		*Southern Basin*		*Northern Basin*		*1*	*2*	*3*	*4*
	Mean	*Range*	*Mean*	*Range*	*Mean*	*Range*	*Mean*	*Range*	*Mean*	*Mean*	*Mean*	*Mean*
Ti	4110	3740-4330	4160	3780-4440	4100	3860-4470	3590	3290-3750	2320	—	—	2000
V	90	71-104	91	85-104	95	90-114	98	92-104	67	—	98	150
Cr	45	40-57	49	47-53	54	49-59	56	52-62	55	—	84	100
Mn	228	167-305	170	134-192	160	141-182	164	143-191	311	1130	550	150
Fe(%)	3.88	3.15-4.12	4.19	3.62-4.68	4.32	4.20-4.74	4.52	4.27-4.77	2.0	4.61	3.68	2.0
Co	15	11-20	15	12-18	13	11-17	14	8-17	8	26	12	10
Ni	21	18-23	23	20-26	25	25-26	25	24-27	26	28	67	50
Cu	13	12-17	12	11-13	13	12-15	14	13-16	34	22	30	70
Zn	71	59-78	75	69-81	75	73-81	74	71-78	64	170	—	<300
P_2O_5	1200	850-1400	1210	1000-1500	1440	1200-1700	1520	1400-1900	1600	—	1110	—
Org.C(%)	4.4	3.2-5.8	4.2	3.2-5.2	4.7	3.9-5.7	5.7	5.1-6.7	2.92	12.6	1.5	3.2
Sand(%)	7		5		5.6		3.1		11.2	—	—	—
Silt(%)	49		45		46		30		44.4	—	—	—
Clay(%)	44		50		48		64		43.8	—	—	—
$CaCO_3$(%)	0.3		0.8		2.1		3.5		2.4	—	18.3	—

1. Central basin sediment, Saanich Inlet, B.C. (Gucluer & Gross, 1964; Gross, 1967)
2. Sediments from water-depths greater than 15 m, Norwegian fjord (Piper, 1971)
3. Clay muds, Black Sea (Glagoleva, 1962)
4. Average black shale (Vine & Tourtelot, 1970)

These areas are more or less restricted, and occupied by stationary marine water for extended periods. Conversely, Mn and Ti are most concentrated in the Upper Lake and main river channel, where the sediments contain a high percentage of silt. These areas are relatively unrestricted and are influenced by fluvial discharge.

The Genoa River estuary — a partly anoxic marine basin

The water circulation of the Genoa River estuary has been shown to be 'fjord-like', in that water in its deeper parts may remain undisturbed for months at a time. The flood-tidal delta is analogous to the sill of a fjord, and restricts the circulation of water in the deeper areas of the basin behind it. The Goodwin Sands also act as a barrier, restricting the free exchange of water in and out of the Northern Basin within the estuary. Thus, the bottom waters of the Genoa estuary are stagnant and partly anoxic, similar to the waters of classical reducing marine basins, such as the Norwegian and British Columbia fjords (Ström, 1939; Piper, 1971; Gross, 1967; Gucluer & Gross, 1964; Presley et al., 1972), and the Baltic Sea (Mannheim, 1961) and Black Sea (Caspers, 1957).

Surface sediments from anoxic basins are generally characterized by high organic-matter content, H_2S odour, and a greenish-black to black colour. The sediments from the basinal areas of the Genoa River estuary have all these characteristics, and are also similar in their transition-metal content to some classical anoxic basins (Table 4).

Glagoleva (1962), Gross (1967), Piper (1971), and Presley et al. (1972), have shown that the transition-metal content of sediments from reducing marine basins are governed dominantly

59. Distribution of manganese in bulk-sediment samples

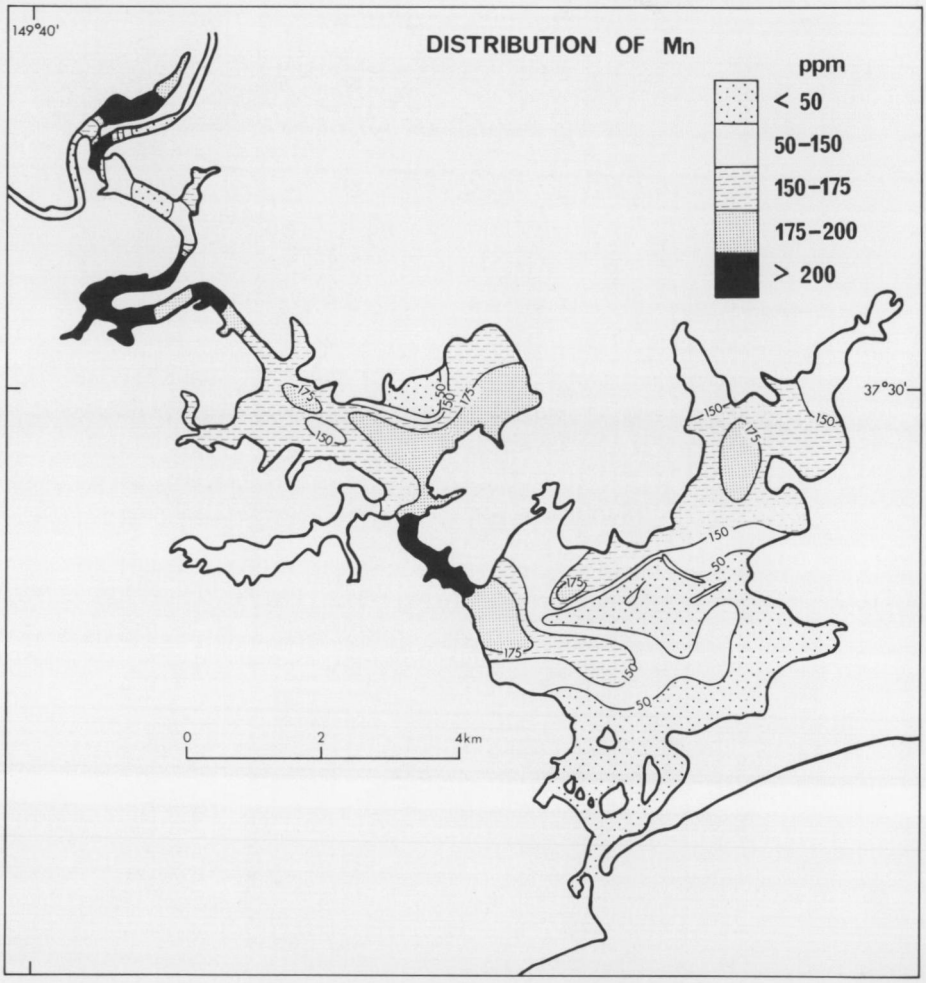

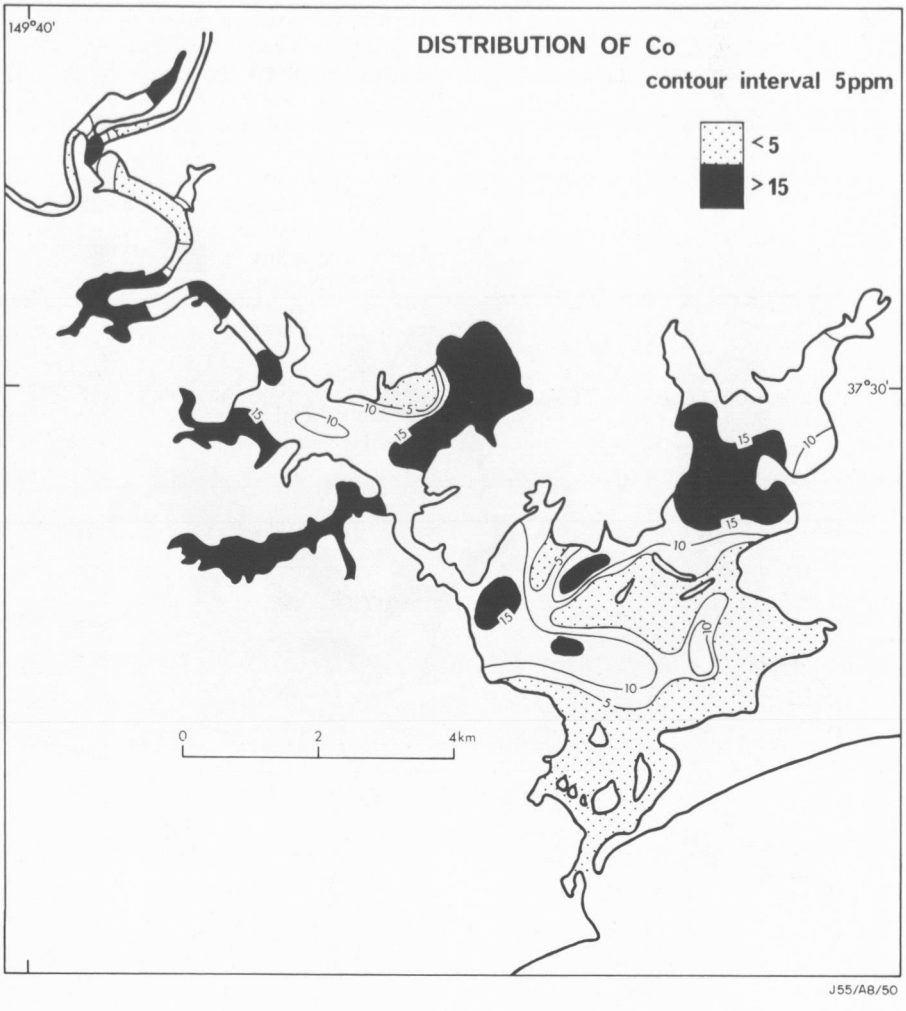

60. Distribution of cobalt in bulk-sediment samples

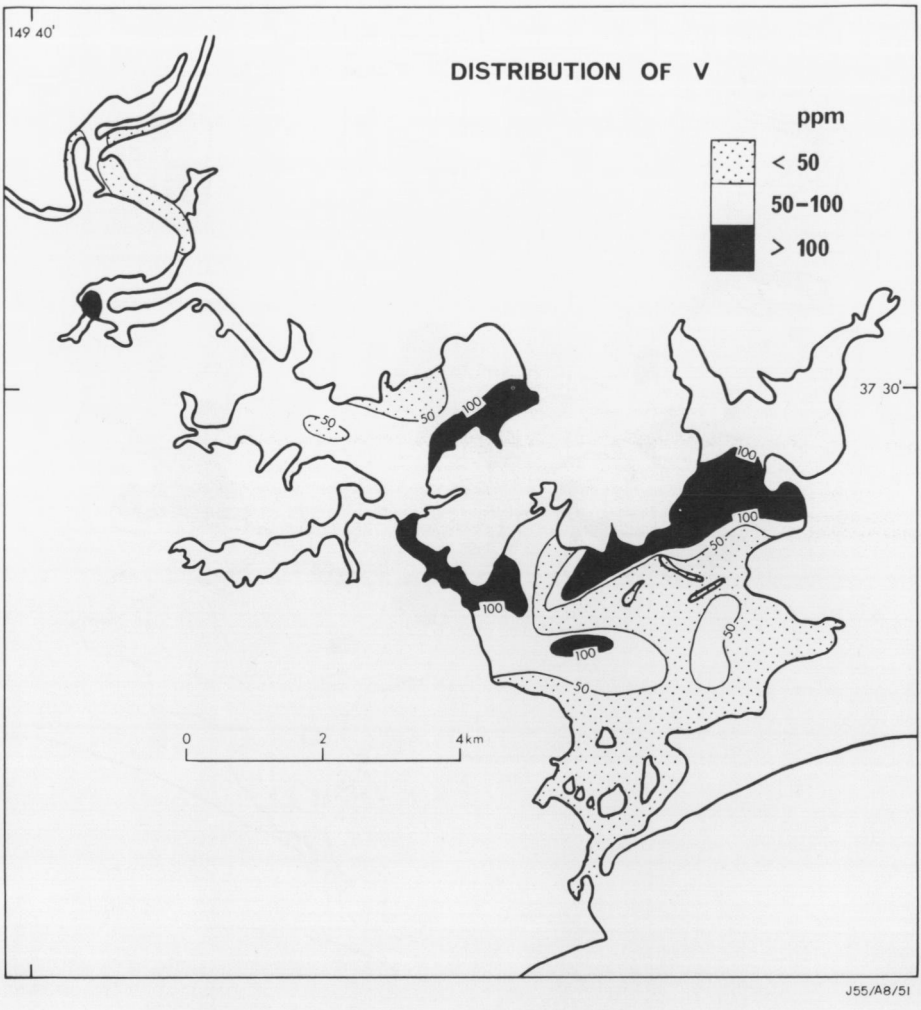

61. Distribution of vanadium in bulk-sediment samples

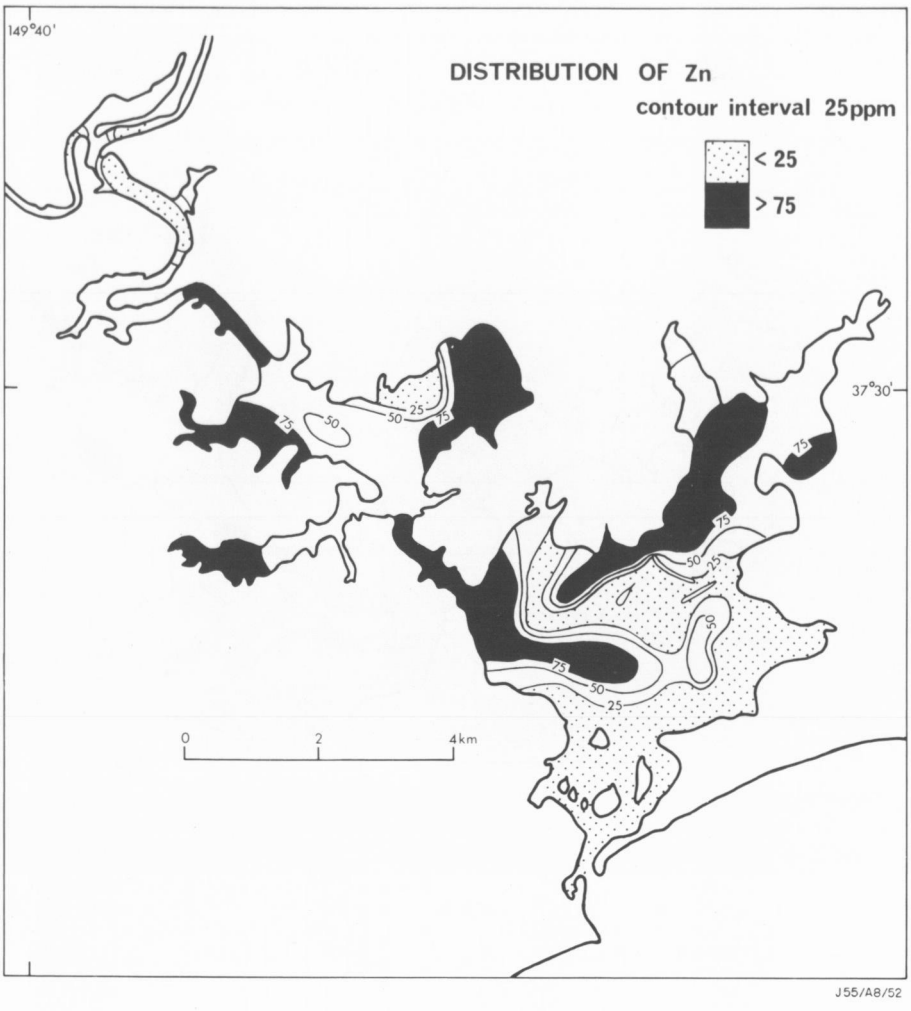

62. Distribution of zinc in bulk-sediment samples

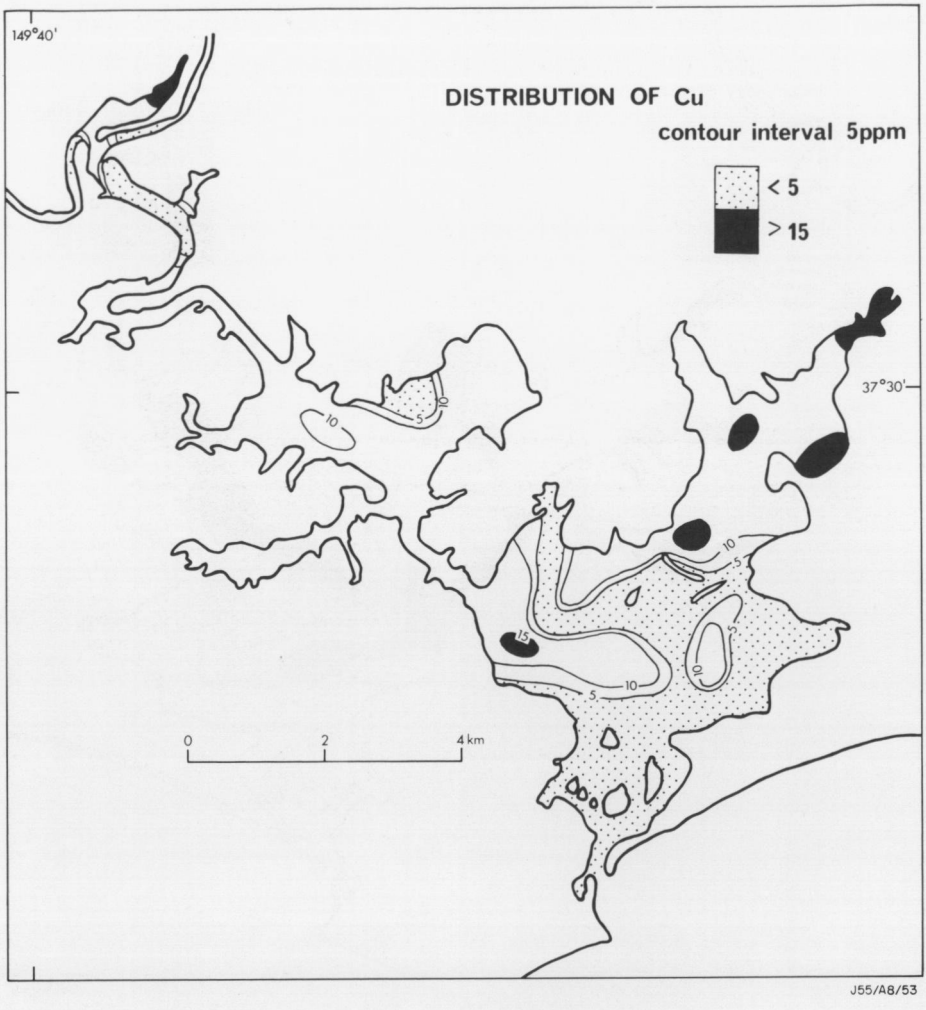

63. Distribution of copper in bulk-sediment samples

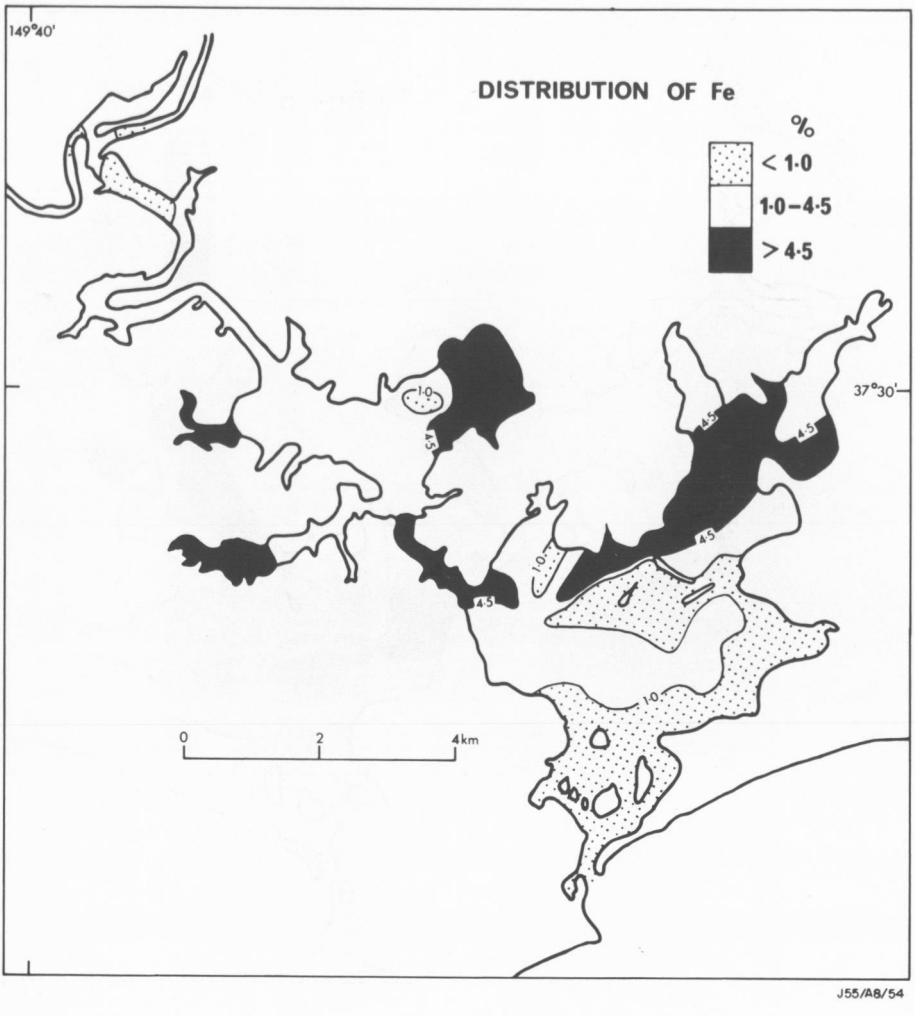

64. Distribution of iron in bulk-sediment samples

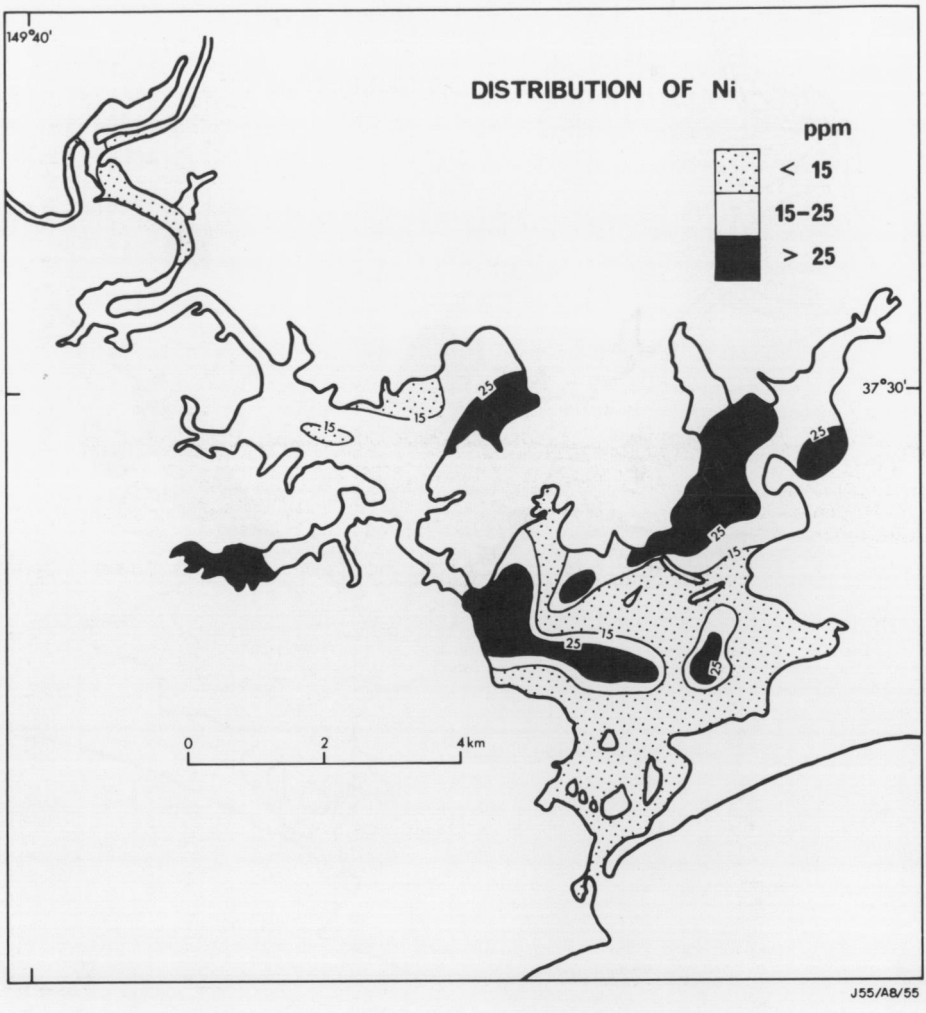

65. Distribution of nickel in bulk-sediment samples

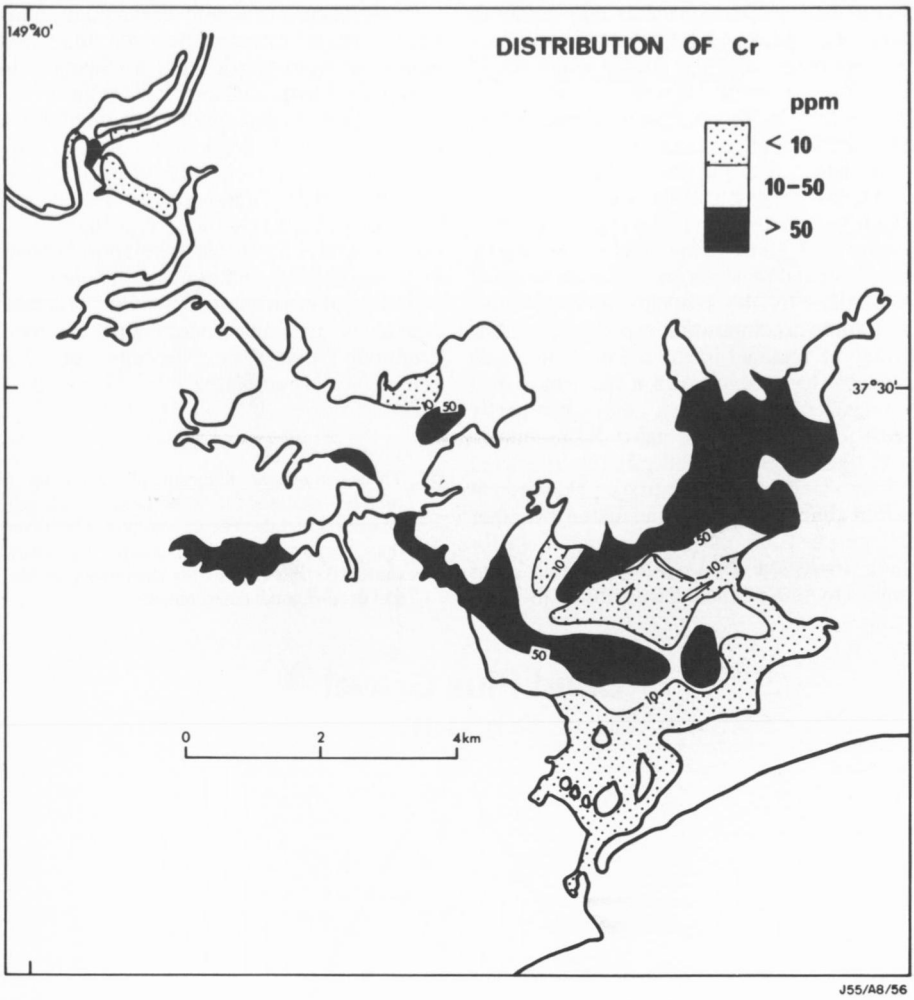

66. Distribution of chromium in bulk-sediment samples

by detrital sources, and to a very minor extent by organic matter. Very little of the transition-metal content is attributed by these workers to enrichment by removal from sea water under reducing conditions. Similar conclusions for the Genoa River estuary are recorded in another paper (Reinson, 1976).

The relationships of the transition metals and P_2O_5 to organic carbon in the muddy sediments are shown graphically in Figures 68 and 69.

Accumulation of phosphate

According to Kaplan & Rittenberg (1963) phosphorus is supplied to marine (basin) sediments in the form of organic phosphate, detrital phosphate minerals, and as phosphate adsorbed on

hydrolysates and oxidates such as clay minerals and ferric hydroxide. No detrital phosphate minerals were detected in the muddy sediments of the Genoa River estuary. Highest phosphate concentrations occur in the Northern Basin, where clay-size material and organic matter are most abundant. There is a strong positive correlation between P_2O_5 and organic carbon (Fig. 69), and between P_2O_5 and clay-size material (Fig. 57), which suggests that P_2O_5 concentrations are controlled by fine-grained detrital minerals and the abundance of organic matter. In the reducing environments, PO_4^{3-} (a soluble decomposition product of organic matter) may be retained in the sediment if excess Fe is available to combine with it (Kaplan & Rittenberg, 1963). This process may be partly responsible for the relatively higher P_2O_5 concentrations in the organic-rich and clay-rich restricted areas of the Genoa River estuary. However it appears that abundance of organic matter (whether it is decomposed or not) is the main factor controlling increased P_2O_5 concentrations over that supplied by fine-grained detrital minerals.

Phosphate is not greatly enriched in muds of the Genoa River estuary, nor for that matter in sediments from fjords such as Saanich Inlet, or large-scale basins such as the Black Sea (Table 4). In fact, ancient shales contain as much P_2O_5 (1600 ppm, Turekian & Wedepohl, 1961) as the muddy sediments of the Genoa River estuary. Thus it is apparent that lagoonal, restricted estuarine environments such as the Genoa River estuary, are not favourable for the accumulation of phosphorus in significant amounts. Therefore, such depositional environments would not appear to be analogous to the environment in which the Cambrian phosphate deposits of northwest Queensland accumulated.

67. Three-component diagram of sediments (77 bulk samples) analysed for organic carbon, phosphate, and transition metals. The 42 samples which contain less than 15 percent sand-plus-gravel are considered as characterizing the muddy sediments of the basinal and deep-channel environments

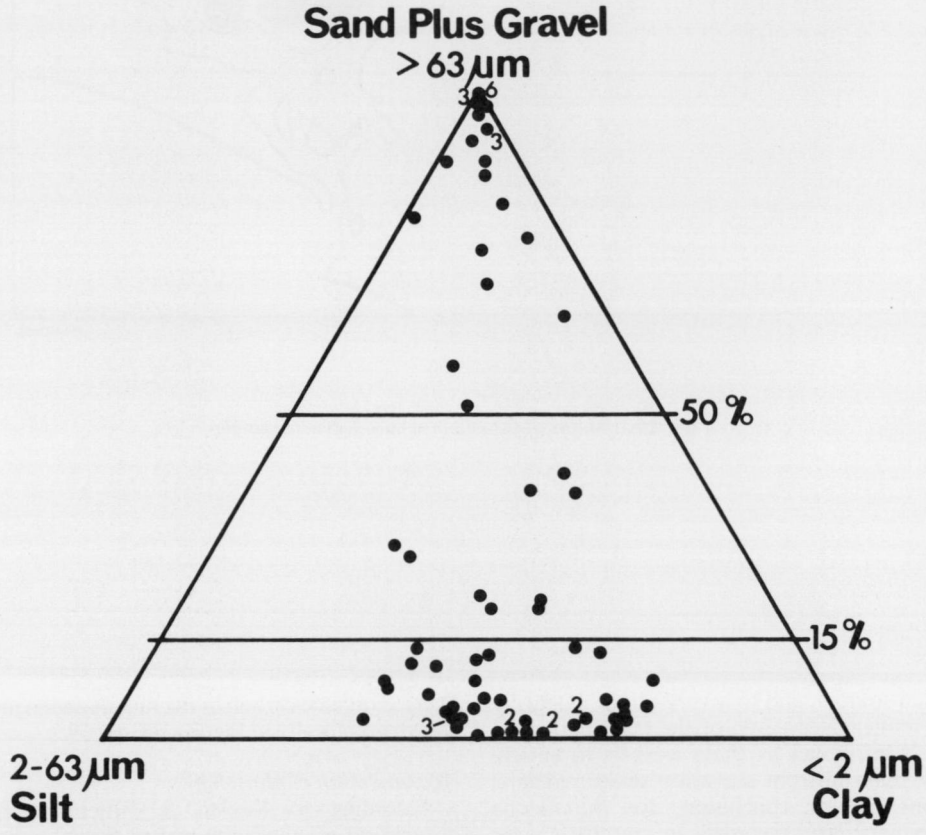

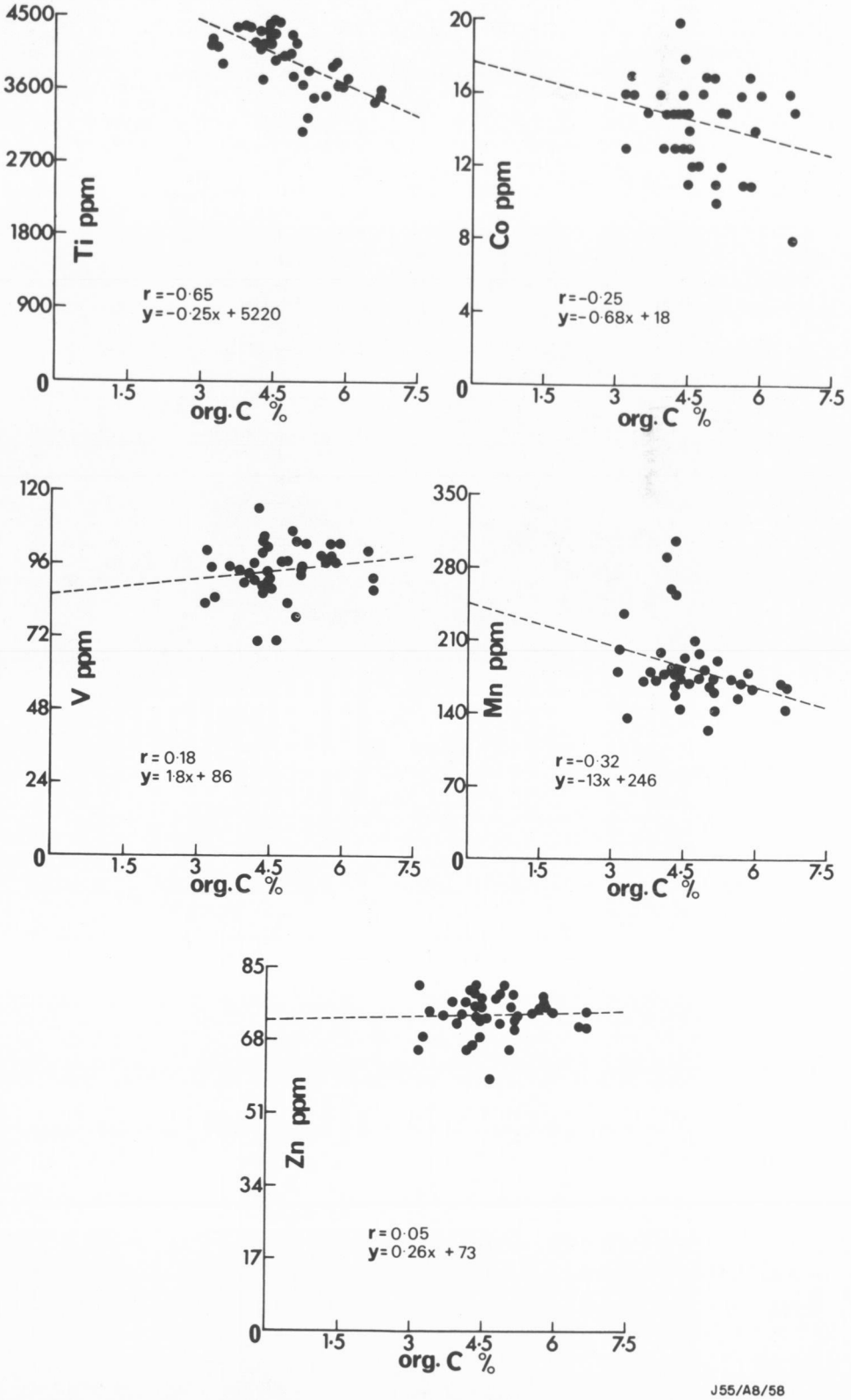

68. Relationships of Ti, V, Co, Mn, and Zn to organic carbon in muddy sediments

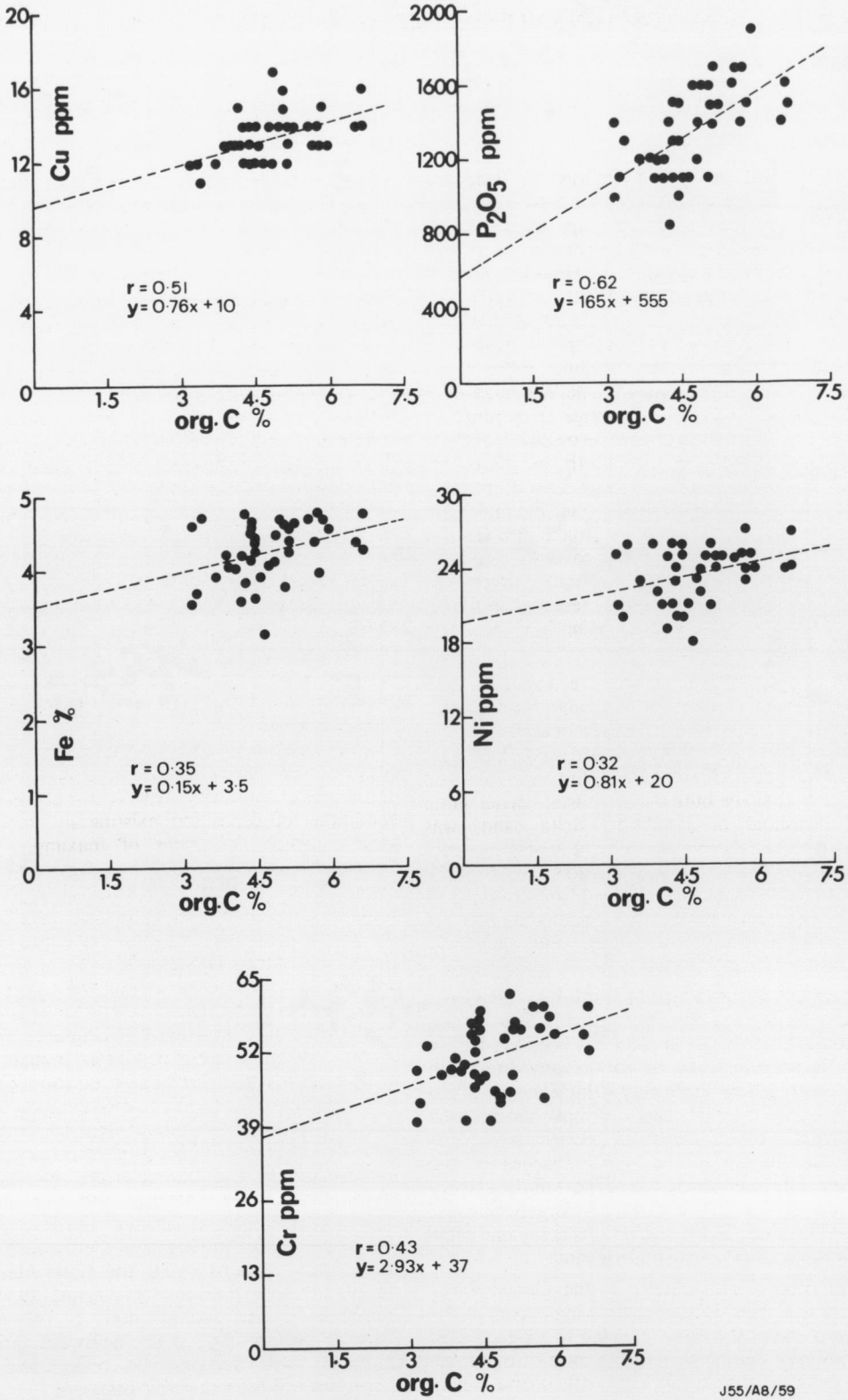

69. Relationships of Cu, Fe, P_2O_5, Ni and Cr to organic carbon in muddy sediments

SEDIMENTATION MODEL FOR THE BAR-BUILT ESTUARY

The bar-built estuary, as defined by Pritchard (1967), is a common feature of the East Australian coast from Sydney south to Cape Howe. In all cases these estuaries formed when river valleys were drowned during the early Holocene marine transgression. Subsequent growth of spits and barriers across the mouths of these estuaries during the late Holocene produced semi-enclosed estuaries and lagoons, such as Mallacoota Inlet. Examples of other estuaries of this type include Wagonga Inlet at Narooma, Birroul and Turonga lakes north of Dalmeny, Lake Illawarra, the Tuross lakes, and the numerous coastal lagoons south of Narooma. South of Mallacoota, along the East Gippsland coast, lagoonal estuaries also occur; examples are Tamboon Inlet and Sydenham Inlet. Bird (1967a, b) and Jennings & Bird (1967) have discussed the general morphology and depositional patterns of these lagoonal estuaries and noted that in-filling, shallowing and natural reclamation have occurred in varying degrees within them.

Many of these estuaries show recurrent patterns of depositional features, in particular, fluvial deltas at river mouths in the upper reaches of the estuaries, and thresholds of marine sand (flood-tidal deltas) at seaward entrances (Bird, 1967b). Bird considers that the bulk of the coastal barrier sand, and threshold or flood-tidal delta sand, was supplied by shoreward movement across the shelf during the Holocene transgression. He suggests that fluvial sand, and sand eroded from coastal outcrops, have contributed only small quantities of detritus to coastal barrier-bar, and flood-tidal deltaic deposits.

Wagonga Inlet is a typical South Coast lagoonal estuary which Bird (1967b) studied in some detail. He found that threshold sand has been washed in from the sea and blown in from coastal dunes and that the threshold itself is growing inward, filling the estuary. Fluvial sand is not contributing significantly to the threshold growth; it is being deposited mainly in the upper reaches of the estuary. The intervening basinal part of the estuary is receiving fine fluvial sediments, largely silts and clays. This finer fluvial sediment is being buried by the landward advance of marine sand.

The depositional pattern in the Genoa River estuary is similar, in that shallowing occurs at the seaward end of the estuary owing to the landward migration of marine sand in the form of the flood-tidal delta (or threshold). Very little coarse fluvial detritus extends further seaward than the Upper Lake. The basins between the upper reaches and the seaward end of the estuary are characterized by muddy sediments.

The detailed documentation of the hydrology and distribution of sediments of the Genoa River estuary supports the suggestion by Bird (1967b), that estuaries of this type along the east Australian coast are being filled in by coarse marine detritus, and very little fluvial sand is being carried through to the sea. This has important implications concerning coastal morphology and the stability of the present sediment cover on the shelf, because the quantity of nearshore sand is being depleted through permanent in-filling and reclamation of these coastal areas. As pointed out by B. G. Thom (personal communication), the reduction in volume of nearshore sands, which act as a buffer to storm-wave attack, leaves the stabilized coastal areas open to erosion by the sea. As emphasized previously, seaward erosion of the coastal barrier seems to be occurring in the Mallacoota area at the present time and progradation of the barrier seems to have stopped.

The landward infilling and formation of flood-tidal deltas in eastern Australian estuaries also has an influence on the water circulation and chemical conditions of deposition existing in the basinal areas between the zones of maximum fluvial deposition and maximum marine deposition. In the Genoa River estuary the restriction imposed on water circulation by the flood-tidal delta renders the basinal areas partially stagnant during normal runoff and during drought. This leads to anoxic conditions in the bottom waters, and halmyrolytic and early diagenetic reactions tend to occur during deposition of fine-grained sediment. Similar depositional patterns and conditions probably exist in lagoonal estuaries throughout the South Coast.

A generalized model of sedimentation in the typical southeast Australian lagoonal estuary is presented in Figure 70. Most of the estuary will be shallow-basinal and characterized by lagoonal muds, which have chemical and mineralogical compositions similar to those of fjords and large-scale restricted marine basins. If the seaward end of the estuary remains open, the flood-tidal delta (threshold) will continue to migrate landward, transgressing the basinal mud. If the marine entrance becomes sealed up, landward threshold migration will decrease or cease, and mud deposition will become dominant.

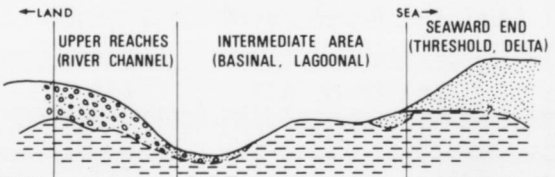

DEPOSITIONAL REALM	Fluvial	Mixed	Marine
DEPOSITIONAL RATE	Rapid-intermittent	Slow-continuous	Rapid-continuous
SEDIMENT TYPE	Dirty sand with gravel	Mud	Clean sand and gravel
DOMINANT MINERALOGY	Quartz & feldspar (rock fragments)	Clay minerals (including mica)	Quartz
DETRITAL CARBONATE	None	Rare	Common
ORGANIC MATTER	Intermediate	High (3% to 7% or more)	Low
PHOSPHATE	Intermediate	High	Low
CONDITION OF BOTTOM WATERS	Oxidizing to weakly reducing	Partially or strongly reducing	Oxidizing
ROCK EQUIVALENT	Arkosic Sandstone or lith-arkosic-sst	Shale to black shale	Quartzose sandstone

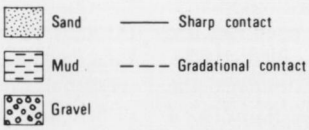

70. Sedimentation model for typical lagoonal estuary, southeastern Australia

REFERENCES

ASHTON, D. A. 1969 — Botany of East Gippsland. *Proc. R. Soc. Vic.*, 82, 69-76.

BANSE, K., FALLS, C. P. & HOBSON, L. A., 1963 — A gravimetric method for determining suspended matter in sea water using Millipore filters. *Deep Sea Res.*, 10, 639-42.

BERNER, R. A., 1964 — Iron sulfides from aqueous solution at low temperatures and atmospheric pressure. *J. Geol.*, 72, 293-306.

BERNER, R. A., 1971 — PRINCIPLES OF CHEMICAL SEDIMENTOLOGY. *New York, McGraw-Hill.*

BIRD, E. C. F., 1964 — COASTAL LANDFORMS. *Canberra, Aust. Nat. Univ. Press.*

BIRD, E. C. F., 1965 — A GEOMORPHOLOGICAL STUDY OF THE GIPPSLAND LAKES. *Canberra, Aust. Nat. Univ. Press.*

BIRD, E. C. F., 1967a — Coastal lagoons of southeastern Australia. *In* JENNINGS, J. N. & MABBUTT, J. A., (Eds.), LANDFORM STUDIES FROM AUSTRALIA AND NEW GUINEA. *Canberra, Aust. Nat. Univ. Press,* 365-85.

BIRD, E. C. F., 1967b — Depositional features in estuaries and lagoons on the south coast of New South Wales. *Aust. Geogr. Studies,* 5, 113-24.

BISCAYE, P. E., 1965 — Mineralogy and sedimentation of Recent deep-sea clay in the Atlantic Ocean and adjacent seas and oceans. *Bull. geol. Soc. Amer.*, 76, 803-32.

BOWDEN, K. F., 1967 — Circulation and diffusion. *In* LAUFF, G. H. (Ed.), ESTUARIES *Publ. Amer. Ass. Adv. Sci.* 83, 15-36.

BROWN, G. (Ed.), 1961 — THE X-RAY IDENTIFICATION AND CRYSTAL STRUCTURES OF CLAY MINERALS *London, Mineralogical Soc.*

CARNE, J. E., 1897 — Geology of the southeast border of New South Wales. *Dep. Mines N.S.W. Ann. Report for 1896,* 100.

CARNE, J. E., 1898 — Report on the geology and mineral resources of the southeast border of New South Wales between Cape Howe and the head of the Murray River. *Dep. Mines N.S.W. Ann. Rep. for 1897,* 151-60.

CASPERS, H., 1957 — The Black Sea and the Sea of Azov. *In* HEDGPETH, J. W. (Ed.), TREATISE ON MARINE ECOLOGY AND PALEOECOLOGY, V. 1. *Mem. geol. Soc. Amer.*, 67, 801-89.

COASTAL RESEARCH GROUP, UNIVERSITY OF MASSACHUSETTS, 1969 — Coastal environments of Northeastern Massachusetts and New Hampshire. Guidebook, *Soc. econ. Paleont. Miner.*, Eastern Section field trip, May, 1969.

COOK, P. J. & MAYO, W., in press — Sedimentology and Holocene history of a tropical estuary (Broad Sound, Queensland). *Bur. Miner. Resour. Aust. Bull.* 170.

DE KEYSER, F. & COOK, P. J., 1972 — Geology of the Middle Cambrian phosphorites and associated sediments of northwestern Queensland. *Bur. Miner. Resour. Aust. Bull.* 138.

DREVER, J. I., 1971 — Early diagenesis of clay minerals, Rio Ameca basin, Mexico. *J. sediment. Petrol.*, 41, 982-94.

DUN, W. S., 1897 — The occurrence of Lower Silurian graptolites in New South Wales. *Geol. Surv. N.S.W. Rec.* 5, 124-27.

DUN, W. S., 1898 — The occurrence of Devonian plant-bearing beds on the Genoa River. *Geol. Surv. N.S.W. Rec.* 5, 124.

EASTON, A. K., 1970 — THE TIDES OF THE CONTINENT OF AUSTRALIA. *Res. Pap. Horace Lamb Cent. Oceanogr. Res., Flinders Univ. S.A.*, No. 37.

FOLK, R. L., 1968 — PETROLOGY OF SEDIMENTARY ROCKS. *Austin, Hemphills.*

GEOLOGICAL SOCIETY OF AMERICA, 1951 — Rock-Color Chart. *New York, Geol. Soc. Amer.*

GEOLOGICAL SURVEY OF VICTORIA, 1967 — Mallacoota, Vic. 1:250 000 geological Series J55-8, Provisional Edition.

GIBBS, R. J., 1967 — Quantitative X-ray diffraction analysis using clay mineral standards extracted from the samples to be analysed. *Clay Minerals,* 7, 79-90.

GIBSON, D. L., 1971 — The solid and surficial geology of the catchment of the Upper Genoa River, New South Wales and Victoria. *B.Sc. thesis, Aust. Nat. Univ.* (unpubl.).

GLAGOLEVA, M. A., 1962 — Regularities in the distribution of chemical elements in modern sediments of the Black Sea. *Dokl. (Proc.) Acad. Sci. USSR* (Geochem. Sect.), 136, 1-4.

GRIFFIN, G. M. & INGRAM, R. L., 1955 — Clay minerals of the Neuse River estuary. *J. sediment. Petrol.*, 15, 194-200.

GRIM, R. E., 1968 — CLAY MINERALOGY. *New York, McGraw-Hill.*

GRIM, R. E. & LOUGHNAN, F. C., 1962 — Clay minerals in sediments from Sydney Harbour, Australia. *J. sediment. Petrol.*, 32, 240-48.

GROSS, M. G., 1967 — Concentration of minor elements in diatomaceous sediments of a stagnant fjord. *In* LAUFF, G. H. (Ed.), ESTUARIES, *Publ. Amer. Ass. Adv. Sci.* 83, 273-82.

GUCLUER, S. M. & GROSS, M. G., 1964 — Recent marine sediments in Saanich Inlet, a stagnant marine basin. *Limnol-Oceanogr.*, 9, 359-76.

HAILS, J. R. & HOYT, J. H., 1968 — Barrier development on submerged coasts: Problems of sea-level changes from a study of the Atlantic coastal plain of Georgia, U.S.A., and parts of the East Australian coast. *Z. Geomorph., Supplementband,* 7, 24-55.

HALL, L. R., 1959 — Mallacoota (N.S.W. portion), 1:250 000 geological series J55-8. *Dep. Mines. N.S.W. explan. Notes,* 3-16.

HARTWELL, A. D., 1970 — HYDROGRAPHY AND HOLOCENE SEDIMENTATION OF THE MERRIMACK RIVER ESTUARY, MASSACHUSETTS. *Amherst, Coastal Research Center, Univ. Massachusetts,* Cont. No. 5.

HORNE, R. A., 1969 — MARINE CHEMISTRY. *New York, Wiley-Interscience.*

HORRER, P. L., 1967 — Methods and devices for measuring currents. *In* LAUFF, G. H. (Ed.), ESTUARIES. *Pub. Amer. Ass. Adv. Sci.* 83, 80-92.

JENNINGS, J. N. & BIRD, E. C. F., 1967 — Regional geomorphological characteristics of some Australian estuaries. *In* LAUFF, G. H. (Ed.), ESTUARIES. *Publ. Amer. Ass. Adv. Sci.* 83, 121-28.

KAPLAN, I. R. & RITTENBERG, S. C., 1963 — Basin sedimentation and diagenesis. *In* HILL, M. N. (Ed.), THE SEA (3). *New York, Wiley-Interscience*, 583-619.

LANGFORD-SMITH, T. & THOM, B. G., 1969 — New South Wales coastal morphology. *J. geol. Soc. Aust.*, 16, 572-80.

LINDFORTH, D. J., 1969 — The climate of East Gippsland. *Proc. Roy. Soc. Vic.*, 82, 27-36.

MACKENZIE, F. T. & GARRELS, R. M., 1966a — Chemical mass balance between rivers and oceans. *Amer. J. Sci.*, 264, 507-25.

MACKENZIE, F. T. & GARRELS, R. M., 1966b — Silica-bicarbonate balance in the ocean and early diagenesis. *J. sediment. Petrol.*, 36, 1075-84.

MANHEIM, F. T., 1961 — A geochemical profile in the Baltic Sea. *Geochim. cosmoch. Acta*, 25, 52-70.

NAIDU, A. S., BURRELL, D. C. & HOOD, D. W., 1971 — Clay mineral composition and geological significance of some Beaufort Sea sediments. *J. sediment. Petrol.*, 41, 691-94.

NELSON, B. W., 1960 — Clay mineralogy of the bottom sediments, Rappahannock River, Virginia. *In* SWINEFORD, Ada (Ed.), CLAYS AND CLAY MINERALS (Proc. 7th Nat. Conf., Washington, 1958). *London, Pergamon*, 135-47.

NELSON, B. W., 1963 — Clay mineral diagenesis in the Rappahannock estuary: an explanation. *In* BRADLEY, W. F. (Ed.), CLAYS AND CLAY MINERALS (Proc. 11th Nat. Conf., Ottawa, 1962). *Oxford, Pergamon*, 210.

NEW SOUTH WALES CONSERVATION AND IRRIGATION COMMISSION, 1968 — Water Resources of the Towamba and Genoa valleys. *Wat. Conserv. Irrig. Comm. N.S.W. Rep.*, 10.

PIERCE, J. W. & SIEGEL, F. R., 1960 — Quantification in clay mineral studies of sediments and sedimentary rocks. *J. sediment. Petrol.*, 39, 187-93.

PIPER, D. Z., 1971 — The distribution of Co, Cr, Cu, Fe, Mn, Ni and Zn in Framvaren, a Norwegian anoxic fjord. *Geochim. cosmoch. Acta*, 35, 531-50.

POWERS, M. C., 1957 — Adjustments of land-derived clays to the marine environment. *J. sediment. Petrol.* 27, 355-72.

PRESLEY, B. J., KOLODNY, Y., NISSENBAUM, A., & KAPLAN, I. R., 1972 — Early diagenesis in a reducing fjord, Saanich Inlet, British Columbia, II- Trace element distribution in interstitial water and sediment. *Geochim. cosmoch. Acta*, 36, 1073-90.

PRITCHARD, D. W., 1967 — What is an estuary: physical viewpoint. In LAUFF, G. H. (Ed.), ESTUARIES. *Publ. Amer. Ass. Adv. Sci.*, 83, 3-5.

REINSON, G. E., 1973 — Aspects of weathering and sedimentation in the Genoa River basin and estuary, N.S.W.-Vic. *Ph.D. thesis, Aust. Nat. Univ.* (unpubl.).

REINSON, G. E., 1976 — Hydrogeochemistry of the Genoa River basin, New South Wales-Victoria. *Aust. J. Mar. Freshwat. Res.*, 27, 165-86.

RUSSELL, K. L., 1970 — Geochemistry and halmyrolysis of clay minerals, Rio Ameca, Mexico. *Geochim. cosmoch. Acta*, 34, 893-907.

SCAFE, D. W. & KUNZE, G. W., 1971 — A clay mineral investigation of six cores from the Gulf of Mexico. *Mar. Geol.*, 10, 69-85.

STEINER, J., 1966 — Depositional environments of the Devonian rocks of the Eden-Merimbula area, N.S.W. Ph.D. thesis, *Aust. Nat. Univ.* (unpubl.).

STOFFERS, P. & MÜLLER, G., 1972 — Clay mineralogy of Black Sea sediments. *Sedimentol.*, 18, 113-21.

STRAHLER, A. N., 1969 — PHYSICAL GEOGRAPHY. *New York, John Wiley and Sons.*

STRÖM, K. M., 1939 — Land-locked waters and the deposition of black muds. *In* TRASK, P. D. (Ed.), RECENT MARINE SEDIMENTS, A SYMPOSIUM. *Tulsa, Amer. Ass. Petrol. Geol.*, 356-72.

THOM, B. G., 1965 — Late Quaternary coastal morphology of the Port Stephens-Myall Lakes area, N.S.W. *J. Roy. Soc. N.S.W.* 98, 23-36.

TUREKIAN, K. K. & WEDEPOHL, K. H., 1961 — Distribution of the elements in some major units of the earth's crust. *Bull. geol. Soc. Amer.*, 72, 175-92.

VENKATARATHNAM, K. & RYAN, W. B. F., 1971 — Dispersal patterns of clay minerals in the sediments of the eastern Mediterranean Sea. *Mar. Geol.*, 11, 261-82.

VINE, J. D. & TOURTELOT, E. B., 1970 — Geochemistry of black shale deposits — a summary report. *Econ. Geol.*, 65, 253-72.

WILLIS, J. H., 1969 — Census of vascular flora indigenous to East Gippsland. *Proc. Roy. Soc. Vic.*, 82, 77-103.

APPENDIX 1
METHODS USED IN PREPARATION AND ANALYSIS OF SEDIMENT SAMPLES

Laboratory preparation and procedures

Figure A1 is a flow diagram which shows the procedures followed in the various analyses. There were three basic lines of analytical procedure: preparation and determination of major grain-size fractions; separation and preparation of sand, silt and clay fractions for mineralogical analysis; and preparation of bulk samples for chemical analysis.

Preparation and determination of grain size, and separation of samples for mineralogical analysis

Most samples consisted mainly of mud, so they were split by quartering while wet until the desired size of sample was reached. The mud samples were not dried because it would have been difficult to disaggregate them after baking. Samples which consisted predominantly of sand-sized material were dried at 40°C, and then split with a chamber-sample splitter. The samples were then treated with 10-percent H_2O_2 in a water bath to remove organic matter. Following this, the samples were washed two or three times with distilled water to remove sea-water salts and enhance dispersion. Next, samples were dispersed in 250 ml of 0.1 N sodium oxalate solution in an ultrasonic bath for 15 minutes. After dispersion the sample was wet sieved with distilled water through a 63 μm sieve. The material retained on this sieve was kept for mineralogical analysis. In addition, the samples which contained gravel were sieved through a 2000 μm sieve, and the proportion of gravel determined by weighing. The mud fraction was subjected to a pipette analysis according to the procedures described by Folk (1968). Thus, the percentages by weight of four size fractions of each sample were obtained. A suspension of the clay-size fraction was decanted from the pipetting cylinder and retained for clay mineral analysis.

About 250 ml of suspension was extracted from the mud fraction of each suspended sample, and the clay-size fraction was removed by repeated centrifuging, using the method described by Hathaway (1956). The silt-size fraction was dried and retained for mineralogical analysis.

Preparation for chemical analysis

About 1 kg of wet sample was split from each bulk sample by quartering, and dried at 40°C. The samples were not washed before drying, because it was felt that washing might remove some heavy metals such as iron from the sample. The samples were then ground and mixed in an agate ball mill to produce a homogeneous powder, ready for any form of chemical analysis.

Methods in mineralogical analysis

Sand-size fraction

The sand-size fraction of each sample was treated with 1N HCl to remove carbonates. The coarse sand-size fraction (larger than 500 μm) was then separated by sieving, and the fine to medium sand-size fraction (63 μm to 500 μm) retained for mineral identification.

A micro-split of the fine to medium sand was then stained for feldspar identification (Hayes & Klugman, 1959). The composition of each sample was determined by counting 400 or more grains in randomly selected grid-squares under the binocular microscope. The samples were also counted in a similar manner before feldspar staining because the staining technique appeared to destroy most mica particles. From these two counting procedures the percentages of the major minerals present in the 63 μm to 500 μm fraction of each sample were obtained.

Silt-size fraction

The silt-size fraction obtained by centrifuging was ground with a mortar and pestle and analysed by X-ray diffraction. Each sample powder was pressed into an aluminium holder and irradiated with a standard Phillips X-ray unit operated at 40 kV and 24 ma, using Ni-filtered Cu K α radiation. The samples were scanned in the range 2° to 50°2Θ using 1°, 0.2°, and 1° slits, at a speed of 2°2Θ per minute. Full-scale deflection of 2 x 10 cps and a time constant of 4 were found to be the optimum working conditions for inter-sample comparison of the ranges of minerals in the samples.

Relative abundance of the major minerals in the silt-size fractions of the samples was determined by a method similar to that described by Schultz (1964). The three main minerals in the silt-size fraction are quartz, feldspar and clay minerals. The abundance of quartz and feldspar is interpreted from the strongest diffraction peaks for each mineral. These are the quartz peak at 26.6°2Θ, and the feldspar peaks at 27.5° and 28°2Θ.

The intensities of these peaks were compared to intensity factors derived by irradiating prepared mixtures of known amounts of feldspar in a clay-size material (smaller than 1 μm) derived from the estuarine muds by centrifuging. The standards then had an absorption factor similar to the actual samples. The standards were mixed in a similar proportion to the composition range of the minerals in the samples and were as follows, in percent by weight:

	Quartz	*Feldspar*	*Clays*
Mix 1	70	10	20
Mix 2	60	15	25
Mix 3	50	20	30
Mix 4	40	25	35
Mix 5	30	30	40
Mix 6	20	35	45
Mix 7	10	40	50

The set of standard mixtures was prepared using a plagioclase-orthoclase mixture containing about 65 percent plagioclase. From these data intensity curves were constructed for feldspar and quartz. The feldspar curve was constructed by adding the intensities of the two feldspar peaks. In most samples, feldspar content was too low to distinguish the two types accurately. These curves were used to estimate the amount of quartz and feldspar in each sample, by comparing the intensities of the quartz and feldspar in the samples to those in the standards. Total amount of clay minerals was derived by assuming that the percentage of the sample which is not quartz and feldspar constitutes the clay-mineral portion. The estimated clay-mineral percentages are probably too high and most likely include amorphous material, iron oxides, and other minor constituents.

Schultz (1964) suggested that errors of up to +10 percent are probable using a method such as this, and that minerals present in amounts of 2 percent or less are not always detected. Despite this, the method is considered adequate for obtaining the relative composition of groups of samples.

Clay-size fraction

The minus-2 μm fraction was mounted on ceramic discs, 19 mm in diameter, which fit the spinner attachment of the X-ray diffractometer. These oriented mounts were obtained by mounting the ceramic tile on a vacuum-suction apparatus, which was then placed into a suspension of the minus-2 μm fraction. The clay particles were sucked on to the disc, and after a sufficient amount of material had adhered to it, the disc was then allowed to dry at room temperature.

The oriented mounts of clay-size material were irradiated with standard Philips diffraction equipment which was operated at 40 kV and 24 ma, using Ni-filtered Cu K α radiation. The samples were irradiated using ¼° entrance and exit slits, and a 0.1° scatter slit, at 1°2Θ per minute with a chart speed of 800 mm/hr.

Four diffractograms were obtained of each oriented clay mount:

1) Untreated; scanned from 2° to 32°2Θ,
2) saturated with ethylene glycol in a vacuum desiccator for 24 hr; scanned from 2° to 14°2Θ,
3) Heat-treated at 450°C for 30 minutes; scanned from 2° to 26°2Θ,
4) heat-treated at 600°C for 1 hour; scanned from 2° to 26°2Θ.

An additional diffractogram or 'slow-scan' (Biscaye, 1964), was obtained on half of the samples, in the range 24 to 26°2Θ. The conditions used were a scanning speed of $^1/_8$°2Θ/minute, chart speed of 400 mm/hr, ¼° entrance and exit slits, and a 0.1° scatter slit.

Calcium Carbonate

The method outlined by Walraven (1968), which is a modification of that described by Hulseman (1966), was used to determine the amount of $CaCO_3$ in the samples. In this method, a known quantity of sample is treated with 2N HCl in a closed container attached to a manometer filled with kerosene. The volume of gas evolved, which is assumed to be entirely CO_2, is measured by the displacement of kerosene in the manometer. Calcium carbonate in percent by weight is then calculated from the known quantity of sample used and CO_2 evolved. Hulseman (1966) suggested that other components of the sample may interfere to some extent by generating gas other than CO_2. In particular, FeS if present in sufficient quantity may generate H_2S. Iron sulfide is present in most of these samples but the degree to which it interferes with this determination is considered to be negligible. Many samples which displayed colour and odour indicative of sulfide presence gave insignificant readings for $CaCO_3$.

Repeat analyses of a 5-percent $CaCO_3$ standard gave an average of 4.9 percent with a reproducibility within ± 6 percent. Six analyses of a sample containing 23 percent $CaCo_3$ gave a reproducibility within ± 2 percent. The results appear to be sufficiently reliable for inter-sample comparison and comparison of groups of samples.

Methods in chemical analysis

Organic carbon

Organic carbon was determined on 77 samples using the method described by Bush (1970). In this method a known weight of sample is treated with warm phosphoric acid to remove carbonates. Then 2 ml of 150-percent (w/v) CrO_3 solution is added to the sample and boiled for 15 minutes. The CO_2 evolved is caught in $Ba(OH)_2$. The $Ba(OH)_2$ is then titrated with HCl, and CO_2 in percent by weight is calculated.

A standard mixture of 4 percent organic carbon was prepared using Analar glucose and pure silica sand. Precision based on 12 determinations of the 4-percent organic standard and an actual sample, was ± 7 percent.

Phosphate

The samples were analysed for phosphate by the Australian Mineral Development Laboratories.

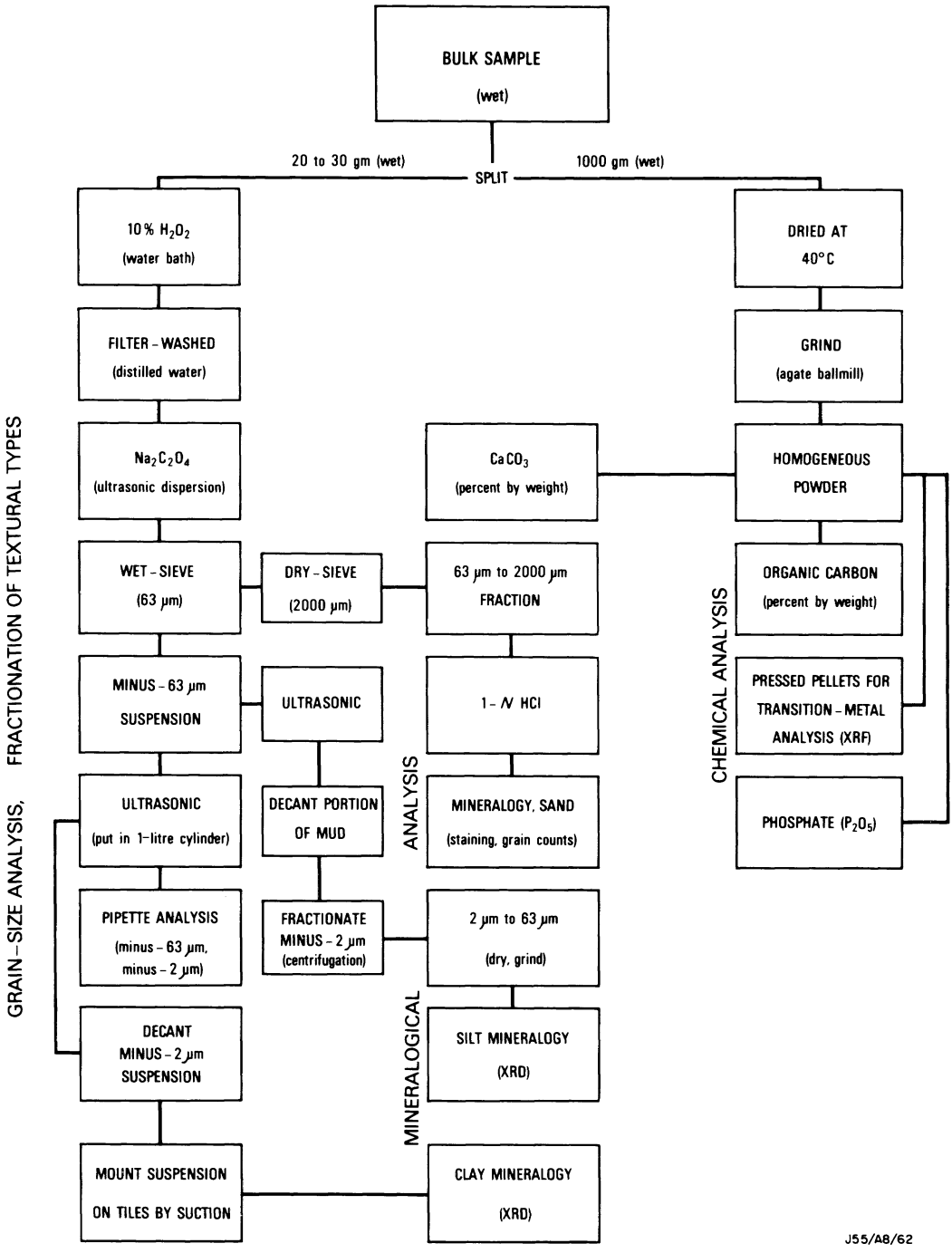

A1. Flow diagram of procedure followed in the analyses of estuarine bottom sediments

Phosphate was determined colorimetrically as P_2O_5, using the vanadomolybdate method. Precision of the method was reported as ± 5 percent or better, at the levels of concentration found in these samples.

Transition metals

Concentrations of Ti, V, Cr, Mn, Fe, Co, Ni, Cu and Zn were determined by X-ray fluorescence spectrography using the methods described by Norrish & Chappell (1967). Undiluted pellets of the powdered samples were prepared in duplicate and measured directly. Mass absorption coefficients for Fe and Zn were measured on sample powders diluted with cellulose. All transition-metal measurements were made in duplicate on separate pellets, using the following analytical conditions:

	X-ray tube	*Analytical line*	*Crystal*	*Coll.*	*Detector*	*Abs. coeff.*	*Emp. low-limit detection (p.p.m.)*
Ti	W	K	LiF (200)	F	F.C.	Fe	20
V	W	K	LiF (220)	F	F.C.	Fe	2
Cr	W	K	LiF (200)	F	F.C.	Fe	2
Mn	W	K	LiF (200)	F	F.C.	Fe	2
Fe	Au	K	LiF (200)	C	S.C.	Fe	20
Co	Au	K	LiF (200)	C	S.C.	Fe	2
Ni	Au	K	LiF (200)	C	S.C.	Zn	2
Cu	Au	K	LiF (200)	C	S.C.	Zn	2
Zn	Au	K	LiF (200)	C	S.C.	Zn	2

The instrument was calibrated against primary synthetic standards, and spectral interference effects, normalized peak and background counts, and final element concentrations were calculated using various computer programs written by B. W. Chappell.

Precision of the analyses was based on the values obtained from the two pellets of each sample. If the concentrations of the duplicate pellets did not agree within 5 percent, they were rejected and the sample was re-run. However, the two measurements were generally well within 5 percent for nearly all samples. The two concentrations measured for each element were averaged to give the final value.

REFERENCES

BISCAYE, P. E., 1964 — Distinction between kaolinite and chlorite in Recent sediments by X-ray diffraction. *Amer. Miner.*, 49, 1281-89.

BUSH, P. R., 1970 — A rapid method for the determination of carbonate carbon and organic carbon. *Chem. Geol.*, 6, 59-62.

FOLK, R. L., 1968 — PETROLOGY OF SEDIMENTARY ROCKS. *Austin, Hemphills.*

HATHAWAY, J. C., 1956 — Procedure for clay mineral analyses used in the sedimentary petrology laboratory of the U.S. Geological Survey. *Clay Miner. Bull.*, 3, 8-13.

HAYES, J. R. & KLUGMAN, M. A., 1959 — Feldspar staining methods. *J. sediment. Petrol.*, 29, 227-32.

HULSEMAN, J., 1966 — On the routine analysis of carbonates in unconsolidated sediments. *J. sediment. Petrol.*, 36, 622-25.

NORRISH, K. & CHAPPELL, B. W., 1967 — X-ray fluorescence spectrography. *In* Zussman, J. (Ed.), PHYSICAL METHODS IN DETERMINATIVE MINERALOGY. *London, Academic Press.*

SHULTZ, L. G., 1964 — Quantitative interpretation of mineralogical composition from X-ray and chemical data for the Pierre Shale. *U.S. geol. Survey. prof. Pap.* 391-C.

WALRAVEN, F., 1968 — Recent marine sedimentation on the continental shelf south of Lae, New Guinea. *Bur. Miner. Resour. Aust. Rec.* 1968/95 (unpubl.).

APPENDIX 2
DESCRIPTIVE FEATURES, TEXTURAL DATA, AND CALCIUM CARBONATE CONTENT OF SEDIMENT SAMPLES

Sample Number	Colour[1]	H_2S Odour	Composition (%) gravel[2]	sand[2]	silt[2]	clay[2]	$CaCo_3$[3]	Terrigenous sand plus gravel[4]
002	yellowish orange	absent	5.1	94.9	0.0	0.0	4.0	96.0
004	yellowish orange	absent	1.0	99.0	0.0	0.0	6.7	93.3
005	yellowish orange	absent	1.5	98.5	0.0	0.0	5.1	94.9
010	yellowish orange	absent	0.0	96.0	2.0	2.0	0.0	96.0
012	greyish orange	absent	0.9	97.1	1.0	1.0	4.9	93.0
013	greyish orange	absent	0.0	100.0	0.0	0.0	5.6	94.0
014	yellowish orange	absent	0.1	99.9	0.0	0.0	5.0	95.0
015	olive-grey	strong	29.3	10.7	35.0	25.0	28.2	12.0
016	greyish orange	absent	0.5	96.5	1.0	2.0	27.0	70.0
018	greyish orange	absent	0.0	94.0	2.3	3.7	11.0	83.0
020	olive-grey	present	20.0	38.0	20.0	22.0	40.0	18.0
032	yellowish brown	absent	0.0	99.0	0.0	1.0	1.7	97.0
033	yellowish brown	absent	7.7	86.3	2.0	4.0	8.5	85.0
034	yellowish brown	absent	0.0	98.0	2.0	0.0	0.0	98.0
035	yellowish brown	absent	0.3	97.7	0.8	1.2	3.7	95.0
036	yellowish brown	absent	0.2	93.8	2.0	4.0	0.4	94.0
038	yellowish brown	absent	0.0	75.0	12.4	12.6	1.3	73.7
040	yellowish orange	absent	0.0	98.0	1.0	1.0	1.7	96.0
042	yellowish orange	absent	0.0	100.0	0.0	0.0	1.7	98.0
050	yellowish orange	absent	0.2	99.8	0.0	0.0	0.0	100.0
052	olive-black	present	0.0	3.0	52.0	45.0	5.5	0.0
053	yellowish brown	absent	0.0	73.0	14.0	13.0	5.0	68.0
054	olive-grey	present	0.0	8.0	58.0	34.0	4.4	3.6
056	olive-grey	present	0.0	3.0	51.0	46.0	0.6	2.4
058	olive-black	present	9.0	62.0	14.0	15.0	0.0	70.0
059	brownish grey	absent	0.2	96.8	1.0	2.0	0.7	96.0
061	olive-black	present	0.0	5.0	48.0	47.0	0.3	4.7
063	olive-black	present	0.0	1.0	47.0	52.0	1.1	0.0
065	olive-black	absent	0.0	3.0	42.0	55.0	4.6	3.0
067	brownish grey	absent	0.0	89.0	5.0	6.0	0.5	88.5
069	brownish grey	absent	3.2	88.8	5.0	3.0	2.4	89.0
071	yellowish orange	absent	0.4	98.6	<1.0	<1.0	0.0	>99.0
077	brownish grey	absent	0.0	77.0	5.0	18.0	0.0	77.0
079	olive-grey	present	0.0	20.0	32.0	48.0	1.4	18.6
081	orange-pink	absent	6.7	93.3	0.0	0.0	4.2	96.0
083	orange-pink	absent	0.0	100.0	0.0	0.0	0.0	100.0
085	brownish black	absent	1.5	78.5	19.0	1.0	1.2	79.0
086	brownish black	absent	0.0	3.0	39.0	58.0	1.0	2.0
087	olive-black	absent	0.0	6.0	44.0	50.0	0.2	5.8
090	olive-grey	absent	0.0	0.3	41.7	58.0	1.0	0.0
091	olive-black	present	24.0	64.0	5.0	7.0	40.0	48.0
092	greyish black	strong	0.1	0.9	33.0	66.0	1.2	0.0
094	orange-pink	absent	2.4	97.6	0.0	0.0	0.2	>99.0
096	orange-pink	absent	0.0	100.0	0.0	0.0	0.0	100.0
098	brownish-grey	absent	0.0	65.0	6.0	29.0	10.0	65.0
100	greyish orange	absent	6.9	75.1	5.0	13.0	13.0	69.0
102	yellowish orange	absent	0.0	100.0	0.0	0.0	0.0	100.0
104	olive-black	absent	1.0	3.0	29.0	67.0	2.2	2.0
106	brownish black	absent	27.9	54.1	6.0	12.0	25.0	57.0
108	olive-grey	present	0.0	38.0	18.0	44.0	0.0	38.0
111	olive-black	present	2.0	3.0	25.0	70.0	1.2	2.0
113	olive-grey	absent	3.9	37.1	18.1	41.0	8.1	33.0
116	greyish black	absent	2.0	3.0	28.0	67.0	1.4	1.5

Sample Number	Colour[1]	H_2S Odour	Composition (%) gravel[2]	sand[2]	silt[2]	clay[2]	$CaCo_3$[3]	Terrigenous sand plus gravel[4]
117	greyish black	present	2.2	1.8	26.0	70.0	3.0	1.0
118	olive-black	strong	1.9	1.1	34.0	63.0	2.2	0.8
120	olive-black	strong	0.0	38.0	34.0	28.0	0.0	38.0
123	olive-black	present	9.7	3.3	27.0	60.0	9.7	3.0
126	olive-black	absent	1.1	1.9	34.0	63.0	1.8	1.2
128	olive-black	present	6.3	36.7	19.0	38.0	6.3	36.0
130	greyish black	absent	3.1	5.9	12.0	79.0	2.6	6.4
132	olive-black	present	4.2	1.8	30.0	64.0	3.0	1.0
133	olive-black	present	9.4	1.6	28.0	61.0	9.4	1.6
134	olive-black	present	11.8	2.2	30.0	56.0	12.0	2.0
135	olive-grey	absent	41.7	9.3	26.0	23.0	40.0	10.0
140	olive-black	present	0.0	1.0	31.0	68.0	1.0	0.0
143	olive-black	present	21.6	8.4	46.0	24.0	18.0	8.4
144	black	strong	0.0	22.0	39.0	39.0	0.7	21.0
145	olive-black	present	3.0	10.0	42.0	45.0	3.5	9.0
147	olive-grey	present	0.0	1.0	41.0	58.0	0.0	1.0
148	olive-grey	present	0.0	1.0	37.0	63.0	0.0	1.0
151	olive-grey	absent	0.0	21.0	31.0	48.0	0.0	21.0
154	dark grey	present	0.7	2.3	30.0	67.0	2.7	0.3
158	olive-black	absent	1.0	19.0	38.0	42.0	1.2	18.8
160	olive-grey	present	0.4	5.6	46.0	48.0	0.7	5.3
162	olive-grey	absent	1.0	3.0	52.0	44.0	1.0	3.0
165	olive-black	present	0.5	2.5	64.0	33.0	1.2	1.8
167	olive-black	present	1.0	2.0	52.0	45.0	0.9	2.0
168	olive-black	present	0.0	4.0	56.0	40.0	0.0	4.0
169	olive-grey	present	0.0	57.0	25.0	18.0	0.0	57.0
170	olive-grey	present	1.9	23.1	44.0	31.0	8.0	17.0
171	olive-grey	present	0.0	3.0	52.0	45.0	0.0	3.0
173	olive-black	present	0.0	0.4	45.0	54.0	0.0	0.1
175	olive-black	present	3.1	6.9	25.0	65.0	3.0	7.0
177	olive-grey	present	1.0	1.0	36.0	62.0	1.0	1.0
179	olive-grey	present	3.5	83.5	6.0	7.0	4.2	82.0
180	olive-grey	absent	6.0	55.0	14.0	25.0	15.0	46.0
181	olive-grey	absent	7.0	24.0	42.0	27.0	12.0	19.0
183	olive-grey	absent	0.0	7.0	53.0	40.0	0.0	7.0
185	olive-grey	present	0.0	3.0	38.0	59.0	0.0	3.0
187	olive-black	present	0.0	2.0	52.0	46.0	0.0	1.7
189	olive-black	present	0.6	0.4	43.0	56.0	0.6	0.4
191	olive-black	strong	2.0	4.0	27.0	67.0	2.0	4.0
194	olive-black	strong	1.0	2.0	29.0	68.0	2.0	1.0
195	black to olive-grey	strong	0.0	1.0	45.0	54.0	0.0	1.0
197	black to olive-grey	strong	0.0	1.0	49.5	49.5	0.0	0.5
199	brownish black	present	0.0	28.0	45.0	27.0	0.0	28.0
200	olive-grey	present	0.0	14.0	51.0	35.0	0.0	13.9
201	greyish black	present	1.3	3.7	51.0	44.0	2.3	2.7
202	olive-grey to black	present	0.0	11.0	50.0	39.0	0.0	10.8
204	brownish grey	absent	0.0	89.0	10.0	1.0	0.0	89.0
205	olive-grey	present	0.0	12.0	53.0	35.0	0.0	12.0
206	light brown	absent	10.4	>85.0	<2.0	<2.0	0.0	>95.4
207	light brown	absent	2.4	>95.0	<1.0	<1.0	0.0	>97.4
208	light brown	absent	0.0	>95.0	<2.0	<2.0	0.0	>95.0
209	olive-grey	absent	2.3	9.7	44.0	44.0	0.0	12.0
210	light brown	absent	3.8	94.2	<1.0	<1.0	0.0	>98.0
211	light brown	absent	14.2	80.0	2.8	3.0	0.0	>94.2
212	olive-grey	present	0.0	9.0	58.0	33.0	0.0	9.0
214	olive-grey	present	0.8	8.2	46.0	45.0	0.5	8.5
218	yellowish orange	absent	0.0	100.0	0.0	0.0	n.d.	—

Sample Number	Colour[1]	H_2S Odour	Composition (%) gravel[2]	sand[2]	silt[2]	clay[2]	$CaCo_3$[3]	Terrigenous sand plus gravel[4]
221	yellowish orange	absent	0.0	100.0	0.0	0.0	n.d.	—
227	yellowish orange	absent	7.4	92.6	0.0	0.0	n.d.	—
231	yellowish orange	absent	0.4	99.6	0.0	0.0	n.d.	—
234	yellowish orange	absent	0.0	100.0	0.0	0.0	n.d.	—
237	yellowish orange	absent	10.5	89.5	0.0	0.0	n.d.	—
240	yellowish orange	absent	0.0	100.0	0.0	0.0	n.d.	—
243	light brown	absent	29.8	Samples 243 to 277:			n.d.	—
244	light brown	absent	20.6	Estimated less than			n.d.	—
245	light brown	absent	0.0	5% silt-plus-clay			n.d.	—
246	light brown	absent	2.8				n.d.	—
247	light brown	absent	0.0				n.d.	—
248	light brown	absent	0.0				n.d.	—
249	greyish orange	absent	0.0				n.d.	—
250	light brown	absent	0.0				n.d.	—
251	greyish orange	absent	6.0				n.d.	—
252	yellowish brown	absent	0.0				n.d.	—
253	yellowish brown	absent	0.0				n.d.	—
254	yellowish brown	absent	50.9				n.d.	—
255	yellowish brown	absent	6.0				n.d.	—
256	yellowish brown	absent	4.3				n.d.	—
257	yellowish brown	absent	0.0				n.d.	—
258	yellowish brown	absent	0.0				n.d.	—
259	yellowish brown	absent	0.0				n.d.	—
260	light brown	absent	51.2				n.d.	—
261	moderate yellowish brown	absent	0.0				n.d.	—
262	moderate yellowish brown	absent	0.4				n.d.	—
263	moderate yellowish brown	absent	6.8				n.d.	—
264	moderate yellowish brown	absent	4.4				n.d.	—
265	moderate yellowish brown	absent	0.0				n.d.	—
266	moderate yellowish brown	absent	0.0				n.d.	—
267	moderate yellowish brown	absent	0.0				n.d.	—
268	moderate yellowish brown	absent	0.0				n.d.	—
269	moderate yellowish brown	absent	0.0				n.d.	—
270	moderate yellowish brown	absent	6.8				n.d.	—
271	moderate yellowish brown	absent	6.3				n.d.	—
272	moderate yellowish brown	absent	0.0				n.d.	—
273	moderate yellowish brown	absent	0.0				n.d.	—
275	moderate yellowish brown	absent	0.0				n.d.	—
276	moderate yellowish brown	absent	0.0				n.d.	—
277	yellowish brown	absent	0.0				n.d.	—
280	yellowish orange	absent	10.7	86.3	0.0	0.0	10.1	97.0
282	yellowish orange	absent	0.9	99.1	0.0	0.0	3.0	97.0
285	yellowish orange	absent	0.8	99.2	0.0	0.0	2.0	98.0
289	greyish orange	absent	1.6	98.4	0.0	0.0	6.3	94.0
291	greyish orange	absent	3.8	96.2	0.0	0.0	5.7	94.3
293	greyish orange	absent	0.8	99.2	0.0	0.0	3.5	96.0

1. Colour determined on wet sample using Rock-Color Chart of Geological Society of America (1951)
2. Percent by weight of organic-free sediment
3. Percent by weight of total sample. Samples in which $CaCo_3$ was not determined are designated 'n.d.'
4. Percent coarse fraction of total sample not attributed to $CaCo_3$

APPENDIX 3

Mineralogy of sand-size fraction of sediment samples (percent by number in 63-500 μm fraction of $CaCo_3$-free sample).

Sample Number	*Quartz*	*Feldspar*	*Mica*	*Heavy Minerals*
002	91	8	<1	<1
004	91	8	0	1
005	91	9	0	0
010	89	9	<1	<1
012	86	13	1	0
013	87	12	<1	<1
014	84	16	0	0
016	85	13	1	<1
018	79	19	2	<1
032	86	12	1	1
033	84	13	2	<1
034	83	17	<1	0
035	89	10	1	<1
036	87	12	<1	<1
038	89	9	1	1
040	92	7	0	<1
042	92	7	0	<1
050	95	4	0	1
052	75	13	8	4
053	90	9	1	0
054	74	14	9	3
056	73	14	9	4
058	89	9	1	1
059	89	9	<1	<1
061	76	14	6	4
063	75	14	9	2
065	74	7	17	2
067	90	9	1	0
069	92	7	0	<1
071	96	3	0	1
077	96	3	0	1
079	90	9	1	0
081	96	3	0	1
083	96	4	0	0
085	96	2	<1	1
086	77	14	8	1
087	76	13	9	2
090	74	14	9	3
091	96	2	<1	1
092	75	14	9	2
094	99	<1	0	<1
096	98	2	0	0
098	96	3	0	1
100	97	2	0	1
102	96	3	0	1
104	96	2	<1	1
106	96	2	<1	1
108	96	2	<1	1
111	97	2	0	1
113	97	2	0	1
116	97	2	0	1
117	98	2	0	0
118	97	2	0	<1
120	96	2	<1	1
123	96	3	0	1

Sample Number	Quartz	Feldspar	Mica	Heavy Minerals
126	95	3	0	2
128	96	2	0	2
130	96	2	0	2
132	96	2	<1	1
133	97	3	0	0
134	97	2	0	1
136	96	2	<1	1
140	97	2	0	1
143	97	2	0	1
144	96	2	<1	1
145	97	0	2	1
147	73	8	17	2
148	75	7	16	2
151	68	25	5	2
154	67	25	6	3
158	79	15	4	2
160	80	14	4	2
162	68	25	5	2
165	77	16	4	3
167	69	24	5	2
168	73	14	9	4
169	68	25	5	2
170	68	25	5	2
171	76	14	6	4
173	75	15	6	4
175	83	17	0	<1
177	85	15	<1	0
179	84	16	0	0
180	83	16	<1	0
181	84	16	0	0
183	64	24	10	3
185	68	26	4	2
187	65	23	10	2
189	79	14	4	3
191	78	16	4	2
194	80	16	2	2
195	64	24	11	1
197	66	22	12	<1
199	65	23	10	2
200	67	23	10	<1
201	65	23	10	2
202	70	21	9	0
204	81	14	4	<1
205	65	23	10	2
206	77	22	<1	<1
207	76	24	0	<1
208	76	24	0	<1
209	71	21	8	0
210	75	24	0	0
211	77	23	0	0
212	70	20	10	0
214	65	21	12	2
280	79	19	2	<1
285	86	13	<1	<1
289	87	12	<1	<1
290	91	9	0	<1
291	91	9	0	0
292	85	15	0	0

APPENDIX 4

Transition-metal, phosphate, and organic-carbon chemistry (ppm, except where stated)

Sample Number	*Ti*	*V*	*Cr*	*Mn*	*Fe(%)*	*Co*	*Ni*	*Cu*	*Zn*	P_2O_5	*Organic carbon (%)*
010	265	4	<2	5	0.15	<2	2	<2	3	200	1.3
012	227	6	<2	16	0.22	<2	2	<2	3	360	0.8
014	151	3	<2	10	0.15	2	2	<2	<2	140	0.2
016	427	12	4	38	0.43	2	3	5	8	500	0.4
018	459	12	9	27	0.40	<2	3	<2	8	350	1.3
033	390	8	5	21	0.32	<2	2	<2	6	300	2.2
035	377	7	5	18	0.27	<2	11	3	5	200	1.2
036	499	9	8	20	0.39	<2	6	4	7	210	0.9
038	1470	31	18	63	1.37	6	8	4	25	420	1.4
040	<20	5	<2	6	0.12	<2	2	<2	<2	190	1.7
050	219	2	3	8	0.05	<2	<2	2	<2	050	0.5
052	3860	94	56	141	4.24	12	25	13	73	1700	5.2
054	3970	90	58	143	4.27	11	25	12	73	1500	4.5
056	4470	94	56	173	4.43	13	25	14	76	1300	4.5
058	2000	41	23	90	1.88	6	12	7	31	550	2.8
061	4350	96	50	178	4.20	13	25	15	77	1200	4.2
063	4450	102	59	172	4.40	15	26	14	78	1300	4.5
065	3890	97	56	153	4.39	11	25	13	76	1700	5.7
067	670	15	9	31	0.66	2	4	2	11	470	1.0
069	395	8	5	21	0.39	2	4	2	7	470	1.2
077	840	20	15	27	0.49	2	6	<2	10	330	1.5
079	3330	77	47	116	4.04	10	23	10	64	1500	4.8
081	264	2	9	5	0.06	<2	4	<2	<2	060	0.4
083	105	2	<2	2	0.04	<2	<2	<2	<2	080	0.2
085	1260	27	12	48	1.06	6	7	<2	19	460	1.5
087	4410	94	49	179	4.20	16	26	13	77	1200	3.9
090	4200	107	54	181	4.69	17	25	14	81	1600	5.0
092	4180	114	55	182	4.74	15	26	14	80	1400	4.3
094	268	4	<2	5	0.10	<2	5	2	<2	150	0.8
096	375	3	7	6	0.12	<2	<2	<2	<2	045	0.8
098	1510	46	19	44	1.39	5	11	7	25	390	3.3
104	3750	103	55	162	4.55	16	24	13	75	1900	6.0
106	880	28	9	63	1.01	5	9	3	17	450	2.0
108	3200	73	46	115	3.73	12	19	10	61	1300	2.5
111	3670	104	62	164	4.64	11	26	15	76	1600	5.1
113	2460	69	37	115	2.84	9	18	10	46	1200	4.3
116	3480	101	55	167	4.37	16	24	14	71	1400	6.6
118	3680	103	60	168	4.77	17	27	14	78	1700	5.8
120	3700	47	32	51	1.67	6	11	7	28	800	3.2
123	3510	103	56	191	4.64	15	25	14	74	1500	5.3
126	3620	92	60	164	4.76	8	27	16	75	1500	6.7
130	3550	99	60	173	4.67	16	25	14	75	1600	5.6
132	3670	97	58	178	4.68	14	25	15	76	1500	5.9
134	3290	93	57	159	4.41	15	24	14	71	1400	5.2
136	2530	74	38	128	3.33	12	18	11	53	900	5.5
140	3540	88	52	143	4.27	15	24	14	71	1600	6.7
143	3130	71	44	118	3.48	11	18	14	62	1100	5.9
144	3000	59	35	79	2.38	11	18	13	47	1400	5.2
145	3100	79	45	122	3.77	10	21	16	66	1100	5.1
147	4180	105	54	253	4.67	13	24	14	79	1500	4.4
154	3920	85	53	134	4.68	16	26	11	75	1300	3.4
160	4200	93	49	197	4.03	15	21	13	74	1200	4.1
162	4380	90	51	172	4.06	13	22	13	72	1100	4.0
165	4330	87	52	156	4.53	16	24	12	79	1100	4.4
167	4270	89	48	165	4.12	15	23	12	76	1100	4.4
169	2980	50	32	132	2.20	8	15	8	42	600	2.1
171	4440	88	48	192	3.92	12	21	13	73	1100	4.6

Sample Number	*Ti*	*V*	*Cr*	*Mn*	*Fe(%)*	*Co*	*Ni*	*Cu*	*Zn*	P_2O_5	*Organic Carbon (%)*
151	3770	81	48	146	3.95	17	21	16	66	1100	5.1
158	4000	84	43	173	3.61	12	21	13	65	1000	3.5
173	4420	100	54	177	4.56	18	24	13	81	1300	4.4
177	4170	100	49	179	4.62	16	25	12	81	1400	3.2
179	610	14	5	27	0.60	3	8	3	10	240	1.0
183	4290	91	47	180	3.62	14	20	12	69	1000	4.5
187	4390	95	48	170	3.92	15	23	12	74	1200	3.7
189	3850	95	48	172	4.59	15	24	12	79	1500	5.2
194	3780	97	44	173	4.48	17	24	12	79	1400	4.9
195	3950	99	44	169	3.97	11	23	13	77	1400	5.8
197	4080	97	45	209	4.08	16	23	14	78	1600	4.8
199	3660	72	39	185	2.86	11	17	10	55	1100	4.9
200	4150	95	43	235	3.71	17	20	12	69	1100	3.3
201	4330	104	46	305	4.14	18	20	12	74	1100	4.4
202	4140	91	40	290	3.58	15	19	13	66	1100	4.2
204	1740	30	15	105	1.13	4	10	4	22	250	1.6
205	4050	71	40	167	3.15	12	18	12	59	1100	4.7
209	3740	71	57	259	3.84	20	21	12	67	850	4.3
212	4210	83	40	200	3.57	13	21	12	66	1000	3.2
214	4300	83	43	197	4.12	17	22	17	72	1200	4.9

R76/1256 Cat. No. 77 2426 9